



Zhao, Y., Vinther, J., Parry, L., Wei, F., Green, E., Pisani, D., Hou, X., Edgecombe, G. D., & Cong, P. (2019). Cambrian Sessile, Suspension Feeding Stem-Group Ctenophores and Evolution of the Comb Jelly Body Plan. *Current Biology*, 29(7), 1112-1125.e2.
<https://doi.org/10.1016/j.cub.2019.02.036>

Peer reviewed version

License (if available):
CC BY-NC-ND

Link to published version (if available):
[10.1016/j.cub.2019.02.036](https://doi.org/10.1016/j.cub.2019.02.036)

[Link to publication record in Explore Bristol Research](#)
PDF-document

This is the accepted author manuscript (AAM). The final published version (version of record) is available online via Elsevier at <https://doi.org/10.1016/j.cub.2019.02.036> . Please refer to any applicable terms of use of the publisher.

University of Bristol - Explore Bristol Research

General rights

This document is made available in accordance with publisher policies. Please cite only the published version using the reference above. Full terms of use are available:
<http://www.bristol.ac.uk/red/research-policy/pure/user-guides/ebr-terms/>

Cambrian sessile, suspension feeding stem-group ctenophores and evolution of the comb jelly body plan

Yang Zhao^{1, 2}, Jakob Vinther^{3, 4*, †}, Luke A. Parry^{3, 5, 6, 7}, Fan Wei^{1, 2}, Emily Green³, Davide Pisani^{3, 4}, Xianguang Hou^{1, 2}, Gregory D. Edgecombe^{2, 5}, Peiyun Cong^{1, 2, 5*}

¹Yunnan Key Laboratory for Palaeobiology, Yunnan University, Kunming 650091, China.

²MEC International Joint Laboratory for Palaeobiology and Palaeoenvironment, Yunnan University, Kunming 650091, China

³School of Earth Sciences, University of Bristol, Wills Memorial Building, Queens Road, Bristol BS8 1RJ, UK

⁴School of Biological Sciences, University of Bristol, Life Sciences, Building, 24 Tyndall Avenue, Bristol BS8 1TQ, UK

⁵Department of Earth Sciences, The Natural History Museum, Cromwell Road, London, SW7 5BD, UK

⁶Department of Natural History (Palaeobiology Section), Royal Ontario Museum, Toronto, Ontario M5S2C6, Canada

⁷Yale Institute for Biosphere studies, Yale University, New Haven, Connecticut, USA

†Lead contact

*Correspondence: jakob.vinther@bristol.ac.uk (J.V.) and cong@ynu.edu.cn (P-Y. C.)

SUMMARY

The origin of ctenophores (comb jellies) is obscured by their controversial phylogenetic position, with recent phylogenomic analyses resolving either sponges or ctenophores as the sister group of all other animals. Fossil taxa can provide morphological evidence that may elucidate the origins of derived characters and shared ancestries among divergent taxa, providing a means to ‘break’ long branches in phylogenetic trees. Here we describe new fossil material from the early Cambrian Chengjiang Biota, Yunnan Province, China, including the putative cnidarian *Xianguangia*, the new taxon *Daihua sanqiong* gen et sp. nov., and *Dinomischus venustus*, informally referred to as ‘dinomischids’ here. ‘Dinomischids’ possess a basal calyx encircled by eighteen tentacles that surround the mouth. The tentacles carry pinnules, each with a row of stiff filamentous structures interpreted as very large compound cilia of a size otherwise only known in ctenophores. Together with the Cambrian tulip animal *Siphusauctum* and the armoured Cambrian scleroctenophores, they exhibit anatomies that trace ctenophores to a sessile, polypoid stem lineage. This bodyplan resembles the polypoid, tentaculate bodyplan of cnidarians, including a blind gastric cavity partitioned by mesenteries. We propose that comb rows are derived from tentacles with paired sets of pinnules that each bear a row of compound cilia. The scleroctenophores exhibit

1 paired comb rows, also observed in *Siphusauctum*, in addition to an organic skeleton, shared
2 as well by *Dinomischus*, *Daihua* and *Xianguangia*. We formulate a hypothesis in which
3 ctenophores evolved from sessile, polypoid suspension feeders, sharing similarities with
4 cnidarians that suggest either a close relationship between these two phyla or a striking
5 pattern of early convergent evolution.

6 7 8 **Introduction** 9

10 Ctenophores are mainly pelagic, predatory animals with a distinct biradial body plan. They
11 use eight external comb rows (ctenes) for locomotion, these being densely packed with cilia
12 up to 2mm long, the largest known cilia among animals [1]. Despite being unequivocally
13 monophyletic and having a diverse Cambrian fossil record [2, 3], the origin of ctenophores
14 and their place in animal phylogeny have been difficult to resolve [4-6]. Ctenophores and
15 cnidarians share diploblasty (two germ layers separated by mesoglea), a large digestive cavity
16 (coelenteron), and radial/biradial symmetry. On this basis, both phyla were historically
17 grouped as Coelenterata [7], and the monophyly of this grouping has also been proposed
18 based on embryology [8]. Other than a diploblastic body organisation, many defining
19 characteristics of ctenophores appear to be autapomorphies and correspondence of body
20 regions and organs to those in other phyla has remained obscure. Alternative hypotheses
21 based on morphology have proposed that ctenophores are the sister group of Bilateria
22 (together forming Acrosomata, named for an acrosome in the sperm [9]), or the deuterostome
23 sister group based on ciliary characteristics [10]. Morphological phylogenetic analyses either
24 recovered Acrosomata [11], placed ctenophores in a polytomy with numerous bilaterians
25 [12], or recovered Coelenterata [13].

26 The first large-scale metazoan molecular phylogeny by Dunn, et al. [4], as well as
27 several subsequent phylogenomic analyses [14-23], recovered ctenophores as the sister group
28 of all other animals. This contrasts with traditional views of sponges in this position based on
29 the absence of symmetry axes, muscles, true tissue layers, a pinocytic digestive system, and
30 nerve cells, and having only a single germ layer. However, other studies proposed that this
31 result might be a tree reconstruction artefact caused by the inability of available models to
32 adequately describe processes of molecular evolution at the root of animals [5, 6, 24-28].

33 The oldest unequivocal ctenophore fossils are found in the early Cambrian
34 Chengjiang Konservat-Lagerstätte [2, 29-31] and middle Cambrian Burgess Shale [3],
35 demonstrating that general features of ctenophores, such as ctene/comb rows and a globose
36 body shape, have ancient origins. Younger taxa are known from the Ordovician [32] and the

Devonian [33, 34]. Of all fossil ctenophores, the Devonian examples most closely resemble extant taxa in having paired tentacles [33, 34]. The Ediacaran *Eoandromeda* also shares some putative similarities with ctenophores [35].

Ctenophores from the Burgess Shale have more numerous comb rows than extant taxa, but share with them a fundamental 8-fold symmetry [3]. These forms lack the paired tentacles with colloblasts that are widespread among extant ctenophores, suggesting a late origin relative to other ctenophore autapomorphies. Ctenophores from the early Cambrian Chengjiang Konservat-Lagerstätte possess a unique organic skeleton and were united as the clade Scleroctenophora by Ou, et al. [2], which was inside crown-group Ctenophora when using a hypothetical outgroup.

Here we describe Cambrian fossils that exhibit a suite of characters indicative of ctenophore affinities. We describe a new species, *Daihua sanqiong* gen. et sp. nov. which resembles *Dinomischus*, a stalked organism originally interpreted as an entoproct [36, 37], and the putative cnidarian, *Xianguangia sinica* [13, 29]. These taxa share circumoral pennate tentacles with large compound cilia. Together with the scleroctenophores and the tulip animal *Siphusauctum* [38] we propose that these tentacles are homologous to the ctenes of extant ctenophores and were primitively used in feeding rather than locomotion. The morphological transitions between a tentaculate feeding appendage with ciliary rows and the comb rows of fossil and extant ctenophores are illustrated by successive sister lineages that share an increasing number of ctenophore apomorphies. The proposed homologous features between taxa with otherwise disparate body plans share the same topological relationship to other anatomical features (such as an organic skeleton), satisfying the criteria of similarity, congruence and conjunction Patterson [39]. Taxa forming the deepest branches of the ctenophore stem group reveal that the earliest members of the ctenophore lineage were sessile, polyp-like animals with circumoral tentacles and radially partitioned gastric cavities, features shared with cnidarians.

Results

Xianguangia

Xianguangia (Figure 1) is a polypoid organism from the Chengjiang Biota [29]. Recent work showed that it has tentacles with ciliated pinnules (Figure 1B,D,E,F) [13]. The body was divided into three sections: a basal holdfast, a ‘column’, and tentacles. Based on our observations, this terminology needs slight modification. The ‘basal holdfast’ sensu Ou et al. [13] is the main body compartment (calyx, (‘Ca’ in Figure 1G-I)), housing the digestive system. The preservation of the calyx suggests light sclerotisation (Figure 1A), discussed

further below. We show here that the ‘column’ [13] and ‘tentacles’ [13] are different parts of the same body unit, with tentacles divided into a proximal and distal region (Fig. 1B).

The proximal part of the tentacle bears a sclerotized, flattened rod (Tentacle rod ‘Ter’ in Figure 1B-F), while the distal part is soft and flexible. Eighteen tentacles have been inferred [13] by doubling the exposed tentacles in lateral view. Each tentacle carries several bilaterally-arranged pinnules (‘Pin’ in Figure 1B-E) in both proximal and distal parts. The pinnules harbour dense lineations/striations that are distally oriented (‘Mci’ in Figure 1D), 19-23 μm thick and up to 600 μm long which we interpret as compound cilia, more specifically macrocilia [13]. A dark organic stain subtends the base of each row of cilia (Figure 1D). The sclerotized rods of the proximal tentacles are ornamented externally with paired, distally converging furrows (Figure 1B). The tentacles were previously inferred to have attached at the distal end of the ‘column’ [13], but we show here that pinnules are present on the proximal portion of the tentacles (Figure 1A, B, E), therefore extending into the ‘column’, indicating the ‘column’ is the basal part of the tentacle. The mouth (‘Mo’ in Figure 1G) is thus defined by the constricted connection into the calyx.

Several small specimens preserve a radially lobate infill within the calyx, demonstrating the presence of radial divisions that compartmentalise the internal body cavity (‘Me’ in Figure 1G-H). By calculating the circumference based on the diameter of the calyx and the width of a medially exposed mesenterial compartment in three specimens, we infer 18 mesenteries. A small specimen (YKLP 13421) preserves a dark stained outline filling the central portion of the calyx and extending into the mesenterial cavities (‘Gu’ in Figure 1G), which we interpret as the integument of the digestive cavity.

New ‘dinomischid’

Systematic palaeontology

Eumetazoa

Total-group Ctenophora

We use the informal name ‘dinomischids’ to refer to *Xianguangia*, *Daihua* and *Dinomischus*. These taxa form a grade in the lower part of the ctenophore stem group (see phylogenetic analysis). All ‘dinomischids’ possess a calyx and 18 tentacles. The calyx has two distinct regions: an apical and a basal portion, which are generally well delineated. The tentacle complex consists of a sclerotized rod, flanked by outer sheaths that emerge from the calyx, and sets of paired pinnules emerging from the tentacles. The pinnules carry a distally facing

row of compound cilia, each about 19-25 μm wide, potentially elaborated as macrocilia as observed in the mouth of living beroids [1], which are held together by a single outer membrane. ‘Dinomischids’ have an organic skeleton, as in scleroctenophores. In the Chengjiang Konservat-Lagerstätte, this skeleton preserves as impressions with prominent relief, similar to co-occurring vetulicolians and arthropods. More robust elements may take on an ochre to rusty red colouration through iron oxide weathering after pyrite. The occurrence of this skeleton was first identified in scleroctenophores [2], and interpreted as possibly chitinous and secreted within, or immediately beneath, the epidermis. Given the mode of preservation and comparison with other sclerotized taxa, it was likely organic in composition although we cannot exclude light mineralisation [2]. In ‘dinomischids’ this skeleton is present in the tentacles, the calyx, the stalk (if present) and invariably the oral surface.

Genus: *Daihua* gen. nov.

Etymology: Chinese: Dai – for a Yunnan minority tribe, and Hua – flower.

Diagnosis: A ‘dinomischid’ stem-group ctenophore characterized by three circumoral domes with paired bracts. Outer sheaths form two pairs of petal-like structures that flank each tentacle and are about 85% the length of the tentacle’s sclerotized portion. The distal, unsclerotized portion of the tentacle is circa 20% of the tentacle’s total length. *Daihua* is most clearly differentiated from *Xianguangia* and *Dinomischus* by the proportions of the calyx, the apical calyx being 50% the height of the total calyx, while the basal portion is less sclerotized and is clearly delimited by a marginal constriction. It tapers to a blunt tip, whereas in *Xianguangia* the basal portion of the calyx is restricted to the basal pit (‘Bpi’ in Figure 1G,H) and is more sclerotized and forms a stalk in *Dinomischus* (‘St’ and ‘Bcal’ in Figure 3B,K). In *Dinomischus* the outer sheaths form a single membrane around each tentacle (Figure 3F,K and S5D,E), while *Daihua* possesses two pairs. *Xianguangia* has no elaboration of its oral surface, whereas *Daihua* has three domes with paired bracts and *Dinomischus venustus* has an oral cone similar to that of *Siphusauctum* (Figure 3C,D).

Locality: Erjie section, Jinning area, Kunming, Yunnan Province.

Species: *Daihua sanqiong*, gen. et sp. nov

Etymology: Chinese: ‘san’ – three, and ‘qiong’ – dome, alluding to the unique circumoral domes on the oral disc.

Diagnosis: As for genus

1 Holotype: YKLP 13401 (Figure 2A-F). Paratypes: YKLP 13428 (Figure 2G); YKLP 13426
2 (Figure 2H).

3
4 Description: The holotype, YKLP 13401, is a large, well-preserved specimen in oral view
5 (Figure 2A,B, Figure S1 and S2), split over the surface of the oral disc (Figure S2A-C), the
6 sclerotized tentacles (Figure 2C,E,F, Figure S2K) and outer sheaths (Figure 2F, Figure S2L).
7 Preparation of the sediment overlying the tentacles in the part exposed well-preserved
8 pinnules (Figure 2C,D, ‘Pin’ in Figure S2G-I). μ CT tomographic scans reveal that portions of
9 the calyx are present in the matrix (Figure S1F-I).

10 Each tentacle consists of a basal part containing a sclerotized rod (‘Ter’) and a distal
11 and flexible portion, about 20% of the total length. On the upper tentacle surface, more than
12 30 paired sets of pinnules are present (Figure S2G-H). They emerge from paired structures on
13 the tentacle, preserved as an organic stain (‘Cu’ in Figure 2E, Figure S2D-F), referred to as
14 the cushion plate for consistency with subsequent comparisons with ctenophores. Along the
15 midline of the tentacle runs an organic line that branches to connect with the cushion plate
16 structures laterally (‘Ne’ in Figure 2E and Figure S2F). We infer this system to be
17 components of a nervous system based on its morphology and preservation mode, innervating
18 the cushion plate at the tentacle base. It has recently been shown that nervous systems
19 preserve as dark, organic stains in the otherwise weathered Chengjiang and Xiaoshiba biotas
20 [40-42] or as reflective organic films in the Burgess Shale [43] and Sirius Passet [44]. Among
21 non-cuticular anatomical features, only melanized tissues, such as the eyes of *Haikouichthys*
22 [45] and nervous tissue and guts preserve as highly organic stains. The extent of the nervous
23 system demonstrates that each tentacle extended beyond the sclerotized rod into a flexible tip
24 (Figure 2A,B), as the enveloping epidermis is not preserved in the holotype.

25 The pinnules (Figure 2C,D, Figure S2G-I) preserve as semi-transparent structures
26 harbouring two sets of organic lines along their entire length. They are about 60-120 μ m wide
27 and can be more than 5 mm long. The pinnulae carry fine, distally oriented, linear structures
28 19 μ m-25 μ m wide and 175-200 μ m long (Figure 2D). These structures resemble cilia in their
29 morphology and trajectory and conform in dimensions to structures referred to as macrocilia
30 in *Xiangiangia* [13] (Figure 1D), as well as striated structures in *Siphusauctum* [46] (Figure
31 4C), described below.

32 Paired sets of membranous outer sheaths flank each tentacle. The inner set (Medial
33 outer sheath, ‘Mos’) is narrow and slightly longer than the outer set (Lateral outer sheath,
34 ‘Los’), which is broader in aspect (Figure 2F, Figure S2K,L). The outer sheaths are flexible
35 and detached from the tentacle, inferred from the varying overlap over the tentacle and their

propensity for becoming displaced. The contact between the lateral outer sheaths of neighbouring tentacles exhibits a kink with some relief (Figure 2E,F). The outer sheaths appear as dark shadows in the μ CT scans, indicating low density and a likely organic composition, corroborated by their dark coloration, perhaps due to melanin, or another recalcitrant pigment [47-49].

The oral disc exhibits a single, large, central teardrop-shaped opening about 2.4 and 1.6 mm wide, interpreted as the mouth (Figure 2AB, Figure S2C). No other large openings are visible on the oral surface, or elsewhere on the calyx (in laterally preserved specimens) that could be interpreted as an anus. Three sclerotized domes emerge on the oral surface from each of which two sets of ribbon-like spikes protrude (bracts, 'Br') (Figure 2A,B, Figure S3G). The bracts are about 1 mm wide and 33 mm long. They fade into the adjacent sediment, suggesting decreasing sclerotization distally. More distinctly colored margins suggest that these were compressed, originally thin walled, cylindrical structures. In specimens preserved in lateral view where the tentacles are contracted, these bracts project aborally (Figure 2G,H).

Other specimens preserved in oral-aboral, or oblique, views reveal two additional sclerotized surfaces beneath the external oral surface (Figure S3). These membranes have a wide concave outer margin (when viewed from above) and a narrower convex inner margin surrounding the mouth opening. The tentacles can be seen to connect with these membranes and appear to pass into the space that they define. On the dorsal membrane, each tentacle connects via two laterally projecting rust-colored lines, separated by a prominent notch ('Dtg' in Figure S3B,C,E). On the ventral oral membrane is a single line ('Vtg' in Figure S3E). These lines connect to a circumoral canal ('Cot' in Figure S3). The grooves connecting the circumoral canal to the tentacles were likely for musculature used in manipulation of the tentacles, which are preserved in either a contracted (Figure 2G,H) or open configuration (Figure 2A). The circumoral canal may have harboured a centralized nerve ring. *Daihua sanqiong* is reconstructed (Figure 2I, Figure S4) as a sessile, polypoid organism which, like *Xianguangia* [13] and *Siphusauctum* [46], used an extensive ciliary apparatus for filter feeding.

Dinomischus venustus

Dinomischus isolatus was originally described from the middle Cambrian Burgess Shale based on three specimens [37] and *D. venustus* was subsequently documented from the Chengjiang Biota [36] (Figure 3). The Czech Republic has a putative occurrence [50] and another species, *D. isolatus*, is described from the middle Cambrian Kaili biota [51]. The

body of *Dinomischus* consists of a stalk with a bulbous base, a cone-shaped calyx, and 18 tentacles [36], although 20 were originally estimated [37]. New material of *D. venustus* collected from the Chengjiang Konservat-Lagerstätte in the Chengjiang and Haikou areas reveals novel features (Figure 3, Figure S5), including rare soft parts and features of internal anatomy,, and confirms the presence of 18 tentacles.

The calyx, stalk and portions of the tentacles appear robust and stiff, sometimes with considerable relief (Figure 3A,B), indicative of an organic skeleton (as in *Daihua* and *Xianguangia*) and likewise supports the calyx, stalk and the basal portion of each tentacle. The tentacles consist of a basal portion that grades into a more flexible distal portion approximately 15% the length of the tentacle. Surrounding each tentacle is a single outer sheath, which tapers to a point at about 80% of the tentacle length (‘Os’ in Figure 3F,G, Figure S5C-E). The single sheaths envelop each tentacle. In some specimens, the tentacles preserve paired dark structures (‘Cu’ in Figure 3F-G) identical to the cushion plates in *Daihua*, and one larger specimen preserves paired sets of pinnules (‘Pin’ in Figure 3H,I). At the calyx base are radially arranged vertical lamellae (Mesenteries, ‘Me’) that partition the gastric cavity (Figure 3A-D, Figure S5A-C), comparable to the mesenteries of cnidarians and *Xianguangia* (Figure 1H). The total number of mesenteries exceeds 12, but could be 18 based on the corresponding tentacle and mesentery number in *Xianguangia*. A dark-stained (sometimes infilled) structure is observed within the calyx of several specimens, extending as a cone (‘Oc’) among the folded tentacles to the distal tip (Figure 3C,D, Figure S5A,B). The dark stain conforms in outline to an internal lining of the digestive system preserved organically. The oral cone and the associated digestive cavity narrow in the transition between the apical and medial portion of the calyx and the latter extend to inter-finger amidst the mesenteries (Figures 3D and S5A). These observations are consistent with an extensive, blind, digestive cavity rather than a U-shaped intestine [37]. The inferred digestive cavity (‘Gu’ in Figure 3D) extends in between the mesenterial walls (‘Me’ in Figure 3D) and was partitioned by them. The oral cone is not apparent in *D. isolatus* [37] or in previously described specimens of *D. venustus* [36]. This includes most specimens available here, which could be due to the previously small sample size and variable preservation. The robust external skeleton is most commonly observed, presumably due to a higher preservation potential.

***Siphusauctum*, the tulip animal**

1 *Siphusauctum gregarium* is an iconic taxon from the Burgess Shale Formation Tulip Beds
2 [46]. A second species, *S. lloydguntheri*, occurs in the Spence Shale in Utah [38].
3 *Siphusauctum* exhibits similar characters to *Dinomischus*: calyx (conical structure, sensu
4 O'Brien and Caron [46], 'Ca'), stalk (stem, 'St'), tentacles (comb segments, 'Ten'), tri-
5 hexameric radial morphology, ciliary rows (striations, 'St'), oral cone (body cavity/conical
6 structure, 'Oc') and outer sheaths (external sheath, 'Os') (Fig. 4A-D).

7 The outer sheaths enclose the tentacles in a globular cavity with a single, oral opening
8 and six aboral openings at each tentacle base [46] (Figure 4A-D). The outer sheaths are
9 sometimes identifiable as discrete blades that flay open distally or form a continuous
10 structure that creates a narrow, distal opening around the mouth (originally interpreted as the
11 anus [46]). Medially, the outer sheaths form a discrete protrusion [46] resembling the kinking
12 in the outer sheaths in *Daihua* (Figure 2E,F). The calyx forms a cone that extends up to the
13 single apical opening, terminating in a pore (Figure 4B) that has been interpreted as an anus
14 [46]. Being the single opening and based on comparisons with *Xianguangia*, *Daihua* and the
15 proposed homology with living ctenophore body axes, it is reinterpreted as a mouth here and
16 is hence referred to as an oral cone.

17 Six tentacles emerge from between the calyx and oral cone and appear freely
18 suspended in the globular lumen between the outer sheath and oral cone ('Ten' in Figure
19 4A,B,D). Each tentacle exhibits paired, transverse arrays of dark lineations ('Cu' in Figure
20 4C) connected to a medial dark line, referred to as the axial groove [46]. The dark lineations
21 (transverse grooves in [46]) form a coupled set of lines that connect medially and laterally on
22 either side of the axial groove. From each of these, a dense set of striations emerges in a row
23 formed by organically preserved rods about 40 μm in diameter and ≥ 1.6 mm in length ('Mci'
24 in Figure 4C), similar to macrocilia in *Daihua* and *Xianguangia* in appearance, dimensions
25 and position on the tentacle (Figure 1D, 2D, S2I).

26 *Siphusauctum* shares similarities with *Dinomischus* and *Daihua* in its overall
27 architecture but the ciliary rows are not attached to pinnules in *Siphusauctum* and instead
28 each tentacle forms a broad ribbon which harbours each ciliary row. The organically
29 preserved transverse grooves may be homologous to the paired sets of basal dark stains
30 beneath the pinnules in *Dinomischus* and *Daihua* and are more directly comparable to
31 cushion plate/polstering cell structures, as in living and fossil ctenophores (Figure S6). There
32 is no clear evidence for an organic skeleton. This could be taphonomic, as *Dinomischus*
33 *isolatus* from the Burgess Shale was interpreted as soft bodied originally as well [37], the
34 skeleton only being revealed by the Chengjiang congener.

Scleroctenophora—*Galeactena*

Scleroctenophores are extinct comb jellies with an organic supporting skeleton and eight sets of paired ctene rows. Several species are known from Chengjiang (in the genera *Galeactena*, *Maotianoascus*, *Thaumactena*, *Batofasciculus* and *Trigoides*) [2]. Below we focus on re-describing *Galeactena hemispherica* based on an especially well-preserved specimen, identifying the architecture of the ctene-ciliary organs, and the correspondence of the organic skeleton to that observed in dinomischids.

The anatomy of *Galeactena* is globose, resembling an upside down garlic bulb in outline (Figure 4E-G). The body is supported by an external organic skeleton, which supports each comb row pair externally ('Ter' in Fig. 4E,F) as well as the apical organ ('Ao'), which is housed within a conical aboral extension ('Cal'). The mouth is inferred to lie in an expanded region in front of the comb rows and is similarly supported by an external skeleton, which appears more flexible (Figure 4E).

The ctene-ciliary complex preserves the basal cushion plates in YKLP 13810. The cushion plate structures but not the cilia can be seen in scleroctenophores and Burgess Shale forms. This may be explained by mode of splitting or preservation, if the ciliary organs have separate membranes over each axoneme rather than a single membrane as proposed for 'dinomischids' [13]. These are set in wide, paired rows along each external skeletal rod. Where the skeletal rod (membranous fin, sensu Ou et al. [2]) splits off into the counterpart it is observed that a dark line, consistent with a nerve, runs beneath it and connects to the lateral sets of ctenes ('Ne' in Figure 4E; see also Figure 2G,H in Ou et al. [2]).

The aboral organ is housed in the aboral extension and is preserved as a dark stain, which was identified as a statolith [2], but is at least an order of magnitude larger than those of extant ctenophores [1], conforming better with the preservation of cholesterol-rich cilia that surround statoliths.

The presence of paired ctenes with a nerve running between them differs from living ctenophores and taxa from the Burgess Shale (Figure 5), in which single ctenes have the nerve passing medially underneath. The ctenes are also broader, resembling the condition observed in *Siphosauctum* (Figure 4A-D) more than Burgess Shale and extant ctenophores. The organic skeleton conforms in preservation and topological relationships to the skeleton in 'dinomischids', as it supports the aboral apical organ inside a calyx-like structure as well as elements that support the tentacle-ctene ciliary organs.

The Burgess Shale ctenophores

Three ctenophore genera have been described from the Burgess Shale: *Fasciculus* (Figure 5A-C), *Ctenorhabdotus* (Figure 5D-F) and *Xanioascus* (Figure 5G-I) [3]. They exhibit features more comparable to crown group ctenophores than do scleroctenophores or ‘dinomischids’. *Fasciculus* is characterized by bilaterally paired lobes carrying two sets of comb rows (Figure 5A). One has approximately 64 comb rows, while the other carries ~16 [3]. The comb rows are relatively narrow and the cushion plates are densely set (‘Cu’ in Figure 5B,C, see also Figure S6G,H). A median organic strand preserved in some comb rows (‘Ne’ in Figure 4B,C) was interpreted as a nerve cord [3] and compared to the giant axon in the living ctenophore *Euplokamis* [52]. *Ctenorhabdotus* and *Xanioascus* both possess 24 comb rows, and a well preserved apical region in *Ctenorhabdotus* demonstrates that the combs connect to the apical organ through eight tracts each with three comb rows (Figure 5D,E).

Discussion

Homology of body regions and the phylogenetic position of ‘dinomischids’

The taxa discussed herein share a body region characterized by serial repetition of large cilia in rows either on radially arranged tentacles or on the external body surface as in living ctenophores. The tentacles in *Xianguangia*, *Daihua* and *Dinomischus* carry pinnules with rows of compound cilia of a size only observed in extant ctenophores [1]. At the base of the pinnules of *Daihua* and *Dinomischus* are dark, paired structures (‘Cu’ in Figures 2C,E; 3F,G) that resemble preservation of cushion plates in fossil ctenophores. In *Siphusauctum* these paired rows of compound cilia are also situated on a broad ribbon-like sheet in which cushion plate-like structures subtend each ciliary row (Figure 4A-D), preserved as in scleroctenophores and Burgess Shale ctenophores. Similarly paired and broad ctene rows are present in scleroctenophores, but are attached to the body rather than as tentacles.

An organic skeleton is shared by *Xianguangia*, *Dinomischus*, *Daihua* and scleroctenophores, but is absent in *Siphusauctum* and Burgess Shale taxa. This skeleton supports the apical organ/calyx and the ctene-tentacle-ciliary organs across these taxa, suggesting homology. Homologous body regions are further identified by the position of the mouth and gut. In *Xianguangia*, *Dinomischus*, *Daihua* and *Siphusauctum*, the digestive cavity is positioned inside a calyx. The basal attachment of the calyx region varies from a pit at the base of the calyx in *Xianguangia*, a tapering point in *Daihua*, to more elongate stalks in *Dinomischus* and *Siphusauctum*. *Xianguangia*, *Daihua* and *Dinomischus* have 18 radially arranged tentacles, while *Siphusauctum* exhibits six. These all conform to a triradial

1 arrangement, echoed in the mesenterial divisions in *Xiangiangia* and three oral domes of
2 *Daihua*. In *Dinomischus* and *Siphusauctum* an oral cone is present as well as a calyx region
3 below the tentacles. A similar arrangement is inferred for the scleroctenophores where the
4 ctenes and associated skeletal rods form a distinct body region from the apical region and
5 apical organ. We interpret this apical region of scleroctenophores as homologous with the
6 calyx of *Xiangiangia*, *Dinomischus*, *Daihua* and *Siphusauctum*. In the Burgess Shale taxa,
7 the calyx/apical region is reduced to only the apical organ, as in modern ctenophores.

8 There is a correspondence in components and arrangement of tentacle-ciliary
9 structures of the sessile and stalked taxa and the ctene-ciliary organs of extant and fossil
10 ctenophores (Figure 7). A transformation from a sessile polypoid form with an organic
11 skeleton can be traced via successive sister groups into the more derived stem-group
12 ctenophores from Chengjiang and the Burgess Shale. This scenario is supported by
13 phylogenetic analyses encompassing extant animals and the fossil taxa described herein.
14 These analyses used a dataset of 93 taxa (20 fossils) and 278 adult and embryological
15 characters. The new matrix builds on previously available datasets [2, 11, 13, 53] through the
16 incorporation of new morphological information and an expanded taxon sample (Figure 6,
17 Figure S7).

18 Phylogenetic analyses recover a paraphyletic grade of sessile, polypoid taxa in which
19 ciliary organs are borne on radially arranged tentacles (Figure 6, Figure S7). This grade
20 subtends the scleroctenophores and the ctenophore crown group, indicating an origin of
21 ctenophores from sessile, skeletonized ancestors with a ‘dinomischid’ bodyplan. The skeleton
22 is inferred to have been lost twice independently, once in the node defining the ctenophore
23 crown group and the Burgess Shale taxa, and once in *Siphusauctum*.

24 Our hypothesis indicates a progressive expansion (Figure 7) of the oral surface to
25 become the main body region of living ctenophores. A progressive modification of the
26 tentacle ciliary organs into a ribbon, carrying ciliary rows in *Siphusauctum*, is observed and
27 subtended by the cushion plates, which become attached to the oral dome in
28 scleroctenophores as the outer sheaths are lost (Figure 7). We infer an inversion in which the
29 ciliary rows/ctenes became outwards facing, as in living ctenophores.

30 The calyx forms the main body compartment in the sessile stemward taxa but in
31 Burgess Shale and crown-group ctenophores is reduced to only the apical region. The
32 transformation series proposed here are further supported by ctenophore development [54].
33 The larval cydippid body is largely composed of an inflated dome with an apical mouth [55].
34 The ctenes emerge near the aboral side between the oral region and the apical organ and grow
35 towards the mouth. Furthermore, each ctene is paired in development [56]. The nervous

1 system is centralized into the apical organ, congruent with our proposal that this is
2 homologous to the ‘dinomischid’ calyx, which originally carried the tentacles as well as the
3 digestive system. ‘Dinomischids’ may have had a similar centralized nerve centre, perhaps
4 surrounding the oral entrance (e.g. in *Daihua*, Figure S3). With the expanded oral cone and
5 reduction of the calyx, this centralized nervous system would become concentrated
6 posteriorly, conforming to the apical organ in living ctenophores.

7 The body transformations proposed here may also inform on why ctenophores depart
8 from other metazoans in terms of their genetic machinery, having lost several gene classes
9 (e.g. microRNA processing enzymes [57] and HOX genes [14, 15]). Our hypothesis suggests
10 that living ctenophores have dramatically remodelled their ancestral body plan to become
11 essentially inflated blastopores through expanding their oral surface, while the main body
12 compartment was reduced (Figure 7).

13 *Eoandromeda* is a discoidal Ediacaran macrofossil with eight distinct, spirally
14 arranged rays [35, 58]. Organic preservation in specimens from China [35, 58] is reminiscent
15 of cushion plate preservation and there is evidence for transverse annulation in the
16 distribution of organic material in the fossils. However, narrow putative comb rows would
17 make *Eoandromeda* deeply nested, as these characteristics of the comb rows are shared only
18 with Burgess Shale and crown group taxa. Furthermore, spiral anatomy is not observed in
19 any other stem-group ctenophore. Other spiral discoidal forms are known from the Ediacaran,
20 such as trilobozoans (e.g. *Tribrachidium* [59]), and discoidal forms with similar organic
21 preservation [60], are associated with *Eoandromeda*. *Tribrachidium* exhibits some similarity
22 to the three oral domes of *Daihua*, but this taxon lacks a calyx and tentacles, and possesses a
23 branching set of grooves, which are unknown from ‘dinomischids’. These considerations, and
24 our new evidence for the ctenophore stem group, indicate that *Eoandromeda* is unlikely to
25 represent a ctenophore, despite its octoradial morphology.

26 Based on our phylogenetic hypothesis, we infer that *Siphusauctum* evolved from a
27 ‘dinomischid’ with a robust organic skeleton that became less sclerotized. The late Ediacaran
28 skeletonized metazoan *Namacalathus* [61, 62] resembles *Siphusauctum* in having a calyx
29 with a stalk, an apical opening, and hexaradial symmetry with six lateral openings. The
30 skeleton is inferred to have been highly organic and putatively mineralized [61]. As for
31 *Dinomischus* [37], affinities with lophophorates have been proposed [61]. *Namacalathus*
32 could represent a member of the same lineage as *Siphusauctum* (Figure S7), as they share a
33 similar body plan, but also have a skeleton like ‘dinomischids’ and scleroctenophores. This
34 would extend the stem-group Ctenophora into the latest Ediacaran. The early Cambrian

putative cnidarian *Eolympia* [63] possesses a bipartite calyx, a stalk, and 18 tentacles, suggesting ‘dinomischid’ affinities, as retrieved when included in our analyses (Figure S7).

Implications for early animal evolution

The taxa that we identify as the deepest branches of the ctenophore stem group resemble cnidarians in several respects. Although these similarities prompted the assignment of *Xianguangia sinica* to the cnidarian stem group [13], we recover this taxon as the most early-diverging ctenophore. Compartmentalisation of the digestive system by mesenteries occurs both in *Xianguangia* and in taxa more proximal to the ctenophore crown group (e.g. *Dinomischus*), and such a radially-partitioned gut has been considered a cnidarian synapomorphy, occurring in both anthozoans and medusozoans. A polypoid body plan has been inferred for the cnidarian ancestor [64], resembling the condition in ‘dinomischids’. Reinterpretation of these characters as coelenterate synapomorphies was revealed by analysis of fossils, being lost prior to the diversification of the ctenophore crown group. If the prior assignment of *Xianguangia* to the cnidarian stem group were correct [13], an organic skeleton might have also been present in the ancestral coelenterate, but subsequently lost in the cnidarian stem group. However, all ‘dinomischids’ possess large compound cilia in serial rows that suggest a position in stem-group Ctenophora. We propose that crown-group ctenophores evolved from polypoid ancestors via scleroctenophores, which share an organic skeleton and broad, paired ctenes with the sessile ‘dinomischids’. Ctenes evolved from pinnule-bearing tentacles that attached to an inflated oral surface, which in modern ctenophores is the main body structure (Figure 7). The ‘dinomischid’ calyx, which contains the gut, is homologous with the body of cnidarians and became reduced to the tissue containing the apical organ in Burgess Shale and crown-group ctenophores.

Coelenterata (Figure 6) has been recovered from morphological data [13], and also some phylogenomic analyses of amino acid sequences [24, 25, 65]. However most current analyses instead find ctenophores to be the sister group either of all other metazoans (Ctenophora-sister hypothesis) or of all animals except sponges (Porifera-sister hypothesis) [4-6, 14]. A recent investigation of presence and absence of protein families and their constituent orthogroups across Opisthokonta [28] confirmed that while ctenophoran gene families lack many eumetazoan-specific orthologs (as shown previously [14, 15]), they frequently include paralogs of the missing genes otherwise found in eumetazoans. This suggests that the missing ctenophore-specific, eumetazoan orthologs represent losses [28], rather than primary absences. When presence/absence of protein families rather than of their

constituent orthogroups was used to infer a phylogeny of the Opisthokonta, Coelenterata was strongly supported [28].

The conclusions drawn here build on the congruence of a nested set of detailed similarities that connect the fossils with each other and with extant ctenophores, as well as ctenophoran development. Our interpretation does not rely on the validity of a specific hypothesis for the relative relationships between Cnidaria, Ctenophora and Porifera. The discovery of fossils with a unique combination of characters found in both cnidarians and ctenophores, however, provides more evidence for coelenterate monophyly. If cnidarians and ctenophores are not a clade (as predicted by most recent phylogenomic analyses), then the character distribution we observe in numerous Cambrian non-bilaterians would have to be a striking case of convergence close to the root of animal phylogeny. Among the phylogenetic hypotheses proposed for deep-branching animals, Coelenterata maximizes support from independent lines of evidence, having been recovered from amino acid datasets [24, 25], presence/absence of protein families [28] and morphology [13].

Acknowledgements.

This work is supported by NSFC (41572015) and Key Project of Yunnan Applied Basic Research (2017FA020) to C.P-Y., H.X-G., F.W., and Z.Y., a Leverhulme Trust Research Project (RPG-2015-441) to G.D.E and C. P-Y, and a Yale Institute of Biospheric Studies Fellowship to L.A.P. Simon Powell is thanked for producing several line drawings and reconstructions for this manuscript. Rebecca Gelernter (Nearbirdstudios) made several initial reconstructions for an earlier version of this manuscript. Xiaodong Wang made the reconstruction of *Daihua* in Figure 2. JV thanks members of the Zoological Museum and Biology Institute, University of Copenhagen, for suggestions and comments during a seminar in November 2017. Mark Q. Martindale (Whitney lab), Qiang Ou (China University of Geosciences) and Jean Bernard Caron (ROM) are thanked for sharing images and discussion on ctenophore anatomy. Tom Davies μ CT scanned YKLP 13401a at the University of Bristol.

Author contributions. Y.Z., C.P-Y. and J.V. conceived the project. Y.Z., C.P-Y., L.P. and J.V. designed the research. H.X-G., C.P-Y., Y.Z. and W.F. collected the material. C.P-Y, Y.Z., H.X-G. and W.F. prepared the material. Y. Z. photographed the material. Y.Z., J.V. and L.P. made camera lucida and interpretative drawings. E.G. rendered and segmented the μ CT scans and made the body reconstructions in Figure 7. J.V. supervised and drafted the line

drawings and reconstructions. L.P and G.D.E. designed the phylogenetic analyses. D. P. contributed to the discussion on ctenophore relationships. J.V. wrote the first manuscript draft, together with L.P. and G.D.E. with input from all authors.

Declaration of Interests.

The authors declare no competing interests

References

1. Tamm, S.L. (2014). Cilia and the life of ctenophores. *Invertebrate biology* 133, 1-46.
2. Ou, Q., Xiao, S.-H., Han, J., Sun, G., Zhang, F., Zhang, Z.-F., and Shu, D.-G. (2015). A vanished history of skeletonization in Cambrian comb jellies. *Science advances* 1, e1500092.
3. Conway Morris, S., and Collins, D. (1996). Middle Cambrian ctenophores from the Stephen Formation, British Columbia, Canada. *Philosophical Transactions of the Royal Society of London B: Biological Sciences* 351, 279-308.
4. Dunn, C., Hejnol, A., Matus, D., Pang, K., Browne, W., Smith, S., Seaver, E., Rouse, G., Obst, M., and Edgecombe, G. (2008). Broad phylogenomic sampling improves resolution of the animal tree of life. *Nature* 452, 745 - 747U745.
5. Feuda, R., Dohrmann, M., Pett, W., Philippe, H., Rota-Stabelli, O., Lartillot, N., Wörheide, G., and Pisani, D. (2017). Improved Modeling of Compositional Heterogeneity Supports Sponges as Sister to All Other Animals. *Current Biology*.
6. Pisani, D., Pett, W., Dohrmann, M., Feuda, R., Rota-Stabelli, O., Philippe, H., Lartillot, N., and Wörheide, G. (2015). Genomic data do not support comb jellies as the sister group to all other animals. *Proceedings of the National Academy of Sciences*, 201518127.
7. Frey, H., and Leuckart, R. (1847). *Beiträge zur Kenntniss wirbelloser Thiere: mit besonderer Berücksichtigung der Fauna des norddeutschen Meeres; Mit zwei Kupfertafeln*, (Vieweg).
8. Scholtz, G. (2004). Coelenterata versus Acrosomata—zur Position der Rippenquallen (Ctenophora) im phylogenetischen System der Metazoa. *Sber. Ges. Naturf. Freunde Berlin* 43, 15-33.
9. Ax, P. (1989). Basic phylogenetic systematization of the Metazoa. In *The hierarchy of life*, B. Fernholm, K. Bremer and H. Jörnvall, eds. (Amsterdam: Elsevier Science B.V.), pp. 229-245.
10. Nielsen, C. (1995). *Animal evolution: Interrelationships of living Phyla*, (Oxford University Press).
11. Peterson, K.J., and Eernisse, D.J. (2001). Animal phylogeny and the ancestry of bilaterians: inferences from morphology and 18S rDNA gene sequences. *Evolution & Development* 3, 170-205.

12. Nielsen, C., Scharff, N., and Eibye-Jacobsen, D. (1996). Cladistic analyses of the animal kingdom. *Biological Journal of the Linnean Society* 57, 385-410.
13. Ou, Q., Han, J., Zhang, Z., Shu, D., Sun, G., and Mayer, G. (2017). Three Cambrian fossils assembled into an extinct body plan of cnidarian affinity. *Proceedings of the National Academy of Sciences* 114, 8835–8840.
14. Moroz, L.L., Kocot, K.M., Citarella, M.R., Dosung, S., Norekian, T.P., Povolotskaya, I.S., Grigorenko, A.P., Dailey, C., Berezikov, E., and Buckley, K.M. (2014). The ctenophore genome and the evolutionary origins of neural systems. *Nature* 510, 109-114.
15. Ryan, J.F., Pang, K., Schnitzler, C.E., Nguyen, A.-D., Moreland, R.T., Simmons, D.K., Koch, B.J., Francis, W.R., Havlak, P., and Smith, S.A. (2013). The genome of the ctenophore *Mnemiopsis leidyi* and its implications for cell type evolution. *Science* 342, 1242592.
16. Halanych, K.M. (2015). The ctenophore lineage is older than sponges? That cannot be right! Or can it? *Journal of Experimental Biology* 218, 592-597.
17. Borowiec, M.L., Lee, E.K., Chiu, J.C., and Plachetzki, D.C. (2015). Extracting phylogenetic signal and accounting for bias in whole-genome data sets supports the Ctenophora as sister to remaining Metazoa. *BMC genomics* 16, 987.
18. Whelan, N.V., Kocot, K.M., and Halanych, K.M. (2015). Employing phylogenomics to resolve the relationships among cnidarians, ctenophores, sponges, placozoans, and bilaterians. *Integrative and comparative biology* 55, 1084-1095.
19. Halanych, K.M., Whelan, N.V., Kocot, K.M., Kohn, A.B., and Moroz, L.L. (2016). Miscues misplace sponges. *Proceedings of the National Academy of Sciences* 113, E946-E949.
20. Whelan, N.V., Kocot, K.M., Moroz, L.L., and Halanych, K.M. (2015). Error, signal, and the placement of Ctenophora sister to all other animals. *Proceedings of the National Academy of Sciences* 112, 5773-5778.
21. Whelan, N.V., Kocot, K.M., Moroz, T.P., Mukherjee, K., Williams, P., Paulay, G., Moroz, L.L., and Halanych, K.M. (2017). Ctenophore relationships and their placement as the sister group to all other animals. *Nature ecology & evolution* 1, 1737.
22. Rokas, A. (2013). My oldest sister is a sea walnut? *Science* 342, 1327-1329.
23. Shen, X.-X., Hittinger, C.T., and Rokas, A. (2017). Contentious relationships in phylogenomic studies can be driven by a handful of genes. *Nature ecology & evolution* 1, 0126.
24. Philippe, H., Derelle, R., Lopez, P., Pick, K., Borchellini, C., Boury-Esnault, N., Vacelet, J., Renard, E., Houliston, E., Quéinnec, E., et al. (2009). Phylogenomics revives traditional views on deep animal relationships. *Current Biology* 19, 706-712.
25. Pick, K.S., Philippe, H., Schreiber, F., Erpenbeck, D., Jackson, D.J., Wrede, P., Wiens, M., Alié, A., Morgenstern, B., Manuel, M., et al. (2010). Improved Phylogenomic Taxon Sampling Noticeably Affects Nonbilaterian Relationships. *Molecular Biology and Evolution* 27, 1983-1987.
26. Pisani, D., Pett, W., Dohrmann, M., Feuda, R., Rota-Stabelli, O., Philippe, H., Lartillot, N., and Wörheide, G. (2016). Reply to Halanych et al.: Ctenophore misplacement is corroborated by independent datasets. *Proceedings of the National Academy of Sciences* 113, E948-E949.
27. Simion, P., Philippe, H., Baurain, D., Jager, M., Richter, D.J., Di Franco, A., Roure, B., Satoh, N., Quéinnec, É., and Ereskovsky, A. (2017). A large and consistent

- phylogenomic dataset supports sponges as the sister group to all other animals. *Current Biology* 27, 958-967.
28. Pett, W., Adamski, M., Adamska, M., Francis, W.R., Eitel, M., Pisani, D., and Woerheide, G. (2018). The role of homology and orthology in the phylogenomic analysis of metazoan gene content. *Molecular Biology and Evolution* *IN PRESS*.
 29. Chen, J.-Y., and Erdtmann, B.-D. (1991). Lower Cambrian fossil lagerstatte from Chengjiang, Yunnan, China: Insights for reconstructing early metazoan life. In *The early evolution of Metazoa and the significance of problematic taxa*, M. Simonetta and S. Conway Morris, eds. (Cambridge: Cambridge University Press), pp. 57-76.
 30. Hu, S.-X., Steiner, M., Zhu, M.-Y., Erdtmann, B.-D., Luo, H.-L., Chen, L.-Z., and Weber, B. (2007). Diverse pelagic predators from the Chengjiang Lagerstätte and the establishment of modern-style pelagic ecosystems in the early Cambrian. *Palaeogeography, Palaeoclimatology, Palaeoecology* 254, 307-316.
 31. Chen, J.-Y., Schopf, J.W., Bottjer, D.J., Zhang, C.-Y., Kudryavtsev, A.B., Tripathi, A.B., Wang, X.-Q., Yang, Y.-H., Gao, X., and Yang, Y. (2007). Raman spectra of a Lower Cambrian ctenophore embryo from southwestern Shaanxi, China. *Proceedings of the National Academy of Sciences* 104, 6289-6292.
 32. Young, G.A., Rudkin, D.M., Dobrzanski, E.P., Robson, S.P., Cuggy, M.B., Demski, M.W., and Thompson, D.P. (2013). Great Canadian Lagerstätten 3. Late Ordovician Konservat-Lagerstätten in Manitoba. *Geoscience Canada* 39.
 33. Stanley Jr, G.D., and Stürmer, W. (1987). A new fossil ctenophore discovered by X-rays. *Nature* 328, 61.
 34. Stanley, G.D., and Stürmer, W. (1983). The first fossil ctenophore from the Lower Devonian of West Germany. *Nature* 303, 518-520.
 35. Tang, F., Bengtson, S., Wang, Y., Wang, X.l., and Yin, C.y. (2011). *Eoandromeda* and the origin of Ctenophora. *Evolution & development* 13, 408-414.
 36. Chen, J.-Y., Hou, X.-G., and Lu, H.-Z. (1989). Early Cambrian Hour glass-like rare sea animal *Dinomischus* (Entoprocta) and its ecological features. *Acta Palaeontologica Sinica* 1, 004.
 37. Conway Morris, S. (1977). A new entoproct-like organism from the Burgess Shale of British Columbia. *Palaeontology* 20, 833-845.
 38. Kimmig, J., Strotz, L.C., and Lieberman, B.S. (2017). The stalked filter feeder *Siphusauctum lloydguntheri* n. sp. from the middle Cambrian (Series 3, Stage 5) Spence Shale of Utah: its biological affinities and taphonomy. *Journal of Paleontology* 91, 902-910.
 39. Patterson, C. (1982). Morphological Characters and Homology. In *Problems of Phylogenetic Reconstruction*, Volume 21, K.A. Joysey and A.E. Friday, eds. (London and New York: Academic Press), pp. 21-74.
 40. Ma, X.-Y., Edgecombe, G.D., Hou, X.-G., Goral, T., and Strausfeld, N.J. (2015). Preservational pathways of corresponding brains of a Cambrian euarthropod. *Current Biology* 25, 2969-2975.
 41. Ma, X.-Y., Hou, X.-G., Edgecombe, G.D., and Strausfeld, N.J. (2012). Complex brain and optic lobes in an early Cambrian arthropod. *Nature* 490, 258-261.
 42. Yang, J., Ortega-Hernández, J., Butterfield, N.J., Liu, Y., Boyan, G.S., Hou, J.-b., Lan, T., and Zhang, X.-g. (2016). Fuxianhuiid ventral nerve cord and early nervous system evolution in Panarthropoda. *Proceedings of the National Academy of Sciences* 113, 2988-2993.

43. Ortega-Hernández, J. (2015). Homology of head sclerites in Burgess Shale euarthropods. *Current Biology* 25, 1625-1631.
44. Park, T.-Y.S., Kihm, J.-H., Woo, J., Park, C., Lee, W.Y., Smith, M.P., Harper, D.A., Young, F., Nielsen, A.T., and Vinther, J. (2018). Brain and eyes of *Kerygmachela* reveal protocerebral ancestry of the panarthropod head. *Nature communications* 9, 1019.
45. Shu, D.-G., Morris, S.C., Han, J., Zhang, Z.-F., Yasui, K., Janvier, P., Chen, L., Zhang, X.-L., Liu, J.-N., and Li, Y. (2003). Head and backbone of the Early Cambrian vertebrate *Haikouichthys*. *Nature* 421, 526-529.
46. O'Brien, L.J., and Caron, J.-B. (2012). A new stalked filter-feeder from the middle Cambrian Burgess Shale, British Columbia, Canada. *PloS one* 7, e29233.
47. Vinther, J. (2015). A guide to the field of palaeo colour: Melanin and other pigments can fossilise: Reconstructing colour patterns from ancient organisms can give new insights to ecology and behaviour. *Bioessays* 37, 643-656.
48. Parry, L.A., Smithwick, F., Nordén, K.K., Saitta, E.T., Lozano-Fernandez, J., Tanner, A.R., Caron, J.B., Edgecombe, G.D., Briggs, D.E., and Vinther, J. (2017). Soft-bodied fossils are not simply rotten carcasses—Toward a holistic understanding of exceptional fossil preservation. *BioEssays*.
49. Vinther, J., Briggs, D.E.G., Prum, R.O., and Saranathan, V. (2008). The colour of fossil feathers. *Biol Letters* 4, 522-525.
50. Mikulas, R., and Kordule, V. (1998). A problematic fossil from the Middle Cambrian of the Barrandian area (Czech Republic). *Journal of GEOsciences* 43, 187-190.
51. Peng, J., Zhao, Y.-L., and Lin, J.P. (2006). *Dinomischus* from the Middle Cambrian Kaili Biota, Guizhou, China. *Acta Geologica Sinica (English edition)* 80, 498-501.
52. Mackie, G.O., Mills, C.E., and Singla, C.L. (1992). Giant Axons and Escape Swimming in *Euplokamis dunlapae* (Ctenophora: Cydippida). *The Biological Bulletin* 182, 248-256.
53. Duan, B., Dong, X.-P., Porras, L., Vargas, K., Cunningham, J.A., and Donoghue, P.C. (2017). The early Cambrian fossil embryo *Pseudoooides* is a direct-developing cnidarian, not an early ecdysozoan. *Proc. R. Soc. B* 284, 20172188.
54. Martindale, M.Q., and Henry, J.Q. (2015). Ctenophora. In *Evolutionary Developmental Biology of Invertebrates 1*. (Springer), pp. 179-201.
55. Martindale, M.Q., and Henry, J.Q. (1999). Intracellular fate mapping in a basal metazoan, the ctenophore *Mnemiopsis leidyi*, reveals the origins of mesoderm and the existence of indeterminate cell lineages. *Dev. Biol.* 214, 243-257.
56. Tamm, S.L. (2012). Patterns of comb row development in young and adult stages of the ctenophores *Mnemiopsis leidyi* and *Pleurobrachia pileus*. *Journal of morphology* 273, 1050-1063.
57. Bråte, J., Neumann, R.S., Fromm, B., Haraldsen, A.A.B., Tarver, J.E., Suga, H., Donoghue, P.C.J., Peterson, K.J., Ruiz-Trillo, I., Grini, P.E., et al. Unicellular Origin of the Animal MicroRNA Machinery. *Current Biology*.
58. Tang, F., Yin, C., Bengtson, S., Liu, P., Wang, Z., and Gao, L. (2008). Octoradial spiral organisms in the Ediacaran of South China. *Acta Geologica Sinica-English Edition* 82, 27-34.
59. Hall, C.M., Droser, M.L., Gehling, J.G., and Dzaugis, M.E. (2015). Paleoecology of the enigmatic *Tribrachidium*: New data from the Ediacaran of South Australia. *Precambrian Research* 269, 183-194.

60. Wang, Y., Wang, X., and Huang, Y. (2008). Megascopic symmetrical metazoans from the Ediacaran Doushantuo Formation in the northeastern Guizhou, South China. *Journal of China University of Geosciences* 19, 200-206.
61. Zhuravlev, A.Y., Wood, R., and Penny, A. (2015). Ediacaran skeletal metazoan interpreted as a lophophorate. *Proc. R. Soc. B* 282, 20151860.
62. Grotzinger, J.P., Watters, W.A., and Knoll, A.H. (2000). Calcified metazoans in thrombolite-stromatolite reefs of the terminal Proterozoic Nama Group, Namibia. *Paleobiology* 26, 334-359.
63. Han, J., Kubota, S., Uchida, H.-o., Stanley Jr, G.D., Yao, X., Shu, D., Li, Y., and Yasui, K. (2010). Tiny sea anemone from the Lower Cambrian of China. *PLoS One* 5, e13276.
64. Kayal, E., Bentlage, B., Pankey, M.S., Ohdera, A.H., Medina, M., Plachetzki, D.C., Collins, A.G., and Ryan, J.F. (2018). Phylogenomics provides a robust topology of the major cnidarian lineages and insights on the origins of key organismal traits. *BMC Evolutionary Biology* 18, 68.
65. Nosenko, T., Schreiber, F., Adamska, M., Adamski, M., Eitel, M., Hammel, J., Maldonado, M., Müller, W.E., Nickel, M., and Schierwater, B. (2013). Deep metazoan phylogeny: when different genes tell different stories. *Molecular phylogenetics and evolution* 67, 223-233.
66. Yang, C., Li, X.-H., Zhu, M., Condon, D.J., and Chen, J. (2018). Geochronological constraint on the Cambrian Chengjiang biota, South China. *Journal of the Geological Society*, jgs2017-2103.
67. Ronquist, F., Teslenko, M., Van Der Mark, P., Ayres, D.L., Darling, A., Höhna, S., Larget, B., Liu, L., Suchard, M.A., and Huelsenbeck, J.P. (2012). MrBayes 3.2: efficient Bayesian phylogenetic inference and model choice across a large model space. *Systematic biology* 61, 539-542.
68. Goloboff, P.A., Farris, J.S., and Nixon, K.C. (2008). TNT, a free program for phylogenetic analysis. *Cladistics* 24, 774-786.
69. Goloboff, P.A., and Catalano, S.A. (2016). TNT version 1.5, including a full implementation of phylogenetic morphometrics. *Cladistics* 32, 221-238.

Figure 1. *Xianguangia sinica* from the Chengjiang Lagerstätte

- (A) YKLP 13830a, part. Insert denotes area in B.
- (B) Detail of YKLP 13429a shown in A, detailing sclerotized proximal tentacle rods, distal tentacles and pinnules emerging from the distal and proximal sections of the tentacles.
- (C) ELEM-SJ120376A, complete individual preserving pinnules and macrocilia, shown in D.
- (D) Details of pinnules and rows of macrocilia of specimen in C.
- (E) YKLP 13429a, preserving pinnules in the proximal, sclerotized tentacles.
- (F) Details of pinnules in E.
- (G) YKLP 13421a, small specimen preserving outline of gut in the calyx. The mouth is inferred to be present where the gut constricts in the calyx-tentacle transition.
- (H) YKLP 13415, small specimen preserving gut infilled with sediment, evidencing the presence of mesenterial divisions.
- (I) Schematic sagittal section through *Xianguangia* based on the new observations presented here. For clarity, macrocilia are not drawn.
- (J) Cross section through a distal tentacle.

(K) Transverse section through the proximal tentacle region, indicated with a stippled line in J.

(L) Transverse section through the calyx, illustrating the arrangement of mesenteries inside. Abbreviations: Cal-calyx, Dt-distal tentacle, Ter-tentacle rod, Pin-pinnules, Gu-gut, Me-mesenteries, Mo-mouth, Mci-macroscilia.

Images in C and D provided by Qiang Ou, China University of Geosciences. See also table S1.

Figure 2. *Daihua sanqiong*, gen. et sp. nov from the Chengjiang Lagerstätte

(A) YKLP 13401a, holotype. Specimen preserved in oral view

(B) Camera lucida drawing of YKLP 13401a. Orange denotes tentacle rods, red is pinnules, blue is outer sheaths and grey is oral domes and associated bracts.

(C) YKLP 13401b, holotype. Detail of four tentacles showing the distinct sclerotized tentacle rod with paired dark stains along (cushion plates) and distal pinnules emerging.

(D) YKLP 13401b, holotype. Close up of pinnules shown in C. notice the distinct adapically facing row of striations, interpreted as macroscilia.

(E) YKLP 13401b, holotype. Close up of tentacle, preserving cushion plates and the median dark line, interpreted as a nerve.

(F) YKLP 13401b, holotype. Same view as in E, imaged in low angle light showing the relief and overlap of the lateral and medial outer sheaths. Notice the kink where lateral outer sheaths abut each other between tentacles.

(G) YKLP 13428, paratype. Contracted specimen preserving well delineated apical and basal calyx region and bracts emerging among the distal tentacles

(H) YKLP 13426, contracted specimen preserving bracts and apical calyx. A putative brachiopod is attached to the proximal tentacle on the right side.

(I) Schematic reconstruction of *Daihua* in upper, oblique lateral view when open and lateral view when contracted.

Abbreviations: Acal- apical calyx, Bcal-basal calyx, Br-bracts, Cu-cushion plate, Dt-distal tentacle, Ter-tentacle rod, Pin-pinnules, Mo-mouth, Mci-macroscilia, Los-lateral outer sheath, Mos-medial outer sheath, Bra-bract, Ki-kink. See also Figures S1-S4, Table S1.

Figure 3. *Dinomischus venustus* from the Chengjiang Lagerstätte

(A) YKLP 13412b highly mineralized specimen in lateral aspect preserving tentacles and mesenteries.

(B) Close-up of YKLP 13412b, shown in A.

(C) YKLP 13411, well preserved specimen, preserving the digestive tract (gut-Gu) as well as the oral cone (Oc), infilled with sediment (inf)

(D) Close-up of YKLP 13411, shown in C.

(E) CJHMD 00051a, well preserved specimen preserving basal cushion plates

(F) CJHMD 00051b, counterpart of specimen shown in E.

(G) Close-up of CJHMD 00051b, shown in F.

(H) YKLP 13414b, large specimen preserving tentacular pinnules.

(I) Close-up of YKLP 13414a, shown in H.

(J) Pinnules preserved in YKLP 13414a.

(K) Schematic reconstruction of *Dinomischus venustus* based on the new material in sagittal section (note stalk is attenuated here), tentacle seen from above and in transverse section. Abbreviations: Acal- apical calyx, Bcal-basal calyx, Mes-mesenteries, Pin-pinnules, Te-tentacle, Oc-oral cone, Os-Outer sheath, St-Stalk, Cu-cushion plate, inf-infilling of sediment. See also Figure S5, table S1.

Figure 4. *Siphusauctum gregarium* and the scleroctenophore, *Galeactena hemispherica*.

(A) *Siphusauctum gregarium* ROMIP 61414, specimen preserving lightly splayed out tentacles, outer sheaths and well preserved cushion plates and macrocilia, detailed in C.
(B) *Siphusauctum gregarium* ROMIP 890069, specimen preserving oral dome and surrounding tentacles.
(C) Detail of ROMIP 61414 preserving cushion plates and long macrocilia.
(D) Schematic reconstruction of *Siphusauctum gregarium* in sagittal section with sections of the stalk omitted and a transverse view in the upper section of the body.
(E) *Galeactena hemispherica*, YKLP 13810a. Well preserved specimen showing tentacle rods supporting comb rows and the apical organ housed within a small calyx.
(F) Detail of E, showing the dark stained cushion plates.
(G) Reconstruction of *Galeactena* in sagittal and transverse view. Note that nothing is known about the digestive cavity in scleroctenophores, which is demarcated with a stippled line.
Abbreviations: Cal- calyx, Ten- tentacle, Mci-macroscilia, Oc-Oral cone, Os-outer sheath, Ne-nerve, Cu-Cushion plate, Ao-apical organ. See also Figure S6.
Images of *Siphusauctum* provided by Jean Bernard Caron, ROM. See also table S1.

Figure 5. Ctenophores from the Burgess Shale

(A) *Fasciculus vesanus*, USNM 202151. Complete specimen in lateral view photographed underwater.
(B) Close-up of region shown in (A) showing unpaired comb rows and underlying nerve.
(C) Close-up of region shown in (A) showing unpaired comb rows and underlying nerve.
(D) *Ctenorhabdotus capulus*, ROMIP 50822. Complete specimen in lateral view.
(E) *Ctenorhabdotus capulus*, ROMIP 51439. Complete specimen in oblique view of the apical region.
(F) SEM backscatter image of comb rows, dark material shows features preserved in light elements, presumably carbon.
(G) *Xanioascus canadensis* ROMIP 43186. Complete specimen in oblique view.
(H) *Xanioascus canadensis* ROMIP 43190. Complete specimen in lateral view.
(I) Close-up of specimen shown in (H) showing unpaired comb row.
Abbreviations: Ao – apical organ, Cu- cushion plate, Ne – nerve. See also Figure S6.
Images provided by Jean Bernard Caron, ROM. See also table S1.

Figure 6. Phylogenetic analysis

Bayesian phylogenetic analysis using the mki model on a dataset containing 278 characters and 90 living and fossil taxa. Numbers at nodes are posterior probabilities and the scale bar is in units of expected number of substitutions per site. Dataset is expanded and modified

from previous datasets [2, 11, 13, 53] to include ‘dinomischids’, which form a paraphyletic grade on the ctenophore stem. For additional analyses using other optimality criteria see the supporting information. See also Figure S7 and methods s1.

Figure 7. Body plan evolution and homology among stem ctenophores

Upper panel illustrates the evolution of the tentacle-ctene ciliary organ in coelenterates. While being simple in Cnidaria, the dinomischids evolved rows of compound cilia, either set on pinnules in the early diverging forms, or as a ribbon-shaped tentacle with transverse rows of cilia over a cushion plate structure in *Siphusauctum*. As in the sessile stem-group ctenophores, the scleroctenophores (*Galeactena*) exhibit paired ciliary rows on their tentacle-ctene ciliary organs. Only crown-group ctenophores and the Burgess Shale forms exhibit fused ctenes evidenced by the underlying nerve.

Lower panel illustrates the relative proportions and association of the major body compartments and their homology with the cnidarian outgroup. The main body compartment is the columnar body in polypoid cnidarians, while this is present as the mesentery bearing calyx in stem-group ctenophores. The oral surface becomes expanded in more derived stem groups, while the calyx becomes reduced into the small region harbouring the apical organ in crown-group and Burgess Shale ctenophores.

Color code: yellow—tentacle/ctenes; Darker yellow/brown—sclerotized skeleton; light blue—pinnules; green—outer sheaths; red—oral surface. See also Figure S7.

STAR methods

CONTACT FOR REAGENT AND RESOURCE SHARING

Further information and requests for resources and reagents should be directed to and will be fulfilled by the Lead Contact, Jakob Vinther (Jakob.vinther@bristol.ac.uk).

EXPERIMENTAL MODEL AND SUBJECT DETAILS

Newly studied material of ‘dinomischids’ was collected from the Chengjiang Biota, which mainly occurs in the local *Eoredlichia-Wutingaspis* biozone of the Yu’anshan Member, Chiungchussu Formation in Yunnan Province, Southwest China. The age of the Chengjiang biota has been widely accepted as Cambrian Age 3, Epoch 2, and is recently constrained as not older than $518.03 \pm 0.69/0.71$ Ma [66]. A list of new material figured in this study, including detailed localities, is shown in table S1. Additional figured material is from the middle Cambrian (Wuliuan) Burgess Shale from British Columbia, Canada.

METHOD DETAILS

Fossil preparation and photography

The Chengjiang fossils are prepared, when necessary, with a needle under a Nikon SMZ 800N or SMZ 1000 stereomicroscope. Images of the Chengjiang material were shot with a Canon EOS 5D SR camera mounted with Canon MP-E 65 mm (1-5X) or Canon EF 100 mm

1 macro lenses under cross-polarized light, and were re-leveled with Adobe Photoshop CC
2 2014.2.2. Details were also photographed under a Leica microscope.

3 4 **μCT scanning**

5 The holotype of *Daihua* YKLP 13401a was scanned on a Nikon XTH225ST CT scanner with
6 reflection target. The settings for the scan were 220kV (energy), 78uA (current), 1.5mm Cu
7 filter, 2.829s (exposure time), gain set at 24, 3141 projections and 4 frames per
8 projection. Total scan time was just under 10 hours. The voxel size of the reconstructed
9 dataset was 17.4um.

10 11 **Interpretative drawings**

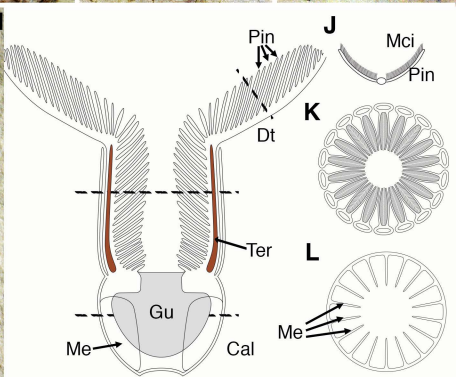
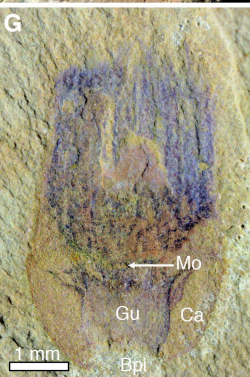
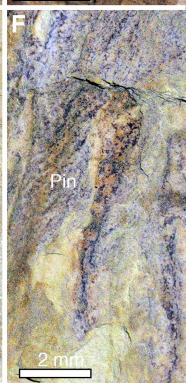
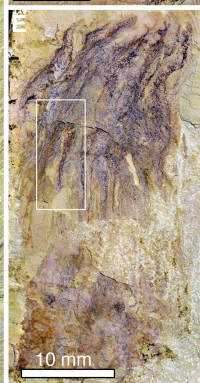
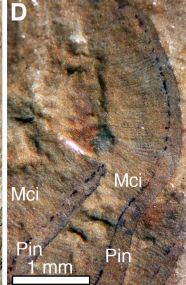
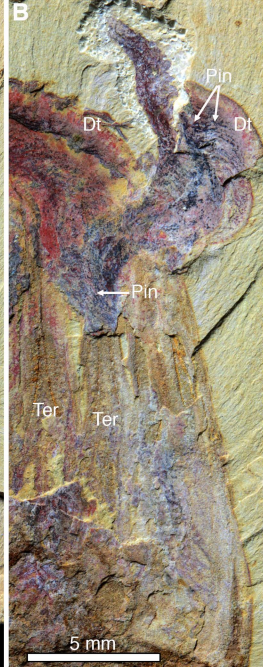
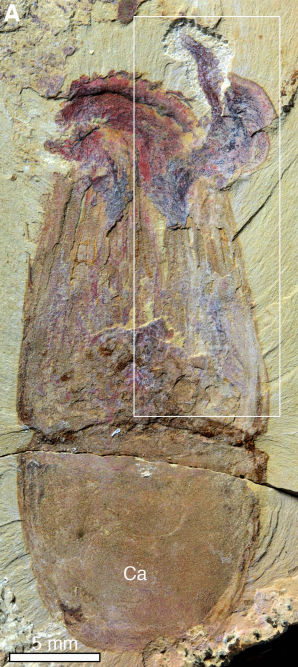
12
13 Interpretative drawings were made using a camera lucida mirror attached to a Heerbrugge
14 microscope and then subsequently inked and colored using Adobe Photoshop. Additional
15 interpretative drawings were made by tracing fossil specimens photographed using
16 different lighting conditions
17 in Adobe Photoshop.

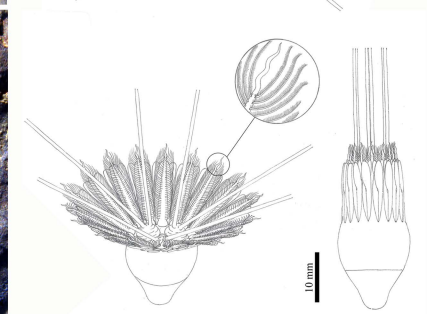
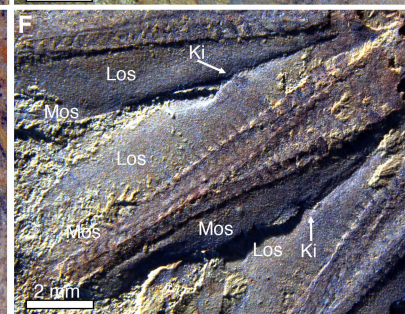
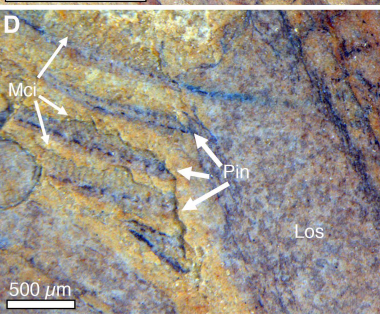
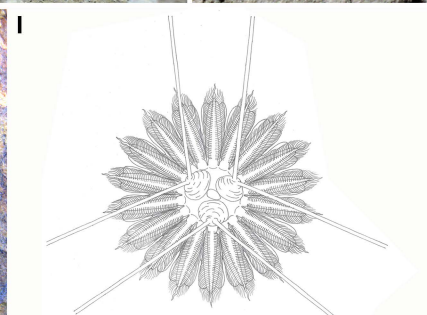
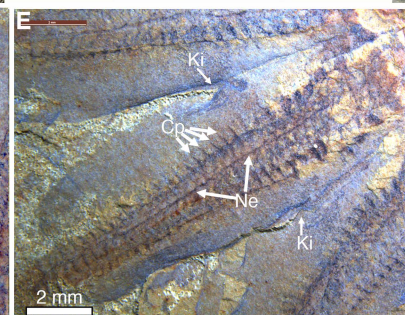
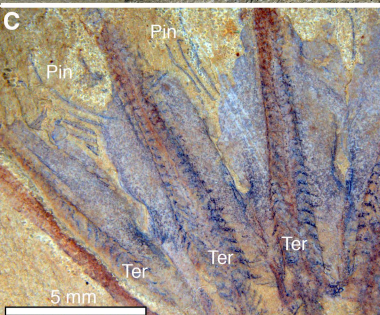
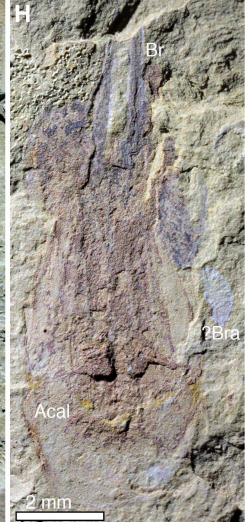
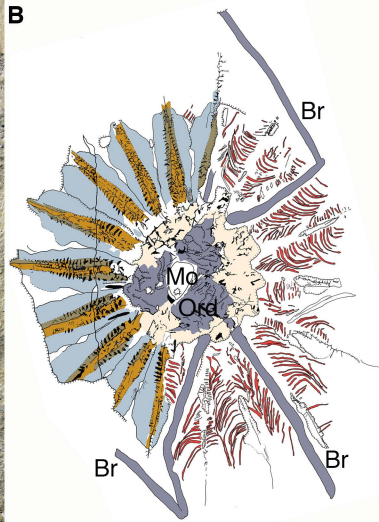
18 19 **QUANTIFICATION AND STATISTICAL ANALYSIS**

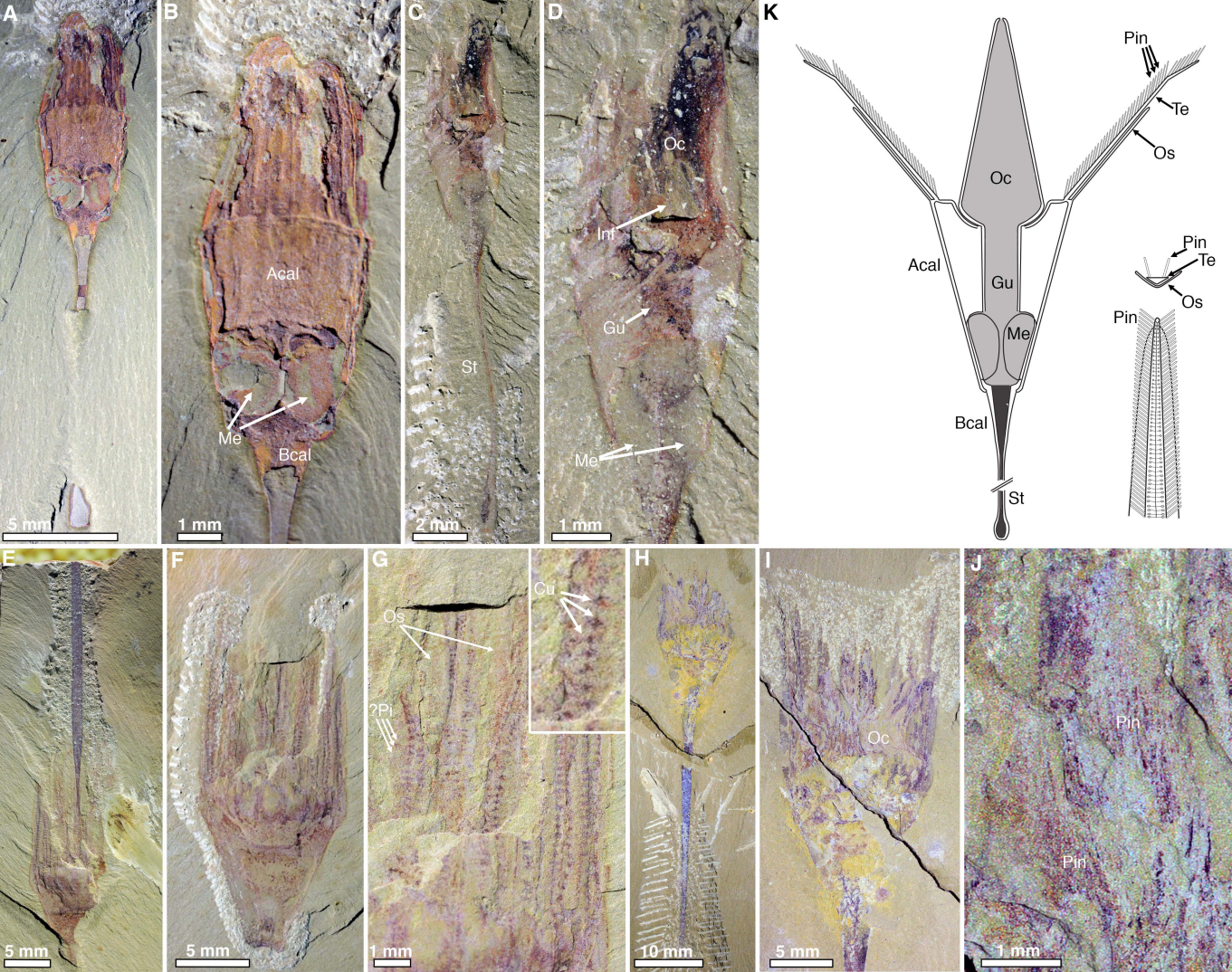
20 21 **Phylogenetic analyses**

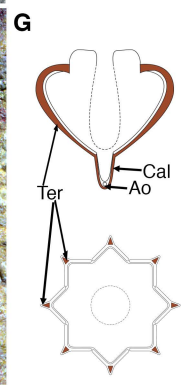
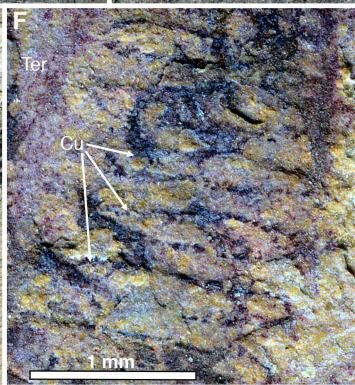
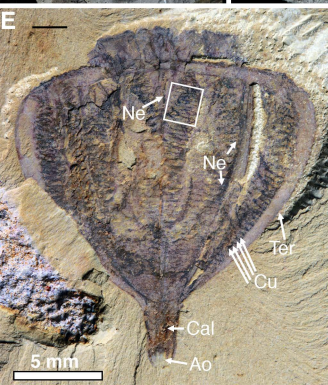
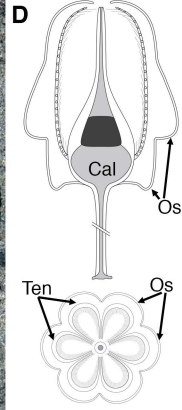
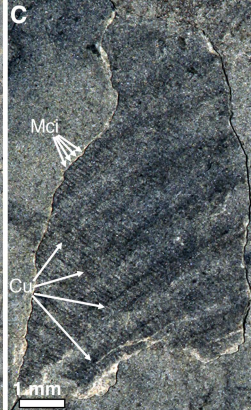
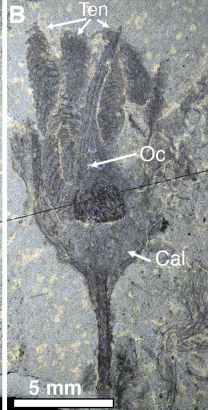
22
23 Morphologic phylogenetic analyses were performed using Bayesian inference under the
24 mkv + gamma model in MrBayes 3.2.6 [67], and under maximum parsimony under equal
25 and implied weighting ($k=10$ and $k=3$) in TNT 1.5 [68, 69]. Bayesian analyses used 15 million
26 generations, and analyses were considered to have converged when the average deviation
27 of split frequencies was <0.01 and ESS scores for all parameters were >200 . Parsimony
28 support values were generated from 1000 replicates of bootstrapping and jackknifing as
29 well as Bremer support for analyses using equal weights. 1000 replicates of symmetric
30 resampling were used for support values for implied weighting at different k values.
31 Additional exploratory analyses not detailed in main text or supplementary figures, such as
32 other implied weighting k values and taxon exclusion experiments, are detailed in the
33 supplementary information.

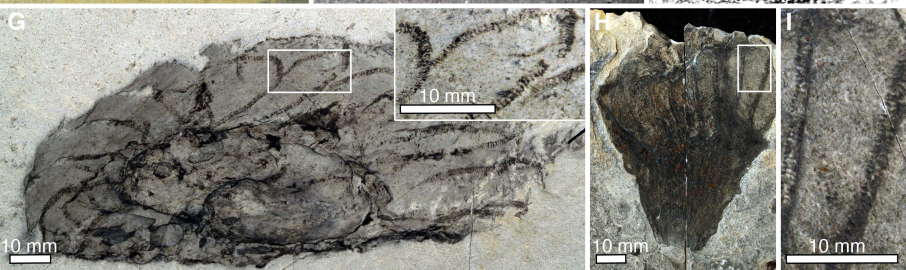
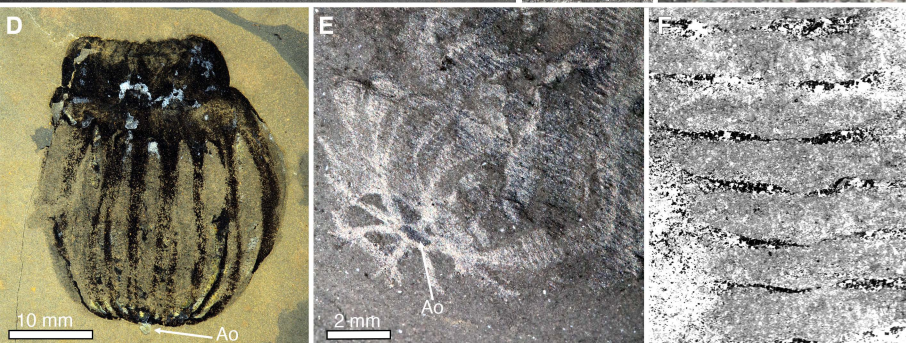
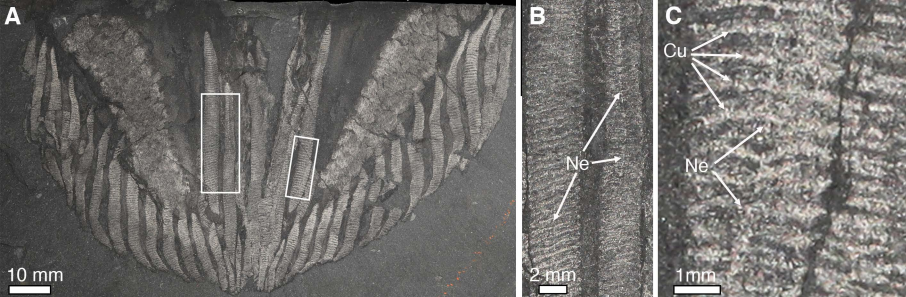
34 35 **Methods S1 - Phylogenetic analysis and character matrix related to Figure 6** 36 **and STAR METHODS**

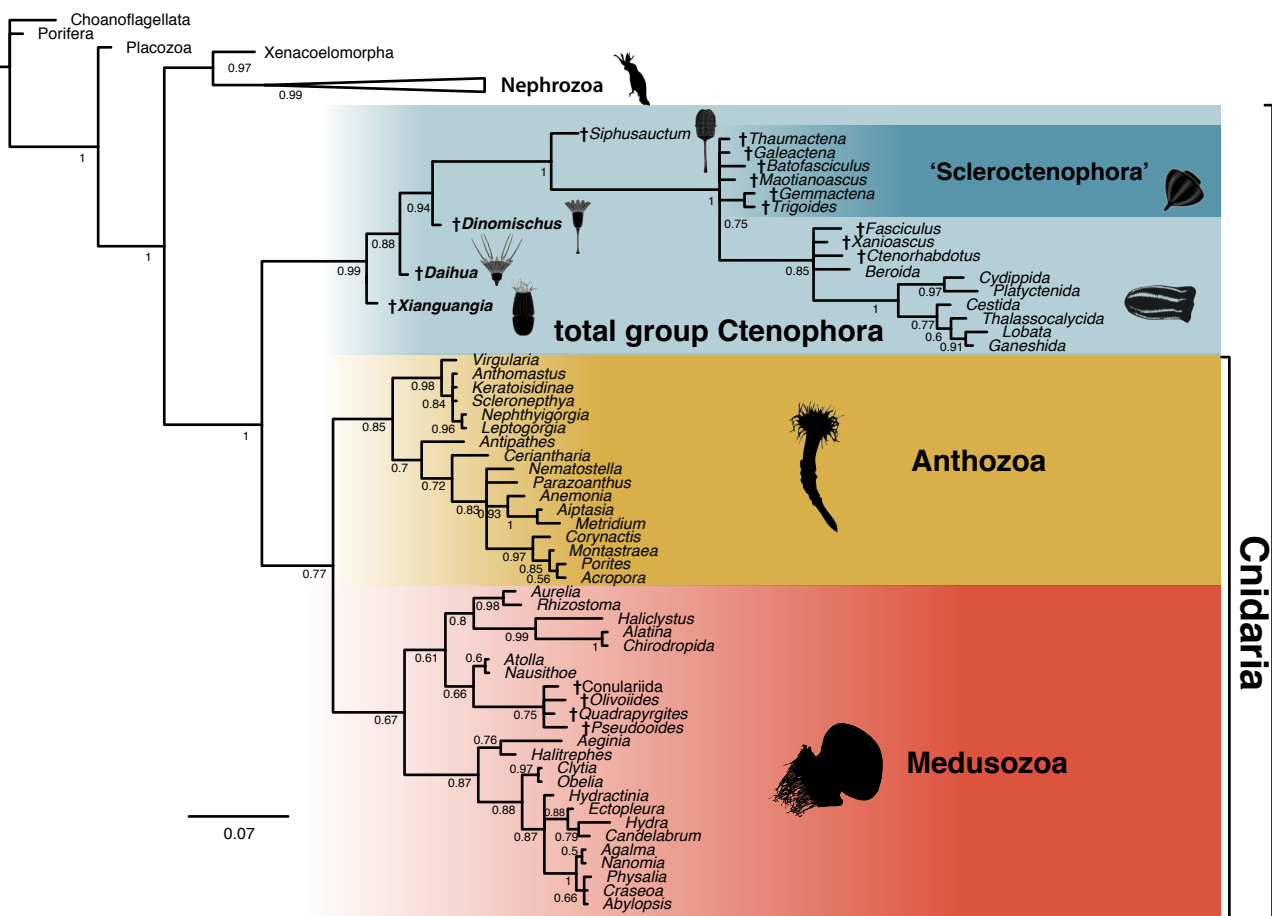






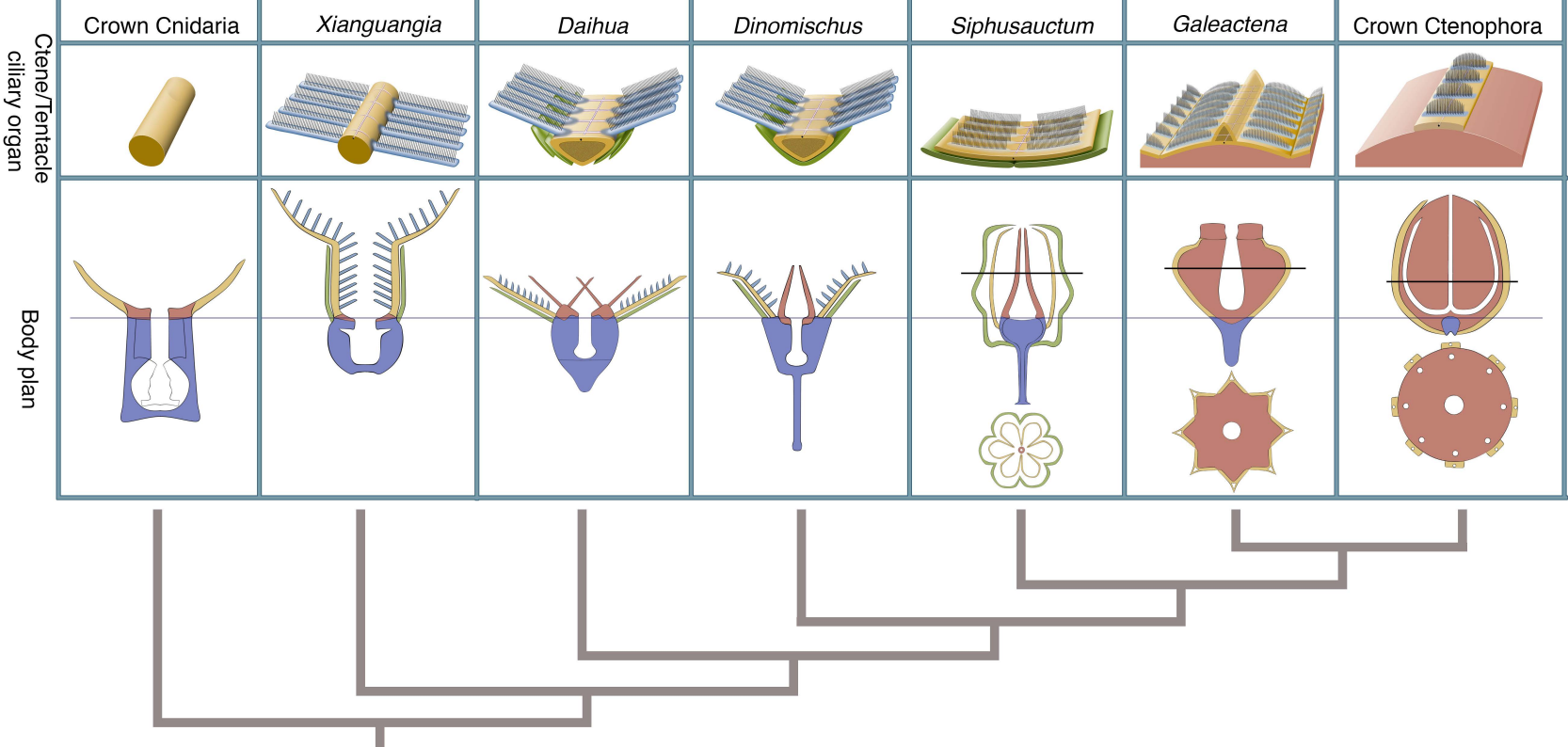






Coelenterata

Cnidaria



Methods S1 - Phylogenetic analysis and character matrix (Related to Figure 6 and STAR Methods)

Our character matrix is modified from a phylum-level matrix of animals that incorporated the genus *Xianguangia* [S1], a matrix consisting of fossil and extant ctenophores [S2], and a character matrix for cnidarians with multiple representatives from the cnidarian classes including candidate ancient cnidarian body fossils [S3]. Changes to these matrices include addition of new and amended morphological observations for *Xianguangia* as well as updates from the published literature and correction of minor coding errors. Characters that were made redundant by new characters were removed from the matrix, as were characters repeated in both [S1] and [S2]. New characters not previously scored in the primary sources for this matrix are marked with an asterisk (*)

Analyses were carried out using maximum parsimony with equal character weights and implied weighting [S4] and using the mk likelihood model in a Bayesian implementation [S5] with four gamma categories used to model rate variation among characters. Our matrix included autapomorphies, so the variable coding correction for the ascertainment bias was used in MrBayes (Iset coding=variable). Consequently only constant characters were excluded from our character matrix during analysis. Parsimony analyses were conducted with equal weights and implied weighting using TNT 1.5 [S4, 6, 7].

Implied weights analyses used concavity values of $k=10$ (following Goloboff, et al. [S7]) and also at a lower concavity value of $k=3$ (frequently used in simulations and other empirical analyses [S8-11]). Results for Bayesian analyses were summarized as a majority rule consensus and parsimony results used the strict consensus. Maximum likelihood analyses were not performed as fully bifurcating trees from morphological data will contain many incorrect nodes [S10] and collapsing poorly supported nodes following bootstrapping recovers trees that are topologically similar to majority rules consensus trees from Bayesian analyses [S12]. Support values for parsimony analyses were generated from 10000 replicates of bootstrapping and jack-knifing as well as Bremer support (for equal weights) and 10000 replicates of symmetric resampling (for implied weights).

We performed two sets of analyses, one that included all taxa scored and another that excluded three fossil taxa (*Sphenothallus*, *Namacalathus* and *Eolympia*). *Sphenothallus* and *Namacalathus* were excluded due to very large amounts of missing data (94 and 95% respectively) and *Eolympia* was excluded as we are unable to exclude the possibility that it represents a juvenile stage of another taxon scored in our matrix (possibly *Daihua*). Results of all analyses recovered *Xianguangia*, *Daihua*, *Dinomischus*, *Siphusauctum* and the Chengjiang scleroctenophores as a paraphyletic grade in the ctenophore stem group. Where included, *Eolympia* and *Namacalathus* were also recovered in the ctenophore stem group, occupying phylogenetic positions proximal to *Daihua* and *Siphusauctum*, respectively.

Sphenothallus collapses Medusozoa to a polytomy in equal weights and Bayesian analyses, but is recovered within the medusozoan crown group in implied weights analyses. This occurs in concert with Hydrozoa becoming paraphyletic, which is not a conventional result for analyses of morphological characters for cnidarians [S13], including the dataset from which our cnidarian characters are derived [S14]. *Sphenothallus* possesses characters that are restricted to Scyphozoa (such as peridermal teeth [S15]) as well as apparent bilateral symmetry, a character that is widespread among anthozoans. *Sphenothallus* has been suggested to occupy a deep position in medusozoan phylogeny [S15], which would require that a polyp-encasing periderm was reduced multiple times during medusozoan evolution.

In all analyses, the dinomischids and *Siphusauctum* form the deepest branches in total-group Ctenophora, subtending a clade of Burgess Shale ctenophores, scleroctenophores and the ctenophore crown group. Support for inclusion of *Xianguangia*, *Daihua* and *Dinomischus* in the ctenophore stem group is high across methods (equal weight bootstrap >89%, implied weight symmetric resampling >86%, posterior probability =1) and the posterior probability of a clade of dinomischids and ctenophores has a posterior probability of 0.98 (full analysis) and 0.94 (reduced taxon sample) in Bayesian analyses.

Our analyses using the full taxon sample recovered beroids in a polytomy with the other extant ctenophores and the Burgess Shale taxa.

Molecular phylogenies place beroids deeply nested in the ctenophore crown group, suggesting that their lack of paired tentacles represents a loss rather than a primitive absence [S16]. When beroids are excluded from the analysis (detailed results not shown), the relationships of the remaining taxa are unchanged and the Burgess Shale ctenophores are recovered as the sister group of extant ctenophores, suggesting that these Cambrian taxa are also members of the stem group, consistent with a relatively late origin of the crown group [S16].

Except where changed by observations detailed in the main paper, our character scores follow those of published matrices. Duplicate characters were identified and omitted and characters that suffer from ‘pseudo-ordering’ [S17] were divided into contingent characters. Character 47 of Ou *et al.* [S1] ‘Separate body cavities in polyps’ was removed, as this character is demonstrably continuous with the digestive tract and is partitioned by mesenteries like the guts of cnidarians. Character 48, ‘Holdfast demarcated by a circumferential constriction’, was likewise removed, as this constriction separates the arms from the body region containing the gastric cavity in *Xianguangia*. Characters for *Eolympia* are scored following [S18].

Character Descriptions

1. Collar complex. Choanoflagellates and the choanocytes of sponges share the presence of a funnel shaped structure composed of microvilli that surround an undulating flagellum. The collar complex is absent in other metazoan groups and uncertain in fossil taxa [S19].

0 absent

1 present

2. Multicellularity with extracellular matrix. ECM is present in sponges and all other animal groups. It is coded as present in Placozoa (following Ou, et al. [S1]) as ECM proteins have been reported from *Trichoplax* [S20]. The included fossil taxa are coded as being multicellular.

0 absent

1 present

3. Septate junctions. Septate junctions are present in all eumetazoan phyla except for vertebrates and ctenophores. Sponges are coded as polymorphic as septate junctions are present only in Calcarea and placozoans are uncertain [S21]. As choanoflagellates lack multicellularity, all cell junction characters (3-6) are coded as inapplicable for choanoflagellates.

0 absent

1 present

4. Tight junctions. These cell junctions are analogous to septate junctions (character 3) but are present only in vertebrates and urochordates [S22].

0 absent

1 present

5. Gap junctions. Gap junctions provide the means for intercellular communication in animals. They are present in most phyla, but are absent in sponges, Placozoa and all cnidarian groups other than Hydrozoa [S23]. Echinoderms lack gap junction proteins [S24]. They have yet to be identified in xenacoelomorphs, which are coded as uncertain as in [S1]

0 absent

1 present

6. Adherens junctions. Adherens junctions/belt desmosomes are present in all animal lineages [S19].

0 absent

1 present

7. Hemidesmosomes. Hemidesmosomes connect epithelial cells to the basal lamina and are present in all animals except all poriferan groups and placozoans [S19].

0 absent

1 present

8. Epithelia.

0 absent

1 present

9. Basal laminae. Basement membranes are present in almost all animal groups, with the exception of all sponges bar homoscleromorphs [S19]. This character is polymorphic in Xenacoelomorpha [S19] and absent in placozoans [S25].

0 absent

1 present

10. Collagen. Collagen is present in all animals, including sponges and placozoans [S20].

0 absent

1 present

11. Nerve cells. Present in all animals with the exception of sponges and placozoans [S19].

0 absent

1 present

12. Acetylcholine used as a neurotransmitter. Present in all bilaterians and ctenophores [S19, S26].

0 absent

1 present

13. Diffuse nervous system. Present in ctenophores and cnidarians [S19] and also Xenacoelomorpha [S27].

0 absent

1 present

14. Hox/ParaHox genes. Present in all animals except ctenophores and sponges [S28].

0 absent

1 present

15. Epidermis with pulsatile bodies. These structures are unique to acoels [S29].

0 absent

1 present

16. Xenacoelomorph cilia. Only in xenacoelomorphs [S30].

0 absent

1 present

17. Diploblasts made of 2 cell layers. We follow Ou *et al.* [S1] in scoring both cnidarians and ctenophores as having a diploblastic level of organization. However this situation has become complicated by the recent proposal that part of the cnidarian endoderm is homologous with the bilaterian mesoderm [S31] and the coding of this character may have to be amended in future. Nevertheless, even if the pharyngeal endoderm of anthozoans represents a homolog of mesoderm, cnidarians are still only made of two cell layers.

0 absent

1 present

18. Triploblasts made of 3 cell layers. Triploblasty is scored as present in all bilaterians. As in character 18, this may have to be adjusted if the conclusions of Steinmetz, et al. [S31] are correct and that the presence of a mesoderm homolog can be generalized to all cnidarians. The presence of triploblasty is scored as contingent on the presence of diploblasty, contra Ou *et al.* [S1].

0 absent

1 present

19. Striated ciliary rootlets. Scored following refs [S23, 30].

0 absent

1 present

20. Spiral cleavage with 4d mesoderm. Spiral cleavage is present in many members of Spiralia (a clade sometimes equated with Lophotrochozoa) with the exception of Gastrotricha, Rotifera, Brachiozoa and Bryozoa, where it is presumed to have been lost or modified [S32].

0 absent

1 present

21. Colloblasts. This cell type is present only in ctenophores with paired tentacles [S19]

0 absent

1 present

22. Coelenteron (gastrovascular cavity). A coelenteron is unique to cnidarians and ctenophores and is present in *Xianguangia*, *Daihua*, *Dinomischus venustus* and *Siphusauctum*.

0 absent

1 present

23. Giant fiber nerve net (GFNN) in medusae

0 absent

1 present

24. Through-gut. No anal opening is identifiable in *Xianguangia*, *Daihua*, *Dinomischus* or *Siphusauctum*. The apical opening in *Siphusauctum* was previously considered an anus [S33], but we consider this unlikely. Although ctenophores have a functional through gut via paired anal pores, we consider these structures as analogous to the bilaterian through-gut and not homologous. Current interpretations of the origin of the bilaterian mouth favour its origination from amphistomy, which is incompatible with an interpretation that the ctenophore anal pores are homologous with a bilaterian anus [S34]

0 absent

1 present

25. U-shaped gut. The presence of a U-shaped gut is contingent on the presence of a through gut.

0 absent

1 present

26. Protonephridia (or homologues)

0 absent

1 present

27. Fate of blastopore. This character is rescored following [S34]

0 protostomy

1 deuterostomy

2 amphistomy

28. Body cuticle with chitin. Taxa lacking this character have been rescored as inapplicable for character 68.

0 absent

1 present

29. Body cuticle with α -chitin

0 absent

1 present

30. Body cuticle molted

0 absent

1 present

31. Segmented body with jointed limbs:

0 absent

1 present

32. Lobopods

0 absent

1 present

33. Slime papillae

0 absent

1 present

34. Telescoping mouth cone with protrudable stylets

0 absent

1 present

35. Respiration via metameric tracheae and spiracles

0 absent

1 present

36. Mixocoel (haemocoel) surrounded by segmented mesoderm

0 absent

1 present

37. Teloblastic segmentation

0 absent

1 present

38. Longitudinal ventral nerve cord(s)

0 absent

1 present

39. Circum-pharyngeal, collar-shaped brain with anterior and posterior rings of perikarya separated by a ring-shaped neuropil. Nematomorphs are recoded as lacking this feature [S35].

0 absent

1 present

40. Introvert with scald rings

0 absent

1 present

41. Flosculi

0 absent

1 present

42. Immunoreactivity of horseradish peroxidase (HRP)

0 absent

1 present

43. Feeding strategy in tentaculate metazoans

0 predominantly micro

1 predominantly macro

44. Trochophores. In addition to the taxa scored in Ou *et al.* [S1], a trochophore larva is also present in some Platyhelminthes [S36].

0 absent

1 present

45. Segmental metanephridia sacculus

0 absent

1 present

46. Chitinous microvillar appendages (chaetae). Chaetae are scored as present in brachiopods, annelids and bryozoans [S37, S38]. They are also scored as present in molluscs, as they are present in stem-group molluscs, as well as aculiferans and some certain conchiferans so we likely present in the last common ancestor of molluscs [S39].

0 absent

1 present

47. Parapodia with dorsal and ventral branches terminated by β -chitinous chaetae

0 absent

1 present

48. Radula

0 absent

1 present

49. Eversible proboscis surrounded by rhynchocoel

0 absent

1 present

50. Complex jaw apparatus in pharynx. Although this was only coded as present in Gnathifera by Ou, et al. [S1], the grasping spines of chaetognaths are possibly homologous to the jaws of gnathiferans [S40].

0 absent

1 present

51. Origin of mesoderm

0 from the blastopore lips and as ectomesoderm

1 from the walls of the archenteron or neural crest

52. Radial cleavage

0 absent

1 present

53. Coelom formation

0 schizocoely

1 enterocoely

54. Trimeric coelom

0 absent

1 present

55. Pharyngeal slits

0 absent

1 present

56. Endostyle (or homologues)

0 absent

1 present

57. Notochord

0 absent

1 present

58. Stomochord

0 absent

1 present

59. Haemal system with axial complex

0 absent

1 present

60. Calcareous endoskeleton composed of separate ossicles

0 absent

1 present

61. Tornaria type larva

0 absent

1 present

62. Longitudinal dorsal nerve cord

0 absent

1 present

63. Zig zag myomeres

0 absent

1 present

64. Endothelium that lines the inner wall of blood vessels

0 absent

1 present

65. Neural crest

0 absent

1 present

66. Neurogenic placodes

0 absent

1 present

67. Dorsoventral axis. The dorsoventral axis and anterior-posterior axis (character 68) are herein considered characters that are unique to bilaterians including Xenacoelomorpha despite the presence of bilateral symmetry in cnidarians [S41-43].

0 absent

1 present

68. Anterior posterior axis

0 absent

1 present

69. Symmetry.

0 bilateral

1 biradial

2 triradial

3 tetraradial

4 pentaradial

5 hexaradial

70. Compression in pharyngeal plane. Characters 70-72 were originally coded as a single character by Ou *et al* (2015). Given some ctenophores have body compression in multiple planes (suggesting independence) this has been expanded into three independent characters (characters 70-72).

0 absent

1 present

71. Compression in oral-aboral axis

0 absent

1 present

72. Compression in tentacular plane

0 absent

1 present

73. Mesoglea

0 absent

1 present

74. Cydippid larvae

0 absent

1 present

75. Ciliary rosettes

0 absent

1 present

76. Lophophore

0 absent

1 present

77. Radially-arranged outgrowths from the interface between the oral and aboral regions. The circumoral extensions of cnidarians (tentacles), dinomischids, *Siphusauctum* and the comb rows of ctenophores are scored as primary homologs. As we propose that ctenes and cnidarian tentacles are end members of this character system, this character is referred to as the ctene/tentacle organ or radial outgrowths.

0 absent

1 present

78. Radial outgrowths fixed in globular configuration*. In extant ctenophores, scleroctenophores, *Siphusauctum* and the ctenophores from the Burgess Shale, the ctene/tentacle organs are arranged in a globular configuration directed towards the mouth. In *Siphusauctum* these structures retain their tentacular morphology and are held in a cavity between the outer sheaths and the oral cone, while they are carried on the oral cone surface in extant ctenophores, scleroctenophores and Burgess ctenophores.

0 absent

1 present

79. Radial outgrowths tentacular*. In cnidarians, dinomischids and *Siphusauctum*, the radially arranged outgrowths form discrete tentacles.

0 absent

1 present

80. Outgrowths with pinnules*. Pinnulae clad with cilia extend from the tentacles in *Xianguangia*, *Dinomischus* and *Daihua*. In *Siphusauctum* the cilia lie on a continuous structure rather than on pinnulae. Many octocorals also possess tentacles with serial branches these taxa are likewise scored as having pinnules as per character 133 in ref [S3].

0 absent

1 present

81. Outer sheaths on external surface of radial outgrowths. A stiff membrane lies on the external surface of the ctene/tentacle organs in dinomischids, *Dinomischus venustus* and *Siphusauctum*.

0 absent

1 present

82. Outgrowths with ciliary rows*. Serialised rows of cilia are present on the ctene/tentacle organs of dinomischids, *Siphusauctum* and ctenophores. Although structures that represent the comb rows are present in many fossil

ctenophores (including scleroctenophores) the cilia themselves are not preserved and so this character is scored as uncertain in these taxa.

0 absent

1 present

83. Cushion rings/plates or polster cells*. In ctenophores the cilia of the comb rows are carried on cushions of specialized cells (polster cells). Although the cilia are often not preserved in fossil ctenophores, the underlying cells are preserved as dark structures (e.g. in the Burgess Shale taxon *Fasciculus*). Such dark structures are also preserved underlying the pinnulae and cilia in dinomischids and *Siphusauctum* but are absent in *Xianguangia*.

0 absent

1 present

84. Cushion rings paired*. In scleroctenophores the comb rows and the underlying cushion plates are paired either side of the skeletal elements that follow the oral-aboral axis. This paired condition is also present in dinomischids and *Siphusauctum*.

0 paired

1 unpaired

85. Ciliary rows paired *. In *Xianguangia*, *Dinomischus*, *Daihua* and *Siphusauctum* the cilia are preserved and occur in paired rows along the ctene/tentacle organs. This character cannot be scored for fossil ctenophores as the cilia are not preserved.

0 paired

1 unpaired

86. Large compound cilia*. Although the ctene organs are preserved in fossil ctenophores from Chengjiang and the Burgess Shale, the cilia have not yet been observed, possibly due to the low number of specimens preserving soft anatomy in addition to the likely mode of splitting perpendicular to the ctene

organs. The compound ciliary organs in the dinomischids also better conform to macrociliary organs with compound cilia held in a single enclosing membrane [S1] rather than individual membranes as in crown group ctenophore ctenes. This may also have taphonomic implications. Consequently, this character is coded as uncertain. The cilia observed in dinomischids and living ctenophores exceed the size known from elsewhere in the animal kingdom (see main text for discussion).

0 absent

1 present

87. Large cilia fused to form locomotory plate*. In extant ctenophores the comb rows are partly fused to form plates for locomotion. Although cilia not visible in taxa proximal to the crown, in dinomischids, *Siphusauctum* and *Xianguangia* the cilia are clearly delimited from each other, not forming a structure like the locomotory cilia of extant ctenophores.

0 absent

1 present

88. Orientation of ciliary rows relative to oral-aboral axis*. In *Xianguangia*, *Dinomischus*, *Daihua* and *Siphusauctum* the cilia face inwards, towards the body axis. In crown-group ctenophores, scleroctenophores and taxa from the Burgess Shale, the ciliary rows face outwards.

0 adaxial

1 abaxial

89. Uniformity of ciliary rows

0 uniform

1 non-uniform

90. Number of ciliary rows/ctenes. The number of comb rows is highly variable among fossil taxa.

0 eight

1 eighteen

2 six

3 twenty-four

4 circa 80

91. Extension of the oral surface to form oral cone*. In *Siphusauctum*, *Dinomischus* and extant ctenophores, the mouth forms an elongated oral cone to which the arms attach in *Siphusauctum*.

0 absent

1 present

92. Aboral region represented only by apical organ*. In extant ctenophores, scleroctenophores and taxa from the Burgess Shale the aboral region forms a distinct apical organ. The apical region is represented by the basal pit or stalk in dinomischids and *Siphusauctum* and consequently it is scored absent in these taxa.

0 absent

1 present

93. Aboral region forming narrow pointed extension*. In scleroctenophores the apical region forms a distinct, narrow pointed extension that is covered by a skeleton continuous with comb rows. Among scleroctenophores this extension is absent only in *Maotianoascus* and is likewise absent in the Burgess Shale taxa. Our analysis optimizes this character as a synapomorphy of a subclade of scleroctenophores (i.e. all taxa except *Maotianoascus*).

0 absent

1 present

94. Gut extending into aboralmost body region*. In dinomischid taxa, the gut occupies the entire aboral region (calyx) which is demonstrated by a radial infill.

0 absent

1 present

95. Stalk extending from apical/aboral region in polyp*. An elongate stalk is present in *Dinomischus* and *Siphusauctum* and some cnidarians [S33, 44].

0 absent

1 present

96. Oral macrocilia

0 absent

1 present

97. Oral lobes

0 absent

1 present

98. Morphology of tip of oral extension

0 narrow

1 voluminous

2 manubrium-like

3 margin of creeping sole

99. Mouth as margin of creeping sole

0 absent

1 present

100. Pharyngeal ridges

0 absent

1 present

101. Sealing ridges of pharynx

0 absent

1 present

102. Macrocilia on pharynx lining inside of mouth

0 absent

1 present

103. Ciliary dome

0 absent

1 present

104. Statolith

0 absent

1 present

105. Balancers

0 absent

1 present

106. Pole plates

0 absent

1 present

107. Aboral papillae

0 absent

1 present

108. Ciliary grooves/ctene axons. The black linear structures running between paired comb rows or underlying unpaired comb rows in fossil ctenophores and dinomischids are interpreted as the ciliary groove, which is part of the nerve system. In extant *Euplokamis*, this is a well-developed axon, comparable in dimensions to that in fossils from the Burgess Shale [S45].

0 absent

1 present

109. Interplate ciliary groove (ICG)

0 absent

1 present

110. Pharyngeal canals

0 absent

1 present

111. Tentacular canals

0 absent

1 present

112. Meridional canals

0 absent

1 present

113. Diverticula of meridional canals

0 absent

1 present

114. Circumoral ring canal

0 absent

1 present

115. Termination of meridional and pharyngeal canals

0 both terminate blindly

1 branch to form a complex network

2 united with the circumoral ring canal

116. Interradial canals

0 absent

1 two

2 four

117. Adradial canals

0 directly branch from the infundibulum

1 branch from interradian canals

118. Aboral canal

0 absent

1 present

119. Anal canals

0 absent

1 present

120. Anal pores

0 absent

1 present

121. Paired ctenophore tentacles

0 absent

1 present

122. Tentilla

0 absent

1 present

123. Disposition of tentilla

0 absent

1 present

124. Tentacle sheaths

0 absent

1 present

125. Opening position of tentacles

0 orally

1 aborally

126. Auricles

0 absent

1 present

127. Brood chambers

0 absent

1 present

128. Sclerotised arms and calyx*. A unique organic skeleton in *Dinomischus*, *Daihua* and also *Xianguangia*, (in addition to its previously recognised occurrence in scleroctenophores [S2]) occurs as a supporting structure along the radial outgrowths (comb rows or tentacles) and also supports the apical rows or tentacles. The sclerotisation of the radially arranged compound cilium bearing structures distinguishes this skeleton from other skeletal structures in cnidarians (e.g. characters 272-274, 277).

0 absent

1 present

129. Tentacles extending beyond skeletal rods and outer sheaths*. In *Daihua* and *Xianguangia*, the distal tips of the ctene/tentacle organs extend beyond the skeleton. In *Dinomischus* and *Siphusauctum* the termination of the tentacle is coincident with the outer sheaths and skeleton (where applicable).

0 absent

1 present

130. Medial structures of skeletal elements

0 absent

1 present

131. Kinked spokes

0 absent

1 present

132. Spinose spokes

0 absent

1 present

133. Radiating flaps/lobes

0 absent

1 present

134. Oral structure separated by circumferential constriction

0 absent

1 present

135. Constriction type

0 skirt or bell

1 lappets

Characters 136-278 are scored following Duan *et al.* [S3] and modifications to codings are noted where applicable.

136. Mesoglea cellularity

0 non-cellular

1 cellular

137. Extracellular digestion

0 absent

1 present

138. Ostia with porocytes

0 absent

1 present

139. Embryonic development

0 direct

1 indirect

140. Cnidae

0 absent

1 present

141. Cnidae in gastrodermis

0 absent

1 present

142. Cnidocil

0 absent

1 present

143. Structure of mitochondrial DNA

0 circular

1 linear

144. Actinopharynx. We have scored the presence of an actinopharynx in *Dinomischus* and *Daihua* as the septate portion of the gut is connected to the mouth by a cylindrical structure resembling the actinopharynx of anthozoans.

0 absent

1 present

145. Siphonoglyph (sulcus)

0 absent

1 present

146. Circular depression on basal disc

0 absent

1 present

147. Giant fibre nerve net (GFNN) in medusae

0 absent

1 present

148. Stenoteles

0 absent

1 present

149. Euryteles

0 absent

1 present

150. Desomonemes

0 absent

1 present

151. Mastigophores

0 absent

1 present

152. Basitrichousisorhizas

0 absent

1 present

153. Apotrichousisorhizas

0 absent

1 present

154. Isorhizas

0 absent

1 present

155. Heterotrichousanisorhizas

0 absent

1 present

156. Birhopaloids

0 absent

1 present

157. Rhopalonemes

0 absent

1 present

158. Spirocyst

0 absent

1 present

159. Ptychocyst

0 absent

1 present

160. Periderm

0 absent

1 present

161. Cuticle layers in periderm

0 one

1 two

162. Chitin expression

0 restricted to a basal area or to podocysts

1 forming a tube

2 forming a thin cuticle

163. Tube extension

0 tube encases polyp

1 tube does not encase polyp

164. Periderm type

0 corneous

1 coriaceous

165. Location of medusa formation

0 lateral budding from an entocodon

1 apical or oral

2 direct development without polyp stage

166. Type of apical medusa formation

0 strobilation

1 without transverse fission

167. Strobilation type

0 polydisk

1 monodisk

168. Propagation through lateral budding

0 absent

1 present

169. Oocyte development

0 oocytes develop without accessory cells

1 oocytes develop with accessory cells

2 oocytes develop within follicles

3 oocytes develop from uptake of somatic or other germ line cells

170. Nectosome

0 absent

1 present

171. Pneumatophore

0 absent

1 present

172. Planula

0 absent

1 present

173. Planula ciliation

0 absent

1 present

174. Number of endodermal cells of the planula

0 absent

1 present

175. Glandular cells in the planula

0 absent

1 present

176. Nerve cells in the planula

0 absent

1 present

177. Relationship between axes of planula and adult

0 oral-aboral axis in the adult derived from the longitudinal axis of the planula

1 oral-aboral axis in the adult derived from the transverse axis of the planula

178. Polypoid phase

0 absent

1 present

179. Polyp organization

0 solitary

1 colonial

180. Polymorphic polyps

0 absent

1 present

181. Number of tentacular whorls

0 one

1 two or more

182. Gut partitioned by septa. We have scored a single character for the presence of gastric septa regardless of which stage of the life cycle this character occurs in, with dependent characters (184 and 185) for the presence of septa in the medusa and polyp phases. This is primarily to establish character polarity, as scoring independent characters for the polyp and medusa phases would necessitate scoring both characters as absent for all non polypoid/medusa forming taxa (i.e. all outgroups such as bilaterians).

0 absent

1 present

183. Septa in polyp*. We consider dinomischids to have a polypoid organization and consequently have scored polyp gastric septa as present in *Dinomischus* and *Xianguangia*. *Siphusauctum* does not appear to have a partitioned gastric cavity and we do not have sufficient material of *Daihua* preserved in lateral view to determine the presence (or otherwise) of this character. *Eolympia* unambiguously possesses a radially partitioned gut [S18].

0 absent

1 present

184. Septa in medusa

0 absent

1 present

185. Mesoglea in polyp septa

0 absent

1 present

186. Pairing of mesentery

0 paired

1 coupled

187. Mesentery pair morphology

0 members the same size

1 members differ in size

188. Paired secondary cycle

0 absent

1 present

189. Mesenterial fusion

0 absent

1 present

190. Number of perfect mesenteries

0 eight

1 ten

2 more than twelve

191. Types of mesentery

0 only perfect mesenteries

1 perfect mesenteries not divisible

2 perfect mesenteries and imperfect mesenteries divisible

192. Directive mesentery

0 absent

1 present

193. Number of directive mesentery pairs

0 one pair

1 two pairs

194. Mesentery formation

0 only primary tentacles

1 new septa arise in the exocoel to either side of the ventral directive

2 from ventral

3 between directive and transverse septa

4 anywhere around the circumference

195. Structure of polyp tentacles

0 hollow

1 solid

196. Type of tentacles

0 one type

1 two types

197. Clustered tentacles

0 absent

1 present

198. Two-tentacle polyp stage

0 absent

1 present

199. Siphonoglyph

0 absent

1 present

200. Number of siphonoglyphs

0 one

1 more than one

201. Mesenteric filament

0 two strips

1 three strips

2 one strip

202. Ridges

0 absent

1 present

203. Embryonic stage retained in the tube morphology

0 absent

1 present

204. Tentacles retractile

0 non retractile

1 retractile

205. Tentacle/coelenteron relationship

0 one tentacle per endocoel and per exocoel

1 one tentacle per exocoel, multiple per endocoel

206. Catch tentacles

0 absent

1 present

207. Arrangement of tentacles

0 scattered

1 one cycle

2 more than one cycle

208. Acrospheres

0 absent

1 present

209. Number of tentacles in polyp. The original formulation of this character [S14] only allowed for the presence of six, eight or more than nine tentacles. We have increased the number of characters to capture the shared presence of 18 tentacles in dinomischids and *Eolympia*.

0 six

1 eight

2 twelve

- 3 sixteen
- 4 eighteen
- 5 more than twenty

210. Marginal spherules

- 0 absent
- 1 holotrichous

211. Acontia

- 0 absent
- 1 present

212. Gonads on mesenteries of 1st cycle

- 0 absent
- 1 present

213. Gonads on mesenteries of second and subsequent cycles

- 0 absent
- 1 present

214. Mesogloal sphincter

- 0 absent
- 1 present

215. Ectodermal longitudinal muscle location

- 0 tentacles and oral disc only
- 1 whole body

216. Basilar musculature

- 0 absent
- 1 present

217. Retractor muscle

0 weak
1 defined

218. Parietal muscle

0 absent
1 present

219. Mesogloea lacunae

0 absent
1 present

220. Acrorhagi

0 absent
1 present

221. Pedal disk

0 absent
1 present

222. Ciliated tract on mesenteric filament

0 absent
1 present

223. Ephyrae

0 absent
1 present

224. Actinula

0 absent
1 present

225. Organisation of the nervous system in polyp

0 nets
1 with nerve rings

226. Canal system

0 absent

1 present

227. Gastrodermic musculature

0 not in bunches

1 organised in bunches of gastrodermal origin

2 organised in bunches of ectodermal origin

228. Medusoid phase

0 absent

1 present

229. Pedalium of coronate type

0 absent

1 present

230. Rhopalia/rhopalioids

0 absent

1 present

231. Complex eyes in rhopalia

0 absent

1 present

232. Nerve ring in medusa. This character was previously pseudo-ordered [S17] in the original matrix [S3] and so has been divided into two characters (233 and 234).

0 absent

1 present

233. Number of rings in nerve ring

0 one

1 two

234. Gastric filaments

0 absent

1 present

235. Coronal muscle

0 well-developed

1 marginal and tiny

236. Pedalium of the cubozoan type

0 absent

1 present

237. Velum

0 absent

1 present

238. Umbrellar margin

0 smooth and continuous

1 lobed

239. Tentacles in medusa

0 absent

1 present

240. Tentacular bulbs

0 absent

1 present

241. Statolith composition

0 MgCaPO_4

1 CaSO_4

242. Septal shape in medusa

0 straight

1 y shaped

243. Radial canals

0 absent

1 present

244. Circular canal. This character was previously pseudo-ordered [S17] in the original matrix [S14] and so has been divided into two characters (245 and 246).

0 absent

1 present

245. Circular canal partial

0 absent

1 present

246. Velarium

0 absent

1 present

247. Coronal furrow

0 absent

1 present

248. Gonadal location

0 manubrium

1 radial canals

249. Statocysts. This character was previously pseudo-ordered [S17] in the original matrix [S14] and so has been divided into two characters (250 and 251).

0 absent

1 present

250. Statocyst location

0 endodermic

1 ectodermic

251. Perradial mesenteries

0 absent

1 present

252. Adult medusoid shape

0 bell

1 pyramidal

2 cubic

3 actinuloid

253. Shape of horizontal cross-section of the medusa

0 circular

1 four-part symmetry

254. Urticant rings

0 absent

1 present

255. Oral arms with suctorial mouths

0 absent

1 present

256. Tentacular insertion

0 at umbrellar margin

1 away from margin

257. Manubrium

0 absent

1 present

258. Nervous system organisation

0 GFNN absent

1 GFNN present

259. Structure of medusa tentacles

0 hollow

1 solid

260. Tentacular morphology

0 straight

1 with angular inflection

261. Peronia

0 absent

1 present

262. Ocelli in medusa

0 absent

1 present

263. Peripheral system

0 absent

1 present

264. Umbrellar furrow

0 absent

1 present

265. Development of the umbrella

0 fully developed

1 aboral cone

266. Number of tentacular whorls

0 one whorl

1 two whorls

267. Velar canals

0 absent

1 present

268. Frenulae

0 absent

1 present

269. Shape of medusa tentacles

0 filiform

1 capitate

270. Zooxanthellae

0 absent

1 present

271. Ectodermal skeleton. This character aims to differentiate taxa that produce their hard parts using their ectoderm from cnidarians, which use their mesoglea to precipitate their skeletons (character 273). This is distinguished from the skeleton of dinomischids and scleroctenophores as the skeleton in those fossil taxa is unique in supporting the tentacles/ciliary organs as well as the entire calyx and stalk region (when present).

0 absent

1 present

272. Composition of ectodermal skeleton

0 proteinaceous

1 calcitic

273. Mesogleal skeleton. This character refers to the skeletons of octocorals, which is formed in the mesoglea and includes spicules. This is distinguished from the skeleton of dinomischids and scleroctenophores, which is unique in supporting the tentacles and forming a continuous skeleton in the calyx/aboral region. Although octocorals also have skeletal elements in the tentacles (spicules, character 277), the tentacles of dinomischids are supported by a continuous skeletal element which may be augmented with stiff membranes (the outer sheaths). The dinomischid/scleroctenophore organic skeleton does appear to be internally secreted and held, which would make it mesogleal.

0 absent

1 present

274. Columella

0 absent

1 present

275. Costae

0 absent

1 present

276. Octocorallian spicules

0 absent

1 present

277. Spicules in tentacle

0 absent

1 present

278. Gorgonin

0 absent

1 present

Character Matrix in NEXUS Format

#NEXUS

BEGIN TAXA;

TITLE Taxa;

DIMENSIONS NTAX=93;

TAXLABELS

Choanoflagellata Porifera Placozoa Xianguangia Daihua

'Dinomisclus_venustus' Siphosauclum Namacalathus Eolymphia Fasciculus

Xanioascus Ctenorhabdotus Gemmactena Thaumactena Galeactena

Batofasciculus Maotianoascus Trigoides Cydippida Lobata Beroida

Platyctenida Cestida Ganeshida Thalassocalycida Bryozoa Brachiopoda

Phoronida Mollusca Annelida Echinodermata Pterobranchia Chaetognatha

Onychophora Arthropoda Nemertea Enteropneusta Urochordata

Cephalochordata Vertebrata Entoprocta Nematoda Nematomorpha Priapulida

Gastrotricha Tardigrada Kinorhyncha Loricifera Gnathifera Xenacoelomorpha

Platyhelminthes sphenothallus Conulariida Olivoiides Quadrapyrgites

Pseudoooides Nematostella Anemonia Aiptasia Metridium Antipathes

Ceriantharia Corynactis Montastraea Porites Acropora Parazoanthus

Anthomastus Keratoisidinae Nephthyigorgia Leptogorgia Scleronephthya

Virgularia Haliclystus Alalina Chirodropida Atolla Nausithoe Aurelia

Rhizostoma Hydra Candelabrum Hydractinia Ectopleura Clytia Obelia

Physalia Craseoa Abylopsis Agalma Nanomia Aeginia Halitrephes

;

END;

BEGIN CHARACTERS;

TITLE 'Matrix';

LINK TAXA = Taxa;

DIMENSIONS NCHAR=278;

FORMAT DATATYPE = STANDARD GAP = - MISSING = ?

SYMBOLS = " 0 1 2 3 4 5 6";

CHARSTATELABELS

- 1 Collar_complex / absent present,
- 2 Multicellularity_with_extracellular_matrix / absent present,
- 3 'Septate junctions (SJs)' / absent present,
- 4 'Tight junctions (TJs)' / absent present,
- 5 'Gap junctions (GJs)' / absent present,
- 6 'Adherens junctions (AJs)' / absent present,
- 7 Hemidesmosomes / absent present,
- 8 Epithelia / absent present,
- 9 Basal_laminae / absent present,
- 10 Collagen / absent present,
- 11 Nerve_cells / absent present,
- 12 Acetylcholine_used_as_a_neurotransmitter / absent present,
- 13 Diffuse_nervous_system / absent present,
- 14 'Hox/ParaHox gene' / absent present,
- 15 Epidermis_with_pulsatite_bodies / absent present,
- 16 Xenacoelomorph_cilia / absent present,
- 17 diploblasts_made_of_2_cell_layers / absent present,
- 18 triploblasts_made_of_3_cell_layers / absent present,
- 19 Striated_ciliary_rootlets / absent present,
- 20 Spiral_cleavage_with_4d_mesoderm / absent present,
- 21 Colloblasts / absent present,
- 22 'Coelenteron (gastrovascular cavity)' / absent present,
- 23 'Giant fiber nerve net (GFNN) in medusae' / absent present,
- 24 'Through-gut' / absent present,
- 25 'U-shaped gut' / absent present,
- 26 'Protonephridia (or homologues)' / absent present,
- 27 Fate_of_blastopore / protostomy deuterostomy amphistomy,
- 28 Body_cuticle_with_chitin / absent present,
- 29 'Body cuticle with ?-chitin' / absent present,
- 30 Body_cuticle_molted / absent present,
- 31 'Segmented body with jointed limbs:' / absent present,
- 32 Lobopods / absent present,
- 33 Slime_papillae / absent present,

34 Telescoping_mouth_cone_with_protrudable_stylets / absent present,

35 Respiration_via_metameric_tracheae_and_spiracles / absent present,

36 'Mixocoel (haemocoel) surrounded by segmented mesoderm' / absent present,

37 Teloblastic_segmentation / absent present,

38 'Longitudinal ventral nerve cord(s)' / absent present,

39 'Circum-pharyngeal, collar-shaped brain with anterior and posterior rings of perikarya separated by a ring-shaped neuropil' / absent present,

40 Introvert_with_scalid_rings / absent present,

41 Flosculi / absent present,

42 'Immunoreactivity of horseradish peroxidase (HRP)' / absent present,

43 Feeding_strategy_in_tentaculate_metazoans / predominantly_micro predominantly_macro,

44 'Trochophores:' / absent present,

45 Segmental_metanephridia_sacculus / absent present,

46 chitinous_microvillar_appendages / absent present,

47 'Parapodia with dorsal and ventral branches terminated by ?-chitinous chaetae' / absent present,

48 Radula / absent present,

49 Eversible_proboscis_surrounded_by_rhynchocoel / absent present,

50 Complex_jaw_apparatus_in_pharynx / absent present,

51 Origin_of_mesoderm / from_the_blastopore_lips_and_as_ectomesoderm from_the_walls_of_the_archenteron_or_neural_crest,

52 Radial_cleavage / absent present,

53 Coelom_formation / schizocoely enterocoely,

54 Trimeric_coelom / absent present,

55 Pharyngeal_slits / absent present,

56 'Endostyle (or homologues)' / absent present,

57 Notochord / absent present,
 58 Stomochord / absent present,
 59 Haemal_system_with_axial_complex / absent present,
 60 Calcareous_endoskeleton_composed_of_separate_ossicles
 / absent present,
 61 Tornaria_type_larva / absent present,
 62 Longitudinal_dorsal_nerve_cord / absent present,
 63 Zig_zag_myomeres / absent present,
 64 Endothelium_that_lines_the_inner_wall_of_blood_vessels /
 absent present,
 65 Neural_crest / absent present,
 66 Neurogenic_placodes / absent present,
 67 Dorsoventral_axis / absent present,
 68 anterior_posterior_axis / absent present,
 69 symmetry / bilateral biradial triradial tetraradial pentaradial
 hexaradial,
 70 compression_in_pharyngeal_plane / absent present,
 71 compression_in_oral_aboral_axis / absent present,
 72 compression_in_tentacular_plane / absent present,
 73 Mesoglea / absent present,
 74 Cydippid_larvae / absent present,
 75 Ciliary_rosettes / absent present,
 76 Lophophore / absent present,
 77 'Radially-arranged outgrowths from the interface between the
 oral and aboral regions' / absent present,
 78 radial_outgrowths_fixed_in_globular_configuration / absent
 present,
 79 radial_outgrowths_tentacular / absent present,
 80 outgrowths_with_pinnules / absent present,
 81 outer_sheaths_on_external_surface_of_radial_outgrowths /
 absent present,
 82 outgrowths_with_ciliary_rows / absent present,
 83 cushion_rings_or_polster_cells / absent present,
 84 cushion_rings_paired / paired_unpaired,

85 Ciliary_rows_paired / paired unpaired,
 86 large_compound_cilia / absent present,
 87 large_cilia_fused_to_form_locomotory_plate / absent
 present,
 88 orientation_of_ciliary_rows / adaxial abaxial,
 89 Uniformity_of_ciliary_rows / uniform non_uniform,
 90 Number_of_ciliary_rows / eight eighteen six twenty_four
 circa_80,
 91 extension_of_the_oral_surface_to_form_oral_cone / absent
 present,
 92 aboral_region_represented_only_by_apical_organ / absent
 present,
 93 apical_organ_forming_narrow_pointed_extension / absent
 present,
 94 gut_extending_into_aboralmost_body_region_ / absent
 present,
 95 'stalk extending from apical/aboral region in polyp' / absent
 present,
 96 Oral_macroscilia / absent_present,
 97 Oral_lobes / absent present,
 98 morphology_of_tip_of_oral_extension / narrow voluminous
 manubrium_like s_margin_of_creeping_sole,
 99 mouth_as_margin_of_creeping_sole / absent present,
 100 Pharyngeal_ridges / absent present,
 101 Sealing_ridges_of_pharynx / absent present,
 102 Macroscilia_on_pharynx_lining_inside_of_mouth / absent
 present,
 103 Ciliary_dome / absent_present,
 104 Statolith / absent present,
 105 Balancers / absent 'present ',
 106 Pole_plates / absent 'present ',
 107 Aboral_papillae / absent 'present ',
 108 Ciliary_grooves / absent 'present ',
 109 'Interplate ciliary groove (ICG)' / absent 'present '

110 Pharyngeal_canals / absent 'present',
 111 Tentacular_canals / absent 'present',
 112 Meridional_canals / absent 'present',
 113 Diverticula_of_meridional_canals / absent 'present',
 114 Circumoral_ring_canal / absent 'present',
 115 Termination_of_meridional_and_pharyngeal_canals /
 Both_terminate_blindly branch_to_form_a_complex_network
 united_with_the_circumoral_ring_canal,
 116 Interradial_canals / absent two four,
 117 Adradial_canals / Directly_branch_from_the_infundibulum
 Branch_from_interradial_canals,
 118 Aboral_canal / absent present,
 119 Anal_canals / absent present,
 120 Anal_pores / absent present,
 121 Paired_ctenophore_Tentacles / absent present,
 122 Tentilla / absent present,
 123 Disposition_of_tentilla / absent present,
 124 Tentacle_sheaths / absent present,
 125 Opening_position_of_tentacles / orally aborally,
 126 Auricles / absent present,
 127 Brood_chambers / absent present,
 128 'Skeletal elements (sclerotised arms and calyx)' / absent
 present,
 129
 tentacles_extending_beyond_skeletal_rods_and_outer_sheaths / absent
 present,
 130 Medial_structures_of_skeletal_elements / absent present,
 131 Kinked_spokes / absent present,
 132 Spinose_spokes / absent present,
 133 'Radiating flaps/lobes' / absent present,
 134 oral_structure_separated_by_circumferential_constriction_
 absent present,
 135 constriction_type / skirt_or_bell lappets_,
 136 mesoglea_cellular / non_cellular cellular,

137 extracellular_digestion / absent present,
 138 ostia_with_porocytes / absent present,
 139 embryonic_development / direct indirect,
 140 Cnidae / absent present,
 141 Cnidae_in_gastrodermis / absent present,
 142 Cnidocil / absent present,
 143 Structure_of_mitochondrial_DNA / circular linear,
 144 Actinopharynx / absent present,
 145 'Siphonoglyph (sulcus)' / absent present,
 146 Circular_depression_on_basal_disc / absent present,
 147 'Giant fiber nerve net (GFNN) in medusae' / absent
 present,
 148 stenoteles / absent present,
 149 euryteles / absent present,
 150 desomonemes / absent present,
 151 mastigophores / absent present,
 152 Basitrichousisorhizas / absent present,
 153 Apotrichousisorhizas / absent present,
 154 Isorhizas / absent present,
 155 Heterotrichousanisorhizas / absent present,
 156 Birhopaloids / absent present,
 157 Rhopalonemes / absent present,
 158 Spirocyst / absent present,
 159 Ptychocyst / absent present,
 160 Periderm / absent present,
 161 Cuticle_layers_in_periderm / one two,
 162 Chitin_expression /
 restricted_to_a_basal_area_or_to_podocysts forming_a_tube
 forming_a_thin_cuticle,
 163 Tube_extension / tube_encases_polyp
 does_not_encase_polyp,
 164 periderm_type / corneous coriaceous,

165 Location_of_medusa_formation /
 lateral_budding_from_an_entocodon apical_or_oral
 direct_development_without_polyp_stage,
 166 Type_of_apical_medusa_formation / strobilation
 without_transverse_fission,
 167 Strobilation_type / polydisk monodisk,
 168 Propagation_through_lateral_budding / absent present,
 169 Oocyte_development /
 oocytes_develop_without_accessory_cells
 _oocytes_develop_with_accessory_cells_oocytes_develop_within_follicles
 oocytes_develop_from_uptake_of_somatic_or_other_germ_line_cells,
 170 Nectosome / absent present,
 171 Pneumatophore / absent present,
 172 planula / absent present,
 173 Planula_ciliation / absent present,
 174 Number_of_endodermal_cells_of_the_planula / absent
 present,
 175 Glandular_cells_in_the_planula / absent present,
 176 Nervous_cells_in_the_planula / absent present,
 177 Relationship_between_axes_of_planula_and_adult /
 oral?aboral_axis_in_the_adult_derived_from_the_longitudinal_axis_of_the_pl
 anula
 oral?aboral_axis_in_the_adult_derived_from_the_transverse_axis_of_the_pla
 nula,
 178 Polypoid_phase / absent present,
 179 Polyp_organization / solitary colonial,
 180 Polymorphic_polyps / absent present,
 181 Number_of_tentacular_whorls / one two_or_more,
 182 gut_partitioned_by_septa_ / absent present,
 183 Septa_in_polyp / absent_ present,
 184 Septa_in_medusa / absent present,
 185 Mesoglea_in_polyp_septa / absent presen,
 186 Pairing_of_mesentery / paired coupled,

187 Pair_morphology / members_same_size
 members_differ_in_size,
 188 Paired_secondary_cycle / absent present,
 189 Mesenterial_fusion / absent present,
 190 Number_of_perfect_mesenteries / eight ten_
 more_than_twelve,
 191 Types_of_mesentery / only_perfect_mesenteries ', perfect
 mesenteries not divisible'
 perfect_mesenteries_and_imperfect_mesenteries_divisible,
 192 Directive_mesentery / absent present,
 193 Number_of__directive_mesentery_pairs / one_pair
 two_pairs,
 194 Mesentery_formation / only_primary_tentacles
 new_septa_arise_in_the_exocoel_to_either_side_of_the_ventral_directive
 from_ventral between_directive_and_transverse_septa
 anywhere_around_the_circumference,
 195 Structure_of_polyp_tentacles / hollow solid,
 196 Type_of_tentacles / one_type two_types,
 197 Clustered_tentacles / absent present,
 198 'Two-tentacle polyp stage' / absent present,
 199 Siphonoglyph / absent present,
 200 Siphonoglyph_count / one more_than_one,
 201 Mesenteric_filament / two_strips_ three_strips_ one_strip,
 202 Ridges_or_peridermal_teeth / absent present,
 203 embryonic_stage_retained_in_the_tube_morphology /
 absent present,
 204 Tentacles_retractile / non_retractile retractile,
 205 'Tentacle/coelenteron relationship' /
 one_tentacle_per_endocoel_and_per_exocoel 'one tentacle per exocoel,
 multiple per endocoel',
 206 Catch_tentacles / absent present,
 207 Arrangement_of_tentacles / scattered one_cycle
 more_than_one_cycle,
 208 Acrospheres / absent present,

209 number_of_tentacles_in_poly / six eight twelve sixteen
 eighteen more_than_twenty,
 210 Marginal_spherules / absent_holotrichous,
 211 Acontia / absent present,
 212 Gonads_on_mesenteries_of_1st_cycle / absent present,
 213 Gonads_on_mesenteries_of_2nd_and_subsequent_cycles /
 absent present,
 214 Mesogloeaal_sphincter / absent present,
 215 Ectodermal_longitudinal_muscle_location /
 tentacles_and_oral_disc_only whole_body,
 216 Basilar_musculature / absent present,
 217 Retractor_muscle / weak defined,
 218 Parietal_muscle / absent present,
 219 Mesogloeaal_lacunae / absent present,
 220 Acrorhagi / absent present,
 221 Pedal_disk / absent present,
 222 Ciliated_tract_on_mesenteric_filament / absent present,
 223 Ephyrae / absent present,
 224 Actinula / absent present,
 225 Organisation_of_the_nervous_system / nets
 with_nerve_rings,
 226 Canal_system / absent present,
 227 Gastrodermic_musculature / not_in_bunches
 organised_in_bunches_of_gastrodermic_origin ', organised in bunches of
 ectodermic origin',
 228 Medusoid_phase / absent present,
 229 Pedalium_of_coronate_type / absent present,
 230 'Rhopalia/rhopalioids' / absent present,
 231 Complex_eyes_in_rhopalia / absent present,
 232 Nerve_ring_in_medusa / absent present,
 233 number_of_rings / one two,
 234 Gastric_filaments / absent present,
 235 Coronal_muscle / well_developed marginal_and_tiny,
 236 Pedalium_of_the_cubozoan_type / absent present,

237 Velum / absent present,
 238 Umbrellar_margin / smooth_and_continuous lobed,
 239 Tentacles_in_medusa / absent present,
 240 Tentacular_bulbs / absent present,
 241 Statolith_composition / MgCaPO_4 CaSO_4 ,
 242 Septal_shape_in_medusa / straight_y_shaped,
 243 Radial_canals / absent_present,
 244 circular_canal / absent present,
 245 circular_canal_partial / absent_present,
 246 Velarium / absent present,
 247 Coronal_furrow / absent present,
 248 Gonadal_location / manubrium radial_canals,
 249 statocysts / absent present,
 250 statocyst_location / endodermic ectodermic,
 251 Perradial_mesenteries / absent present,
 252 Adult_medusoid_shape / bell pyramidal cubic actinuloid,
 253 'Shape of horizontal cross-section of the medusa' / circular
 four_part_symmetry,
 254 Urticant_rings / absent present,
 255 Oral_arms_with_suctorial_mouths / absent present,
 256 Tentacular_insertion / umbrellar_margin
 away_from_margin,
 257 Manubrium / absent present,
 258 Nervous_system_organisation / GFNN_absent
 GFNN_present,
 259 Structure_of_medusa_tentacles / hollow solid,
 260 tentacular_morphology / straight
 straight_with Angular_inflection,
 261 peronia / absent present,
 262 ocelli_in_medusa / absent present,
 263 peripheral_system / absent present,
 264 umbrellar_furrow / absent present,
 265 development_of_the_umbrella / fully_developed_
 aboral_cone,

calcitic,

Choanof

??-----0-0-0--

-----0-----??-----0-0-0-----

-----0-----??-----0-0-0-----

?1?1??????????0----

??0????????100011??????????0?0????0??1?4??????????0?????
 ???

Daihua ?????????????????????1?0-

?????00000?0?00?0?00000-??0?0000?0????0??-
????1011111001000100-11?0-0????????1????????????0?????1100000-
?10?0???1?????????????0-----
??0????????100011????????????0?0?????0??1?4????????????0?????
??

'Dinomischnus_venustus'????????????????????01?0-

?????00000?0?00?0?00000-??0?0000?0??????-
????1011111001000110-11?000????????????-?????????0----??1?00000-
?10?0???0?????????????????0-----
??0????????100011????????????0?0?????0??1?4????????????0?????
??

Siphusauctum ?????????????????????01?0-

?????00000?0?00?0?00000-??0?0000?0?????5??-
????1110111001000210-01?000????????1??-?????????0?????0----10-
?10?0???0?????????????????0-----
??0????????100000????????????0?0?????0??1?0????????????0?????
??

Namacalathus

??0??
??????5?????????????????????????0-
?1????????????????????????????????1?00????????????????????????
?????0-----
????????????1????????????????????????????????????0?????
??

Eolympia

????????????????????1?0?????00?0?0?????00????????????0??
?????0???????100????????????00-?1??-?????????????????????0?---
????????????????1?????????????????0-----
????????????100011?????0?????0?0????????1?4????????????0?????
??

Fasciculus

????????????????????0????????00000?0?00???00000-
??0?0000?0?????1??-????11000?11???1141?00?0?0?????????1??-

?????????0---??0---00-?????????-?????????????0-----
????????????????????????????????????-?????????????-
?????????????0??
????????

Xanioascus

?????????????????????0?????????00000?0??00???00000-
???0?0000?0?00001??-???11000?11???10311000?0?0?????1????-
?????????0---??0---00-?????????-?????????????0-----
????????????????????????????????????-?????????????-
?????????????0??
????????

Ctenorhabdotus

?????????????????????0?????????00000?0??00???00000-
???0?0000?0?00001??-???11000?11???11311000?0?0????????????-
?????????0---??0---010?????????-?????????????0-----
????????????????????????????????????-?????????????-
?????????????0??
????????

Gemmactena

????????????????????????????????????00000?0??00???00000-
???0?0000?0?000000-???11000?1?????00111?0?0?0?????????1??-
?????????0---??10110111?????????-?????????????0-----
????????????????????????????????????-?????????????-
?????????????0??
????????

Thaumactena

????????????????????????????????????00000?0??00???00000-
???0?0000?0?000000-???11000?10?????00111?0?0?0????????????-
?????????0---??10?00110?????????-?????????????0-----
????????????????????????????????????-?????????????-
?????????????0??
????????

Galeactena

????????????????????????????????????00000?0??00???00000-

Batofasciculus

Maotianoascus

Trigoides

Cydippida

Lobata

```
Lobata      0100111111111000101011-100-0-000000-
00000010000000-0--
```

000000000000000110011101100011111110110000100(0
1)001111011111(0 1)(0 1)2211111101100---00-11000-000-----0-----
--?-0---0--0-----0-----0-----??-----
-----0-0--0--

Beroida 0100111111111000101001-100-0-000000-
00000010000000-0--00000000000000110-
1010110001111111001100010100111111101-1112000000---000---00-
11000-000-----0-----?-0---0--0-----0-----
0-----??-----0-0--0--

Platyctenida 0100111111111000101011-100-0-000000-
00000010000000-0--00000000000000111111011000(0
1)111111?0110000001000111110111(0 1)011(0 1)1111011010---00-
11000-000-----0-----?-0---0--0-----0-----
0-----??-----0-0--0--

Cestida 0100111111111000101011-100-0-000000-
00000010000000-0--
0000000000000011001110110001111111011000000000111?0111110(0
1)22111111111000---00-11000-000-----0-----?-0---0--0-----
--0-----0-----??-----0-0--0--

Ganeshida 0100111111111000101011-100-0-000000-
00000010000000-0--
000000000000001100111011000111111100110000100000111?0111110(0
1)2211??11101000---00-11000-000-----0-----?-0---0--0-----
--0-----0-----??-----0-0--0--

Thalassocalycida 0100111111111000101011-100-0-000000-
00000010000000-0--
000000000000001100111011000111111100110000020000111?0111110(0
1)2211??11101000---00-11000-000-----0-----?-0---0--0-----
--0-----0-----??-----0-0--0--

Bryozoa 01101111111110100111100-11100-
0000000000000000100000001000000000001100-0001(0 1)-----0---00-
0000-0000000000?0-0-0-0-0000---000---00--1010-000-----0-----?--
0---0--0-----0-----0-----??-----
0-0--0--

Brachiopoda 0110111111110100111100-(0 1)11(0 1)0-
00000000000000001000000010000000000001100--00010-----0---00-
0000-0000000000?0-0-0-0-0000---000---00--1010--000-----0-----?--
0---0--0-----0-----0-----0-----??-----
0-0--0--

Phoronida 0110111111110100111100-11100-
00000000000000000000000010000000000001100--00010-----0---00-
0000-0000000000?0-0-0-0-0000---000---00--1010--000-----0-----?--
0---0--0-----0-----0-----0-----??-----
0-0--0--

Mollusca 0110111111110100111100-101(0 1 2)(0
1)0000000001000011010100000000000000000001100--0000(0 1)-----0---
00-1000-0000000000?0-0-0-0-0000---000---00--1010--000-----0-----
?--0---0--0-----0-----0-----0-----??-----
---0-0--0--

Annelida 0110111111110100111100-101(0 1 2)0-
0000000110000(0 1)10110000000000000000000001100--00000-----0---00-
1000-0000000000?0-0-0-0-0000---000---00--1010--000-----0-----?--
0---0--0-----0-----0-----0-----??-----
0-0--0--

Echinodermata 0110011111110100111000-10110-
00000000000000000000011111000111000001100--0000(0 1)-----0---00-
1(0 1)00-0000000000?0-0-0-0-0000---000---00--1010--000-----0-----
?--0---0--0-----0-----0-----0-----??-----
---0-0--0--

Pterobranchia 0110111111110100111000-11110-
000000001000000000000011111101101000001100--00000-----0---00-
1000-0000000000?0-0-0-0-0000---000---00--1010--000-----0-----?--
0---0--0-----0-----0-----0-----??-----
0-0--0--

Chaetognatha 0110111111110100111000-10110-
0000000010000-00000011001000000000000001100--00000-----0---00-1000-
0000000000?0-0-0-0-0000---000---00--1000--000-----0-----?-0-----

0--0-----0-----0-----??-----0-0--
0--

Onychophora 011011111110100111000-
1012111011011110001-0100000000000000000001100--00000-----0---
00-1000-0000000000?0-0-0-0-0000---000---00--1000-000-----0-----
?-0---0--0-----0-----0-----??-----
----0-0-0--

Arthropoda 0110111111110100111000-101(0 1)1111000(0
1)1110001-010000000000000000000001100--00000-----0---00-1000-
0000000000?0-0-0-0-0000---000---00--10{0 1}0-000-----0-----?-0--
--0--0-----0-----0-----??-----0-
0--0--

Nemertea 0110111111110100111100-101(0 1)0-
0000000010000-100001000000000000000001100--00000-----0---00-1000-
0000000000?0-0-0-0-0000---000---00--1010-000-----0-----?-0-----
0--0-----0-----0-----??-----0-0--
0--

Enteropneusta 0110111111110100111000-10110-
0000000010000-000000011111101101000001100--00000-----0---00-1000-
0000000000?0-0-0-0-0000---000---00--1010-000-----0-----?-0-----
0--0-----0-----0-----??-----0-0--
0--

Urochordata 0111111111110100111000-10110-
0000000000000-000000010101110000100111100--00000-----0---00-1000-
0000000000?0-0-0-0-0000---000---00--1010-000-----0-----?-0-----
0--0-----0-----0-----??-----0-0--
0--

Cephalochordata 0110111111110100111000-10110-
0000000000000-000000011101110000110001100--00000-----0---00-1000-
0000000000?0-0-0-0-0000---000---00--1010-000-----0-----?-0-----
0--0-----0-----0-----??-----0-0--
0--

Vertebrata 0101111111110100111000-10110-0000000000000-
00000001(0 1)10111000011111100--00000-----0---00-1000-

0000000000?0-0-0-0-0000---000---00--1000-000-----0-----?-0-----
0--0-----0-----0-----0-----??-----0-0--
0--

Entoprocta 011011111110100111100-111010000000-
0000000100000000--0000000000001100--00001-----0---00-1100-
0000000000?0-0-0-0-0000---000---00--1010-000-----0-----?-0-----
0--0-----0-----0-----0-----??-----0-0--
0--

Nematoda 011011111110100111000-101010100000-
011101-0000000000--0000000000001100--00000-----0---00-1000-
0000000000?0-0-0-0-0000---000---00--1000-000-----0-----?-0-----
0--0-----0-----0-----0-----??-----0-0--
0--

Nematomorpha 011011111110100111000-101110100000-
010101-0000000000--0000000000001100--00000-----0---00-1000-
0000000000?0-0-0-0-0000---000---00--1010-000-----0-----?-0-----
0--0-----0-----0-----0-----??-----0-0--
0--

Priapulida 011011111110100111000-101111100000-011111-
0000000000--0000000000001100--00000-----0---00-1000-0000000000?0-0-
0-0-0000---000---00--1010-000-----0-----?-0---0--0-----0-
-----0-----??-----0-0-0--

Gastrotricha 011011111110100111100-10100-000000-010000-
0000000000--0000000000001100--00000-----0---00-1000-0000000000?0-0-
0-0-0000---000---00--1000-000-----0-----?-0---0--0-----0-
-----0-----??-----0-0-0--

Tardigrada 011011111110100111000-
1010111010101?10001-0000000000000000000000001100--00000-----0---
00-1000-0000000000?0-0-0-0-0000---000---00--1000-000-----0-----
?-0---0--0-----0-----0-----0-----??-----
---0-0-0--

Kinorhyncha 011011111110100111000-101?10100000-
111111-0000000000--0000000000001100--00000-----0---00-1000-
0000000000?0-0-0-0-0000---000---00--1000-000-----0-----?-0-----

0--0-----0-----0-----??-----0-0--
0--

Loricifera 011011111110100111000-101?10100000-011111-
000000000--0000000000001100--00000-----0---00-1000-0000000000?0-0-
0-0-0000---000---00--1010--000-----0-----?-0---0--0-----0-
-----0-----??-----0-0-0--

Gnathifera 011011111110100111100-10100-000000-010000-
000000100--0000000000001100--00000-----0---00-1000-0000000000?0-0-
0-0-0000---000---00--1000--000-----0-----?-0---0--0-----0-
-----0-----??-----0-0-0--

Xenacoelomorpha 0100?1?1(0 1)1111111111000-0-0-0-000000-
0?0000-0000000-0--0000000000001100--00000-----0---00-1000-
0000000000?0-0-0-0-0000---000---00--1000--000-----0-----?-0-----
0--0-----0-----0-----??-----0-0--
0--

Platyhelminthes 0110111111110100111100-0-000-000000-
010000-100000000--0000000000001100--00000-----?0---00-1000-
0000000000?0-0-0-0-0000---000---00--1010--000-----0-----?-0-----
0--0-----0-----0-----??-----0-0--
0--

sphenothallus
????????????????????????????00?0????????????????????????
????000?0????????????????????????0????????????????????
????0????????????1????????????????????1??0????1????????11??11??
????????????????10????????????????0????????????????????
????????????????????????????

Conulariida ?????????????????????00?-
???00?0????????0????????????????????003?0????????????
??0??0????????????????????????????0-
????????????????????????11101???0?-0----10-
?111????????????1????????????????????2????????????1
????????1????????????????????

Olivoiides ?????????????????????00?-
???00?0????????0????????????????????004?0????0????????

??0??0????????????????????????????????0-
??????????0????????????????????????1?10?????--0----10-
?11????????????????????11????????????????????1??1?1?????????????
????????????????????????????????????

 Quadrupyrates ????????????????????????00?-
???00?0??????????0????????????????????????003?0????0?????????????
??0??0????????????????????????????????????0-
??????????0????????????????????????1?10?????--0----10-
?11????????????????????11????????????????????1?????????????????
????????????????????????????????????

 Pseudoides ????????????????????????00?-
???00?0??????????0????????????????????????001?0????0?????????????
??0??0????????????????????????????????????0-
??????????0????????????????????????1?10?????--0----10-
????????????????????11???
????????????????????????????????????

 Nematostella 011001111101100101001-0-0-0-000000-
00000010000000-0--0000000000000000-10001010000--0----00-1000-
0000000000?0-0-0-0-0000----000----00-11011110110-0001000000100-----
01--11011010-111-101002111400001110-100203001?000110001000010-----
-----??-----00-0--0-0

 Anemonia 011001111101100101001-0-0-0-000000-
00000010000000-0--00000000000000500-10001010000--0----00-1000-
0000000000?0-0-0-0-0000----000----00-11011110110-0001001000100-----
01--11011010-111-10010211140000111?-1002051011001110111000010-----
-----??-----10-0--0-0

 Aiptasia 011001111101100101001-0-0-0-000000-
00000010000000-0--00000000000000500-10001010000--0----00-1000-
0000000000?0-0-0-0-0000----000----00-11011110110-0001000000100-----
01--11011010-111-100102111400101110-10020501??101110011000010-----
-----??-----10-0--0-0

 Metridium 011001111101100101001-0-0-0-000000-
00000010000000-0--00000000000000500-10001010000--0----00-1000-
0000000000?0-0-0-0-0000----000----00-11011110110-0001000000100-----

01--11011010-111-100102111400101110-1112050101101110011000010-----
-----??-----00-0--0-0

Antipathes 0110011111101100101001-0-0-0-000000-
00000010000000-0--00000000000000500-10001010000--0----00-1000-
0000000000?0-0-0-0-0000----000----00-11011110110-0001001000100-----
0100110110110011-100001011300001120-00010500??0?0000000000010---
-----??-----?100--0-0

Ceriantharia 0110?11111101100101001-0-0-0-000000-
00000010000000-0--00000000000000000-10001010000--0----00-1000-
0000000000?0-0-0-0-0000----000----000110111?????0001001000110-----
01--11011010-111-10?002010201001010-000205001?010000001000000-----
-----??-----?0-0--0-0

Corynactis 0110011111101100101001-0-0-0-000000-
00000010000000-0--00000000000000500-10001010000--0----00-1000-
0000000000?0-0-0-0-0000----000----00-11011110110-0001001000100-----
01--11011010-111-10010210-400000-20-11021500??010000010000010-----
-----??-----?0-0--0-0

Montastraea 0110011111101100101001-0-0-0-000000-
00000010000000-0--00000000000000500-10001010000--0----00-1000-
0000000000?0-0-0-0-0000----000----00-11011110110-0001001000100-----
0100110110110111-10010210-400000-20-10021500??0?0000000000010---
-----??-----1110110-0

Porites 0110011111101100101001-0-0-0-000000-
00000010000000-0--00000000000000500-10001010000--0----00-1000-
0000000000?0-0-0-0-0000----000----00-11011110110-0001001000100-----
0100110110110111-10010210-400000-20-10021300??0?0000000000010---
-----??-----1110110-0

Acropora 0110011111101100101001-0-0-0-000000-
00000010000000-0--00000000000000500-10001010000--0----00-1000-
0000000000?0-0-0-0-0000----000----00-11011110110-0001001000100-----
0100110110110111-10010210-400000-20-10021200??0?0000000000010---
-----??-----1110110-0

Parazoanthus 0110011111101100101001-0-0-0-000000-
00000010000000-0--00000000000000000-10001010000--0----00-1000-

0000000000?0-0-0-0-0000----000----00-11011110110-0001001000100-----
0100110110110111-101102211100001010-10020500??000011001000010---
-----??-----10-0--0-0

Anthomastus 0110011111101100101001-0-0-0-000000-
00000010000000-0--0000000000000000-10001011000--0----00-1000-
0000000000?0-0-0-0-0000----000----00-11011110110-0000001000000-----
0100110110110011-11-000010000001000-00010100??0?0000001000010---
-----??-----?0-1--110

Keratoisidinae 0110011111101100101001-0-0-0-000000-
00000010000000-0--0000000000000000-10001011000--0----00-1000-
0000000000?0-0-0-0-0000----000----00-11011110110-0000001000000-----
0100110110110011-11-00001000000100?00010100??0?0000001000010---
-----??-----?0-1--110

Nephthyigorgia 0110011111101100101001-0-0-0-000000-
00000010000000-0--0000000000000000-10001011000--0----00-1000-
0000000000?0-0-0-0-0000----000----00-11011110110-0000001000000-----
0100110110110011-11-000010000001000-00010100??0?0000001000010---
-----??-----?0-1--111

Leptogorgia 0110011111101100101001-0-0-0-000000-
00000010000000-0--0000000000000000-10001011000--0----00-1000-
0000000000?0-0-0-0-0000----000----00-11011110110-0000001000000-----
0100110110110011-11-000010000001000-00010100??0?0000001000010---
-----??-----?0-1--111

Scleronepthya 0110011111101100101001-0-0-0-000000-
00000010000000-0--0000000000000000-10001011000--0----00-1000-
0000000000?0-0-0-0-0000----000----00-11011110110-0000001000000-----
0100110110110011-11-000010000001000-00010100??0?0000001000010---
-----??-----?0-1--110

Virgularia 0110011111101100101001-0-0-0-000000-
00000010000000-0--0000000000000000-10001011000--0----00-1100-
0000000000?0-0-0-0-0000----000----00-11011110110-0000001000000-----
0100110110111011-11-000010000001000-00010100??0?0000001000010---
-----??-----00-1--0-0

Haliclystus 011001111110110010100100-0-0-000000-
00000010000000-0--00000000000000100-10001010000--0----00-1-00-
0000000000?0-0-0-0-0000----000----00-010111?10000010000100000100-
011-12--10100010-01111--0-----00010--000-000100--0?000000-
0001210100-110001?-10000010-011000100000000000100-0--000

Alatina 011001111110110010100110-0-0-000000-
00000010000000-0--00000000000000100-10001010000--0----00-1-00-
0000000000?0-0-0-0-0000----000----00-010111010001110100100000110-
011-1?--110??010-01110--0-----10010--000-000100--0?000000-
0011210111010100101110010110021000110001000011000-0--000

Chirodropida 011001111110110010100110-0-0-000000-
00000010000000-0--00000000000000100-10001010000--0----00-1000-
0000000000?0-0-0-0-0000----000----00-010111010001110100100000110-
011-1?--110??010-01110--0-----10010--000-000100--0?000000-
0011210111010100101110010110021000110001000011100-0--000

Atolla 011001111110110010100110-0-0-000000-
00000010000000-0--00000000000000300-10001010000--0----00-1000-
0000000000?0-0-0-0-0000----000----00-
110111010001010000100000?????10???--?????0???01111--0-----10000--
???0-010500--0?000000-1001211100-
100011010100011100000001110010000000000-0--000

Nausithoe 011001111110110010100110-0-0-000000-
00000010000000-0--00000000000000300-10001010000--0----00-1000-
0000000000?0-0-0-0-0000----000----00-
1101110100010100001000001110010000--1????010-01111--0-----10000--
100-010500--0?000000-1001211100-
100011010100011100000001110010000000000-0--000

Aurelia 011001111110110010100110-0-0-000000-
00000010000000-0--00000000000000300-10001010000--0----00-1000-
0000000000?0-0-0-0-0000----000----00-110111010001010000110000100-
010111--1??11010-01101--0-----10000--000-000300--0?000000-
1001210100-10001101-111001100000001100010000000000-0--000

Rhizostoma 011001111110110010100110-0-0-000000-
00000010000000-0--00000000000000300-10001010000--0----00-1?00-

0000000000?0-0-0-0-0000----000----00-110111010001010000110000100-
010011--1??00010-01101--0-----10000--000-000300--0?000000-
1001210100-100010-1-1110011000001-11--01000-00-00-0--000

Hydra 011011111110110010100110-0-0-000000-
00000010000000-0--00000000000000300-10001010000--0----00-1100-
0000000000?0-0-0-0-0000----000----00-0100100100011111001000000---00--
13--0-----10-110----0-----?0000--0-0-010?00--0?000000-000000----?-----
??-----00-0--000

Candelabrum 011011111110110010100110-0-0-000000-
00000010000000-0--00000000000000300-10001010000--0----00-1000-
0000000000?0-0-0-0-0000----000----00-
010010010001111100100000101100--03000----110110----0-----?0000--000-
000?00--0?000000-000000----?-----??-----00-0--000

Hydractinia 011011111110110010100110-0-0-000000-
00000010000000-0--00000000000000300-10001010000--0----00-1000-
0000000000?0-0-0-0-0000----000----00-
010110010001111100100000101100--0300???110111110----0-----?0000--
000-010300--0?000000-
000001?????????????????????????????????????00-0--000

Ectopleura 011011111110110010100110-0-0-000000-
00000010000000-0--00000000000000300-10001010000--0----00-1000-
0000000000?0-0-0-0-0000----000----00-
010010010001111100100000101100--03000----1101101---0-----?0000--
000-010500--0?000000-00000100-110001011--1100000-
10000011?001000000000-0--000

Clytia 011011111110110010100110-0-0-000000-
00000010000000-0--00000000000000300-10001010000--0----00-1100-
0000000000?0-0-0-0-0000----000----00-
010110010001110110100000101000--03001??1101111101---0-----10000--
000-010500--0?000000-00000100-1100010110-
1100011100000011000?000000000-0--000

Obelia 011011111110110010100110-0-0-000000-
00000010000000-0--00000000000000300-10001010000--0----00-1100-
0000000000?0-0-0-0-0000----000----00-

010110010001110110100000101000--03001??1101111101---0-----10000--
000-010500--0?000000-00000100-1100010110-
1100011100000011000?000000000-0--000

Physalia 011011111110110010100110-0-0-000000-
00000010000000-0--00000000000000300-10001010000--0----00-1000-
0000000000?0-0-0-0-0000----000----00-010110010001111100101100102-00-
-0?011??1101111101---0-----00000--0-0-0?0?00--0?000000-00000100-
110001001--1100000-00000-11--00000-00-00-0--000

Craseoa 011011111110110010100110-0-0-000000-
00000010000000-0--00000000000000300-10001010000--0----00-1000-
0000000000?0-0-0-0-0000----000----00-010110010001111100101100102-00-
-0?111??1101111101---0-----00000--0-0-0?0?00--0?000000-00000100-
110001001--1100000-00000-11--00000-00-00-0--000

Abylopsis 011011111110110010100110-0-0-000000-
00000010000000-0--00000000000000300-10001010000--0----00-1000-
0000000000?0-0-0-0-0000----000----00-010110010001111100101100102-00-
-0?111??1101111101---0-----00000--0-0-0?0?00--0?000000-00000100-
110001001--1100000-00000-11--00000-00-00-0--000

Agalma 011011111110110010100110-0-0-000000-
00000010000000-0--00000000000000300-10001010000--0----00-1000-
0000000000?0-0-0-0-0000----000----00-010110010001111100101100102-00-
-0?101??1101111101---0-----00000--0-0-0?0?00--0?000000-00000100-
110001001--1100000-00000-11--00000-00-00-0--000

Nanomia 011011111110110010100110-0-0-000000-
00000010000000-0--00000000000000300-10001010000--0----00-1000-
0000000000?0-0-0-0-0000----000----00-010110010001111100101100102-00-
-0?101??1101111101---0-----00000--0-0-0?0?00--0?000000-00000100-
110001001--1100000-00000-11--00000-00-00-0--000

Aeginia 011011111110110010100110-0-0-000000-
00000010000000-0--00000000000000300-10001010000--0----00-1000-
0000000000?0-0-0-0-0000----000----00-0101100100010000011000000-----
03001??00110-0101---0-----0000--0-0-010?00--0?000000-0100-100-
??0001110?-010000100000010?1010100000000-0--000

Halitrephes 011011111110110010100110-0-0-000000-
00000010000000-0--00000000000000300-10001010000--0----00-1000-
0000000000?0-0-0-0-0000----000----00-0101100100011100001000000-----
03001??00000-0101---0-----0000--0-0-010?00--0?000000-0100-100-
1100010100-11000110000100111000000000000-0--000

;

END;

Supplemental References

- S1. Ou, Q., Han, J., Zhang, Z., Shu, D., Sun, G., and Mayer, G. (2017). Three Cambrian fossils assembled into an extinct body plan of cnidarian affinity. *Proceedings of the National Academy of Sciences*, 201701650.
- S2. Ou, Q., Xiao, S., Han, J., Sun, G., Zhang, F., Zhang, Z., and Shu, D. (2015). A vanished history of skeletonization in Cambrian comb jellies. *Science advances* 1, e1500092.
- S3. Duan, B., Dong, X.-P., Porras, L., Vargas, K., Cunningham, J.A., and Donoghue, P.C. (2017). The early Cambrian fossil embryo *Pseudoooides* is a direct-developing cnidarian, not an early ecdysozoan. *Proc. R. Soc. B* 284, 20172188.
- S4. Goloboff, P.A., Carpenter, J.M., Arias, J.S., and Esquivel, D.R.M. (2008). Weighting against homoplasy improves phylogenetic analysis of morphological data sets. *Cladistics* 24, 758-773.
- S5. Lewis, P.O. (2001). A likelihood approach to estimating phylogeny from discrete morphological character data. *Systematic Biology* 50, 913-925.
- S6. Goloboff, P.A., Farris, J.S., and Nixon, K.C. (2008). TNT, a free program for phylogenetic analysis. *Cladistics* 24, 774-786.
- S7. Goloboff, P.A. (1997). Self-Weighted Optimization: Tree Searches and Character State Reconstructions under Implied Transformation Costs. *Cladistics* 13, 225-245.

- S8. Goloboff, P.A., Torres, A., and Arias, J.S. (2017). Weighted parsimony outperforms other methods of phylogenetic inference under models appropriate for morphology. *Cladistics*.
- S9. Legg, D.A., Sutton, M.D., and Edgecombe, G.D. (2013). Arthropod fossil data increase congruence of morphological and molecular phylogenies. *Nature communications* 4.
- S10. Parry, L.A., Edgecombe, G.D., Eibye-Jacobsen, D., and Vinther, J. (2016). The impact of fossil data on annelid phylogeny inferred from discrete morphological characters. *Proceedings of the Royal Society B* 283, 20161378.
- S11. Puttick, M.N., O'Reilly, J.E., Tanner, A.R., Fleming, J.F., Clark, J., Holloway, L., Lozano-Fernandez, J., Parry, L.A., Tarver, J.E., and Pisani, D. (2017). Uncertain-tree: discriminating among competing approaches to the phylogenetic analysis of phenotype data. In *Proc. R. Soc. B*, Volume 284. (The Royal Society), p. 20162290.
- S12. O'Reilly, J.E., Puttick, M.N., Parry, L., Tanner, A.R., Tarver, J.E., Fleming, J., Pisani, D., and Donoghue, P.C. (2016). Bayesian methods outperform parsimony but at the expense of precision in the estimation of phylogeny from discrete morphological data. *Biology Letters* 12, 20160081.
- S13. Brown, J.W., Parins-Fukuchi, C., Stull, G.W., Vargas, O.M., and Smith, S.A. (2017). Bayesian and likelihood phylogenetic reconstructions of morphological traits are not discordant when taking uncertainty into consideration: a comment on Puttick et al. *Proc. R. Soc. B* 284, 20170986.
- S14. Marques, A.C., and Collins, A.G. (2004). Cladistic analysis of Medusozoa and cnidarian evolution. *Invertebrate Biology* 123, 23-42.
- S15. Dzik, J., Baliński, A., and Sun, Y. (2017). The origin of tetra-radial symmetry in cnidarians. *Lethaia* 50, 306-321.
- S16. Whelan, N.V., Kocot, K.M., Moroz, T.P., Mukherjee, K., Williams, P., Paulay, G., Moroz, L.L., and Halanych, K.M. (2017). Ctenophore relationships and their placement as the sister group to all other animals. *Nature ecology & evolution* 1, 1737.

- S17. Brazeau, M.D. (2011). Problematic character coding methods in morphology and their effects. *Biological Journal of the Linnean Society* 104, 489-498.
- S18. Han, J., Kubota, S., Uchida, H.-o., Stanley Jr, G.D., Yao, X., Shu, D., Li, Y., and Yasui, K. (2010). Tiny sea anemone from the Lower Cambrian of China. *PLoS One* 5, e13276.
- S19. Nielsen, C. (2012). *Animal evolution: interrelationships of the living phyla*, (Oxford University Press).
- S20. Srivastava, M., Begovic, E., Chapman, J., Putnam, N.H., Hellsten, U., Kawashima, T., Kuo, A., Mitros, T., Salamov, A., and Carpenter, M.L. (2008). The *Trichoplax* genome and the nature of placozoans. *Nature* 454, 955.
- S21. Ganot, P., Zoccola, D., Tambutté, E., Voolstra, C.R., Aranda, M., Allemand, D., and Tambutté, S. (2014). Structural molecular components of septate junctions in cnidarians point to the origin of epithelial junctions in eukaryotes. *Molecular biology and evolution* 32, 44-62.
- S22. Günzel, D., and Yu, A.S. (2013). Claudins and the modulation of tight junction permeability. *Physiological reviews* 93, 525-569.
- S23. Peterson, K.J., and Eernisse, D.J. (2001). Animal phylogeny and the ancestry of bilaterians: inferences from morphology and 18S rDNA gene sequences. *Evolution & development* 3, 170-205.
- S24. Burke, R., Angerer, L., Elphick, M., Humphrey, G., Yaguchi, S., Kiyama, T., Liang, S., Mu, X., Agca, C., and Klein, W. (2006). A genomic view of the sea urchin nervous system. *Developmental biology* 300, 434-460.
- S25. Schierwater, B., de Jong, D., and DeSalle, R. (2009). Placozoa and the evolution of Metazoa and intrasomatic cell differentiation. *The international journal of biochemistry & cell biology* 41, 370-379.
- S26. Achatz, J.G., and Martinez, P. (2012). The nervous system of *Isodiametra pulchra* (Acoela) with a discussion on the neuroanatomy of the Xenacoelomorpha and its evolutionary implications. *Frontiers in zoology* 9, 27.

- S27. Hejnol, A., and Pang, K. (2016). Xenacoelomorpha's significance for understanding bilaterian evolution. *Current Opinion in Genetics & Development* 39, 48-54.
- S28. Ryan, J.F., Pang, K., Mullikin, J.C., Martindale, M.Q., and Baxevanis, A.D. (2010). The homeodomain complement of the ctenophore *Mnemiopsis leidyi* suggests that Ctenophora and Porifera diverged prior to the ParaHoxozoa. *EvoDevo* 1, 9.
- S29. Lundin, K., and Hendelberg, J. (1996). Degenerating epidermal bodies ("pulsatile bodies") in *Meara stichopi* (Plathelminthes, Nemertodermatida). *Zoomorphology* 116, 1-5.
- S30. Ax, P. (1996). Multicellular animals. A new approach to the phylogenetic order in nature. 1996. (Berlin-Heidelberg: Springer Verlag CrossRef Google Scholar).
- S31. Steinmetz, P.R., Aman, A., Kraus, J.E., and Technau, U. (2017). Gut-like ectodermal tissue in a sea anemone challenges germ layer homology. *Nature ecology & evolution* 1, 1535.
- S32. Giribet, G. (2008). Assembling the lophotrochozoan (=spiralian) tree of life. *Philosophical Transactions of the Royal Society B-Biological Sciences* 363, 1513-1522.
- S33. O'Brien, L.J., and Caron, J.-B. (2012). A new stalked filter-feeder from the middle Cambrian Burgess Shale, British Columbia, Canada. *PloS one* 7, e29233.
- S34. Nielsen, C., Brunet, T., and Arendt, D. (2018). Evolution of the bilaterian mouth and anus. *Nature ecology & evolution* 2, 1358.
- S35. Schmidt-Rhaesa, A., Rothe, B., Wägele, J., and Bartolomaeus, T. (2014). Brains in Gastrotricha and Cycloneuralia—a comparison. *Deep metazoan phylogeny: the backbone of the Tree of Life. New insights from analyses of molecules, morphology, and theory of data analysis.* Berlin: De Gruyter, 93-104.
- S36. Nielsen, C. (2005). Trochophora larvae: cell-lineages, ciliary bands and body regions. 2. Other groups and general discussion. *Journal of Experimental Zoology Part B: Molecular and Developmental Evolution* 304, 401-447.

- S37. Lüter, C. (2000). Ultrastructure of larval and adult setae of Brachiopoda. *Zoologischer Anzeiger* 239, 75-90.
- S38. Gordon, D.P. (1975). The Resemblance of Bryozoan Gizzard Teeth to “Annelid-like” Setae. *Acta zoologica* 56, 283-289.
- S39. Vinther, J., Parry, L., Briggs, D.E.G., and Van Roy, P. (2017). Ancestral morphology of crown-group molluscs revealed by a new Ordovician stem aculiferan. *Nature*.
- S40. Fröblius, A.C., and Funch, P. (2017). Rotiferan Hox genes give new insights into the evolution of metazoan bodyplans. *Nature communications* 8, 9.
- S41. Spangenberg, J.E., Bagnoud-Velásquez, M., Boggiani, P.C., and Gaucher, C. (2014). Redox variations and bioproductivity in the Ediacaran: Evidence from inorganic and organic geochemistry of the Corumbá Group, Brazil. *Gondwana Research* 26, 1186-1207.
- S42. Genikhovich, G., Fried, P., Prünster, M.M., Schinko, J.B., Gilles, A.F., Fredman, D., Meier, K., Iber, D., and Technau, U. (2015). Axis patterning by BMPs: cnidarian network reveals evolutionary constraints. *Cell reports* 10, 1646-1654.
- S43. Leclère, L., and Rentzsch, F. (2014). RGM regulates BMP-mediated secondary axis formation in the sea anemone *Nematostella vectensis*. *Cell reports* 9, 1921-1930.
- S44. Kimmig, J., Strotz, L.C., and Lieberman, B.S. (2017). The stalked filter feeder *Siphosauctum lloydguntheri* n. sp. from the middle Cambrian (Series 3, Stage 5) Spence Shale of Utah: its biological affinities and taphonomy. *Journal of Paleontology*, 1-9.
- S45. Conway Morris, S., and Collins, D. (1996). Middle Cambrian ctenophores from the Stephen Formation, British Columbia, Canada. *Philosophical Transactions of the Royal Society of London B: Biological Sciences* 351, 279-308.

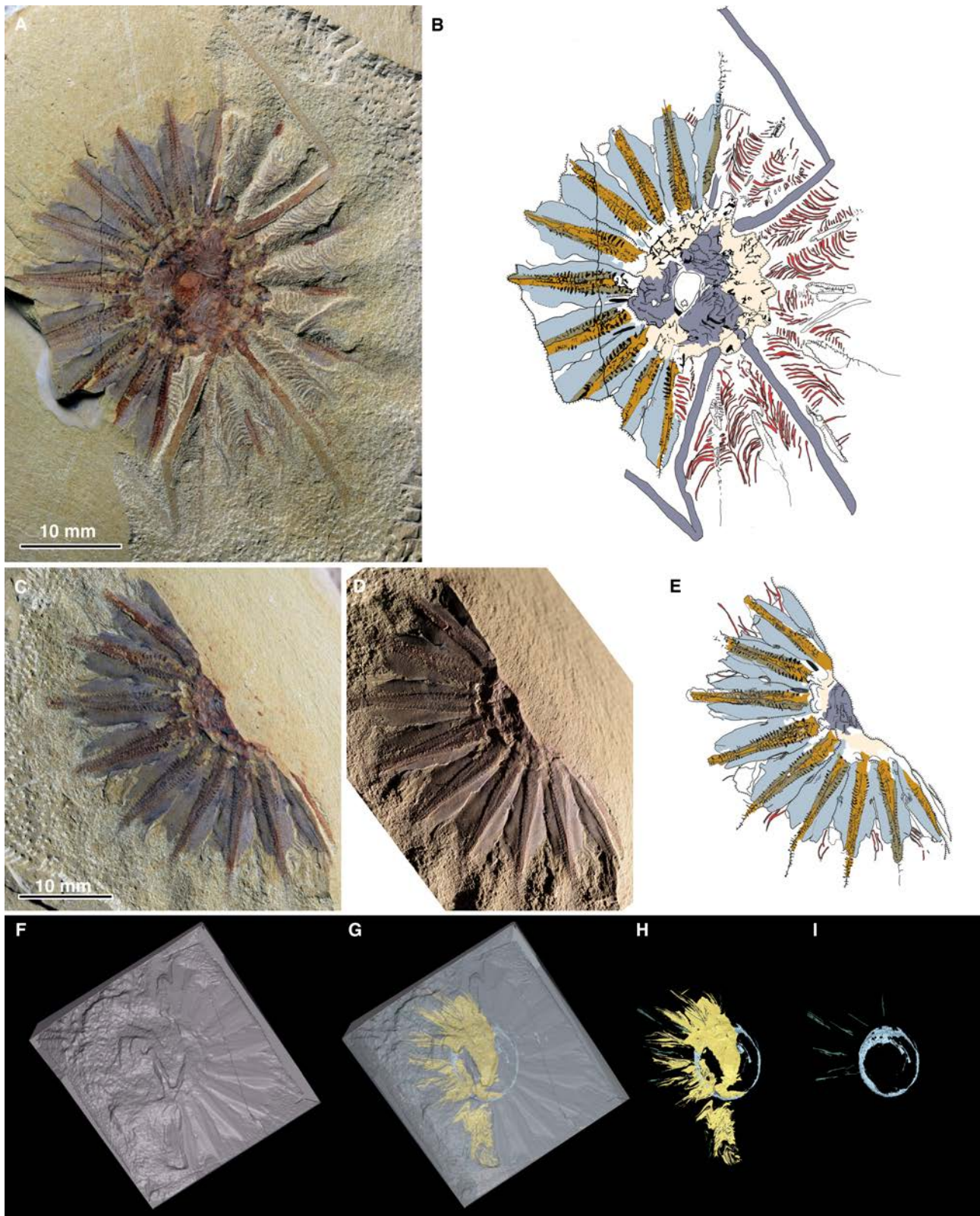


Figure S1 *Daihua sanqiong*, YKLP 13401, holotype. Related to Figure 2. (A) Part, Photographed with crossed polarized light. (B) Camera lucida drawing of part. Pinnules are indicated in red, outer sheaths in light blue, tentacle rods in orange, oral surface in peach, and oral dome and bracts dark grey. (C) Counterpart. Photographed with crossed polarized light. (D) Counterpart, photographed in low angle light. (E) Camera lucida drawing of counterpart. Colour scheme as in counterpart (B). (F) Surface render of scanned area of block. (G) Segmented calyx (light blue), lateral blades (yellow) and arms (green) revealed within matrix. (H) Matrix removed. (I) Lateral blades removed.

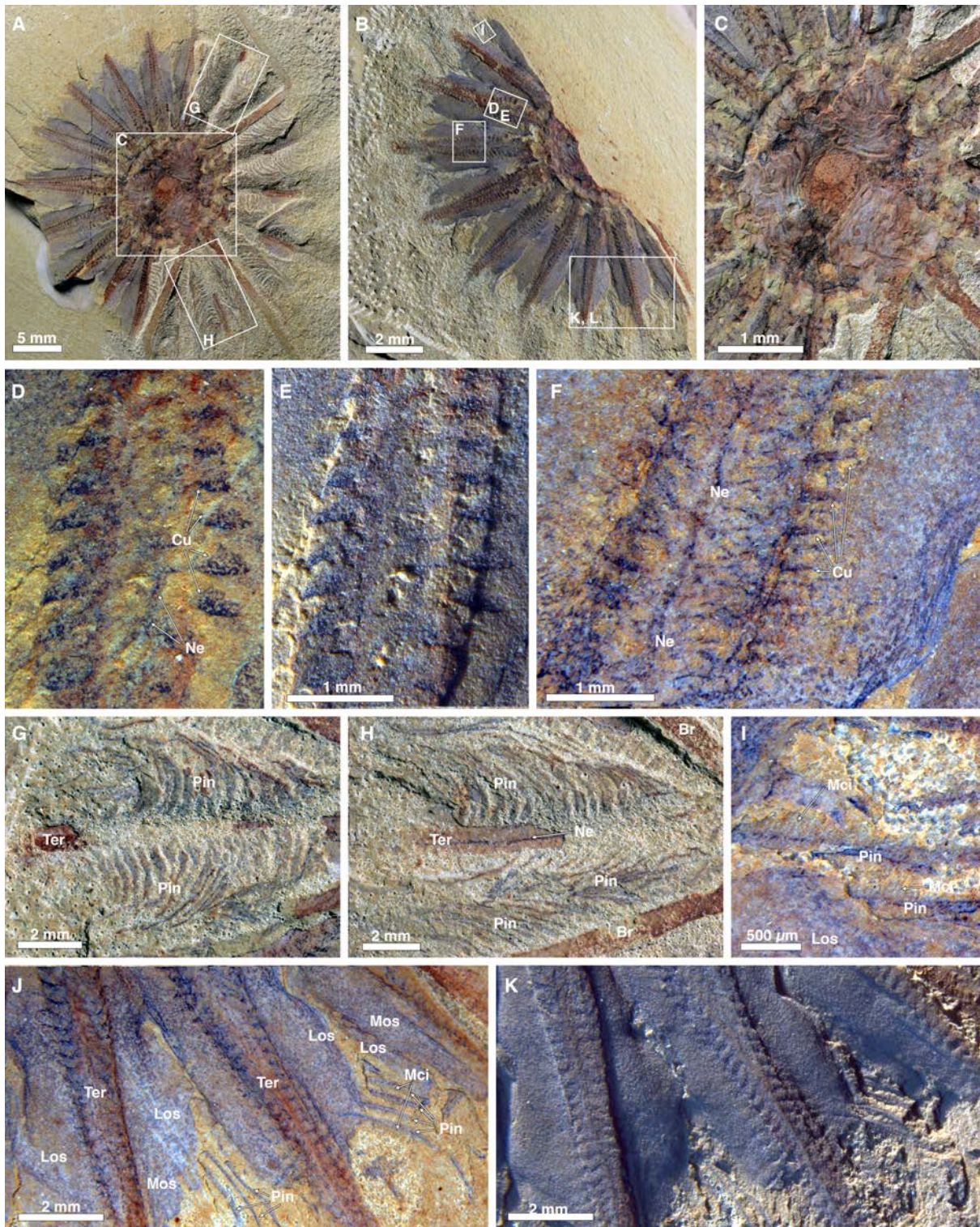


Figure S2 Additional details of the *Daihua sanqiong* holotype, YKLP 13401 Related to Figure 2. (A) Overview of part, boxed areas are subsequent panels. (B) Overview of counterpart, boxed areas are subsequent panels. (C) Detail of oral region, oral domes and the teardrop-shaped mouth opening. (D) Detail of tentacle with cushion plates, median nerve and connectives between cushion plates and nerve. (E) Same view as in D, but in low angle light. Notice that cushion plates cross over the sclerotized tentacle rod. This indicates that the soft tissue was markedly wider than defined by the internal sclerotised rod. (F) Tentacle preserving cushion plates, nerve and more diffuse organic lines that appear to reticulate. This may be a finer reticulate nervous system. (G) Pinnules prepared out from overlying matrix in part. (H) Pinnules prepared out from overlying matrix in part, showing a nerve on the tentacle rod and the adjacent bracts from the oral domes. (I) Details of macrociliary rows on pinnules from a different part of the specimen. (J) Details of tentacles, cushion plates, outer sheaths and pinnules. (K) Same view as in J, but in low

angle light. Abbreviations: Cu-Cushion plate, Ne-nerve, Pin-pinnules, Ter-tentacle rod, Br-bract, Mci-macrotilia, Los-lateral outer sheaths, Mos-medial outer sheaths.

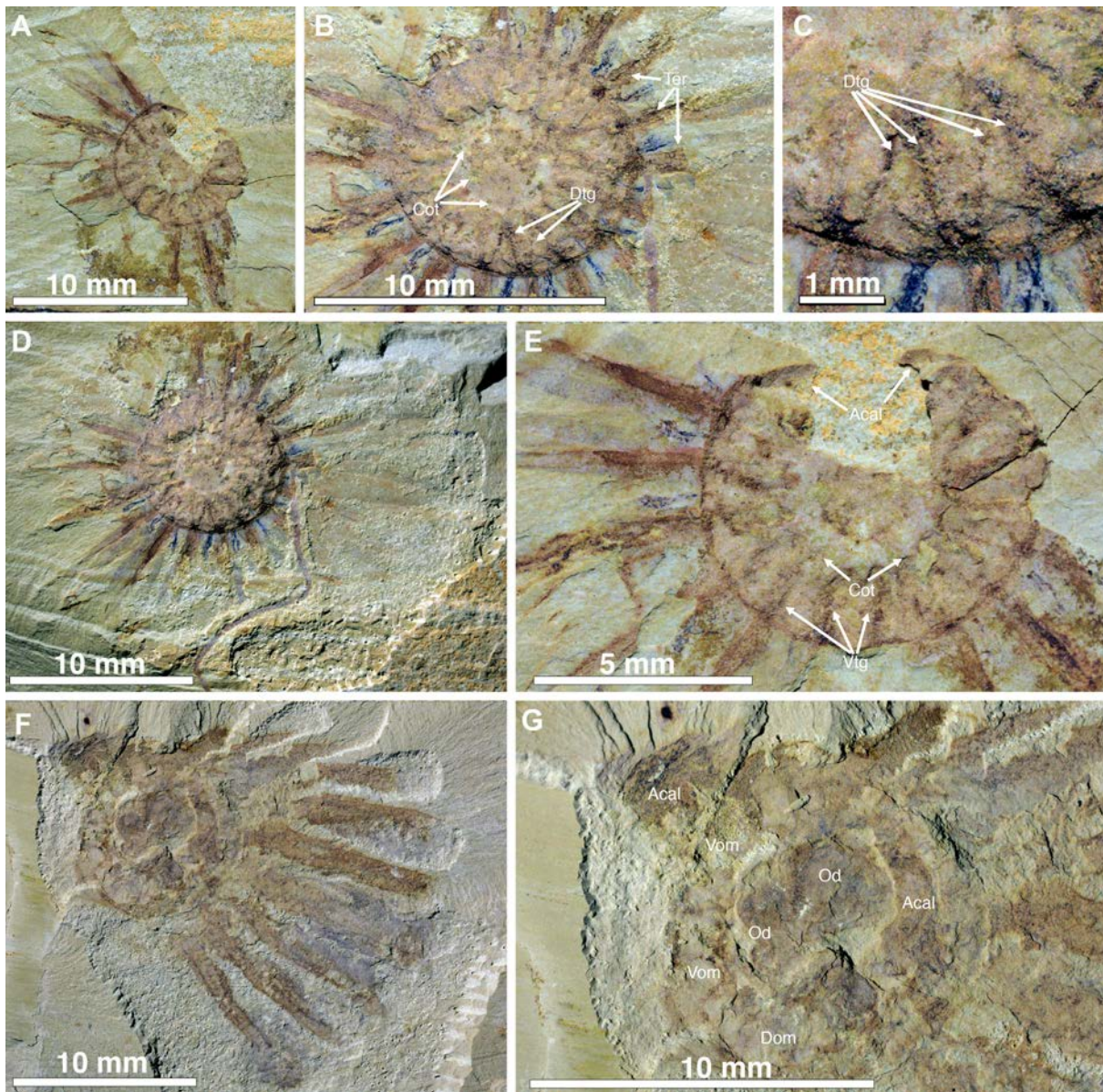


Figure S3. Additional specimens of *Daihua sanqiong*, preserved in oral-aboral view Related to Figure 2. (A) YKLP 13404, part. Oral view, showing ventral oral membrane. (B) YKLP 13404, counterpart. Aboral view, overview of dorsal oral membrane, showing the presence of dorsal tentacle grooves, circumoral tunnel and poorly preserved tentacle rods. (C) YKLP 13404, close-up of counterpart, showing dorsal tentacle grooves. (D) YKLP 13404, counterpart in larger view. A single bract is apparent. (E) YKLP 13404, close-up of part, showing the ventral membrane and the ventral tentacle groove and the circumoral tunnel. Part of the fossil broken off, showing the apical calyx within the sediment. (F) YKLP 13402, specimen viewed in aboral view. (G) YKLP 13402, close-up of specimen. Irregular breakage reveals surfaces of compacted apical calyx, dorsal and ventral oral membrane, and oral dome. Acal-apical calyx, Bcal-basal calyx, Cot-circumoral tunnel, Dom-dorsal oral membrane, Dtg-dorsal tentacle groove, Od-Oral dome, Ter-Tentacle rods, Vom-ventral oral membrane, Vtg-ventral tentacle groove.

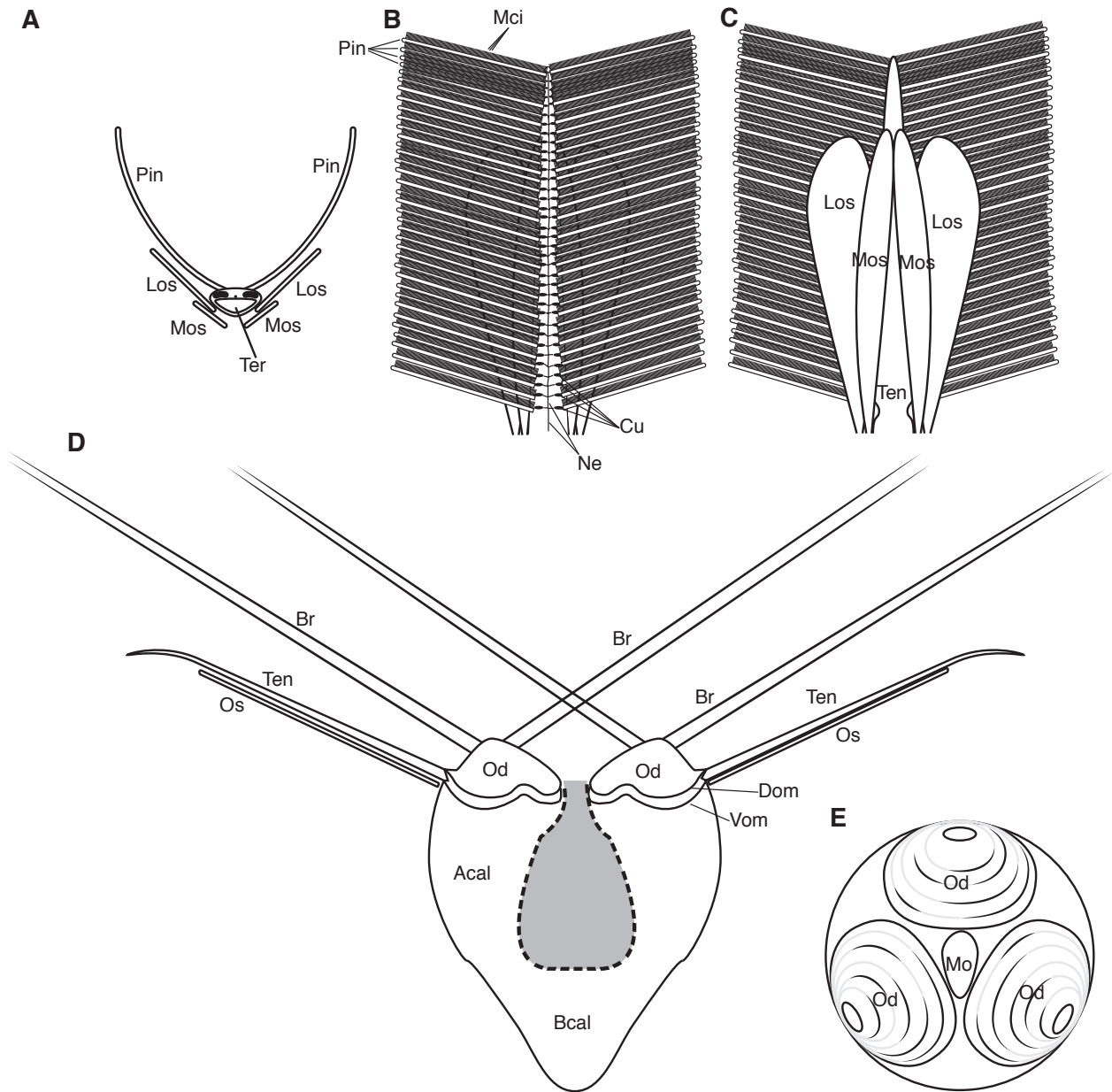


Figure S4 Schematic reconstruction of *Daihua sanqiong*. Related to Figure 2. (A) Tentacle in cross section. (B) Tentacle seen from above. (C) Tentacle seen from below. (D) Sagittal section through body. Note digestive tract is unknown. (E) View of oral surface from above. Abbreviations: Acal-Apical calyx, Bcal-basal calyx, Br-bracts, Los-lateral outer sheath, Mos-medial outer sheath, Os-Outer sheath, Ten-tentacle, Od-oral dome, Mo-mouth, Vom-ventral oral membrane, Dom-dorsal oral membrane, Ter-tentacle rod, Cu-cushion plate, Ne-nerve, Pin-pinnules, Mci-Macrocilia.



Figure S5 Specimens and soft parts of *Dinomischus venustus*. Related to Figure 3. (A) YKLP 13406, specimen preserving oral cone (Oc), gut tract (Gu) inside calyx and mesenteries. (B) YKLP 13408, specimen preserving oral cone (Oc) as organic lining as well as sedimentary infill (Inf) of oral cone. (C) YKLP 13410, specimen preserving multiple mesenteries (Me). (D) YKLP 13430, specimen preserving outer sheaths and lining of digestive tract inside calyx. (E) YKLP 13431, insert showing close-up of outer sheaths.

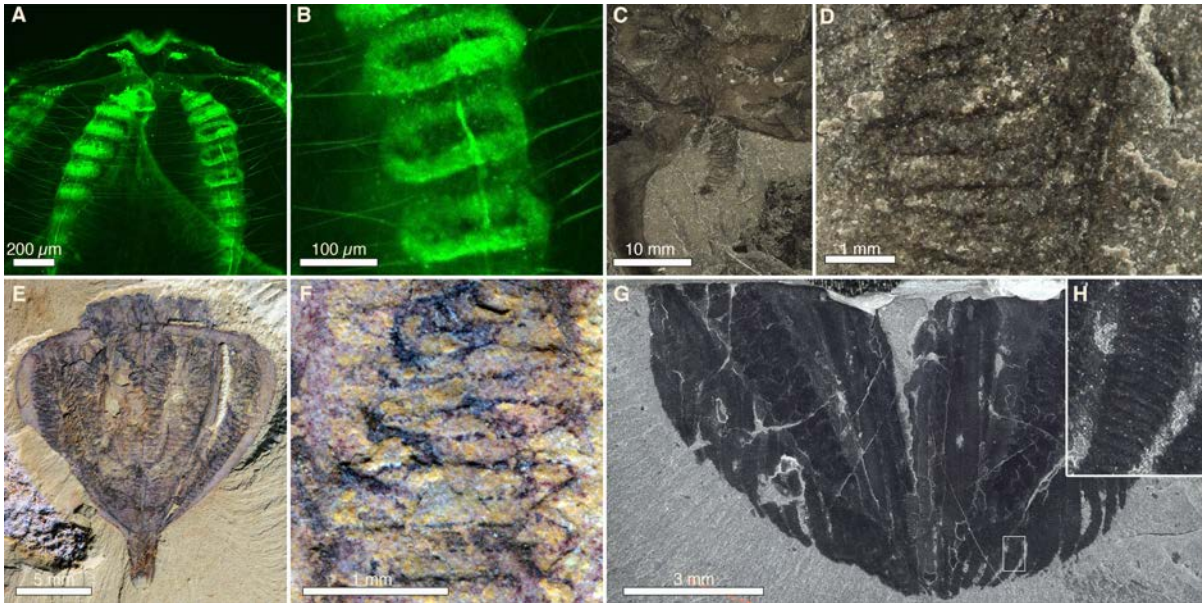
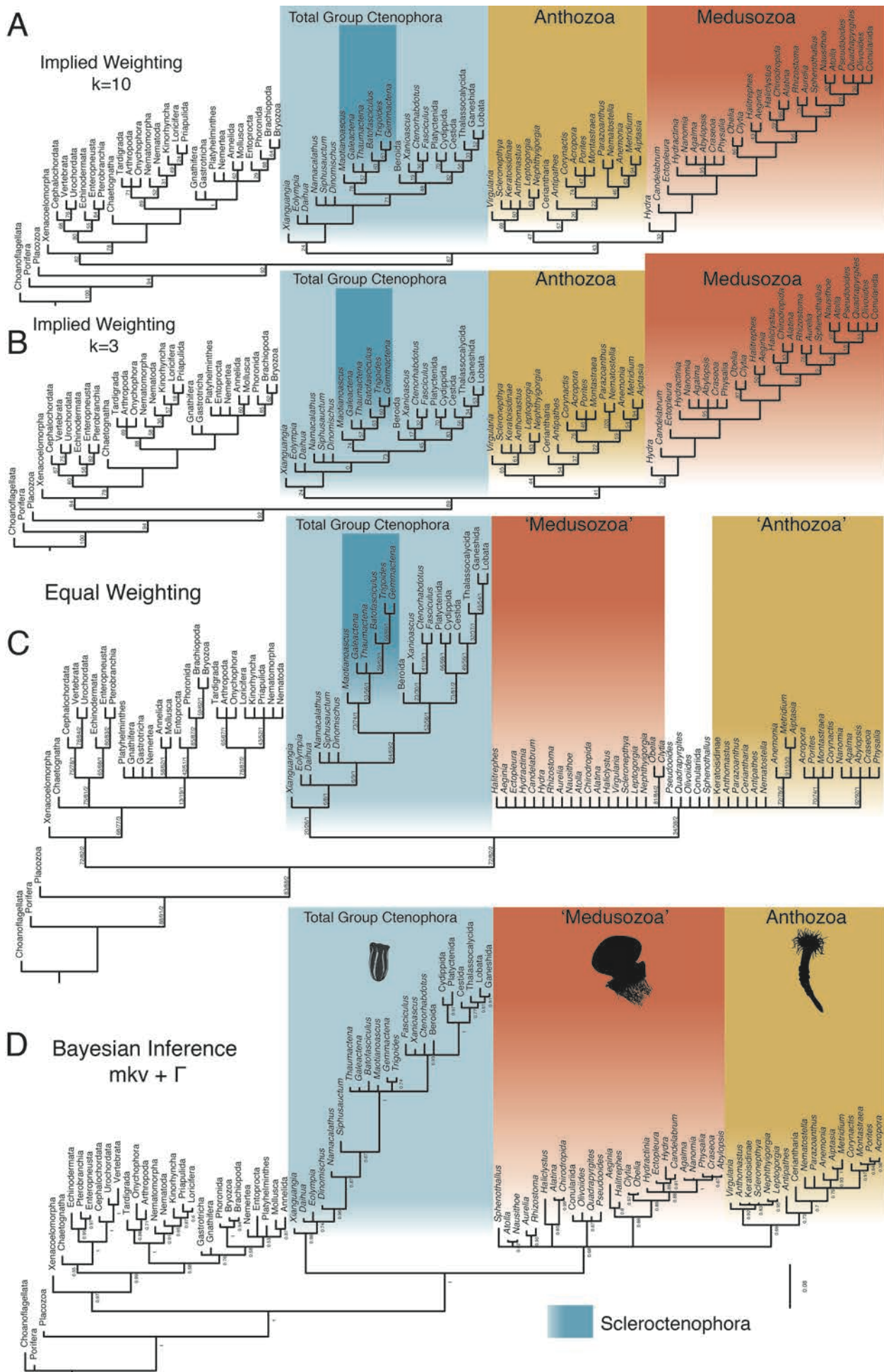
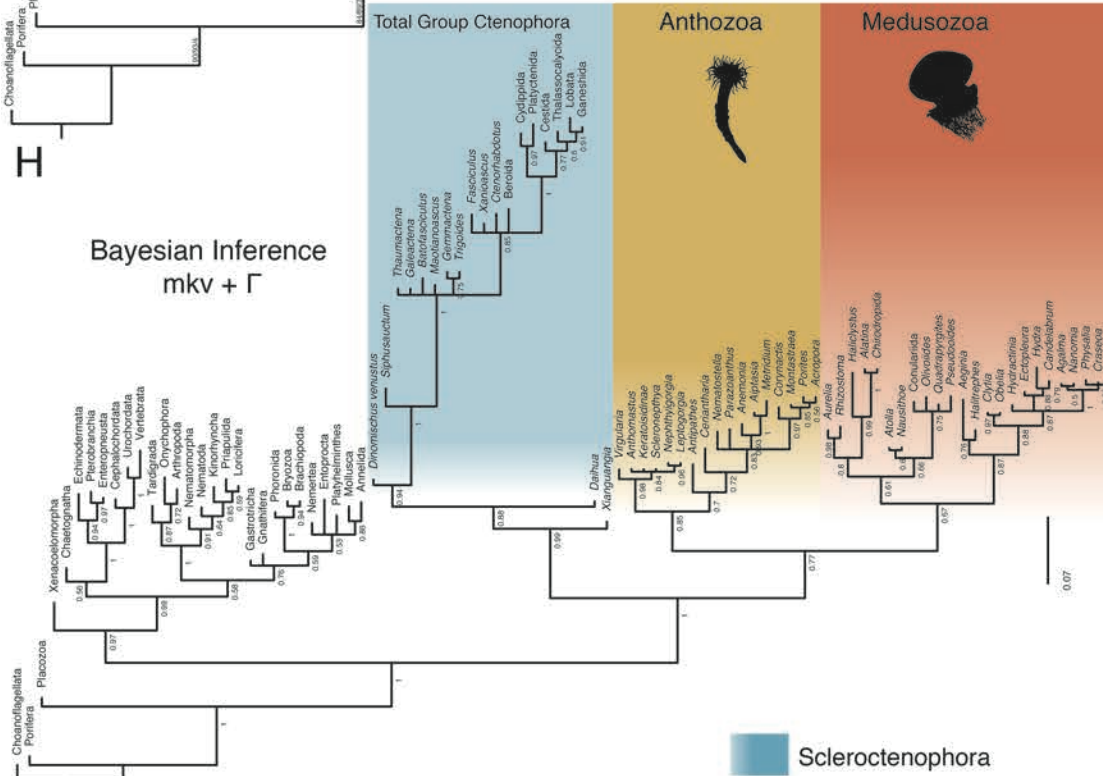
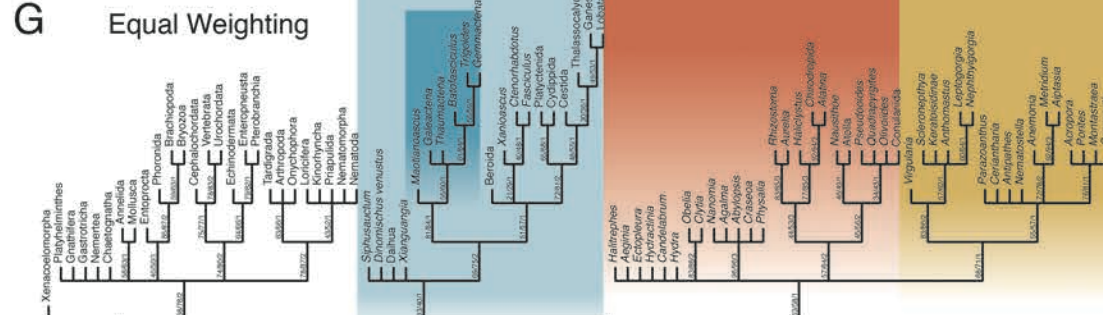
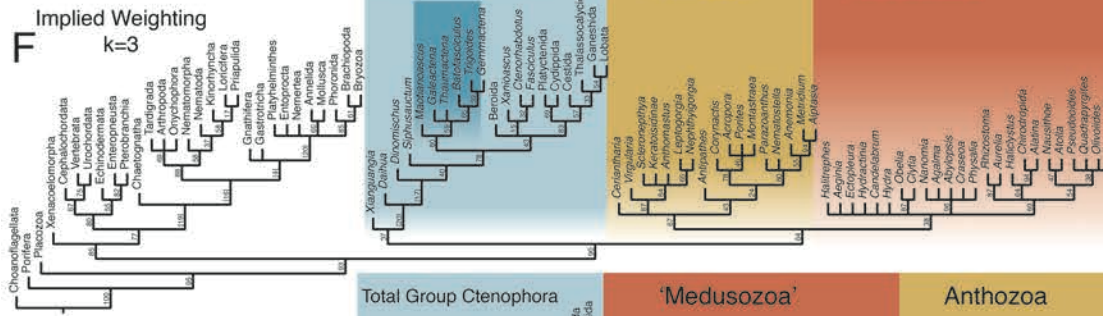
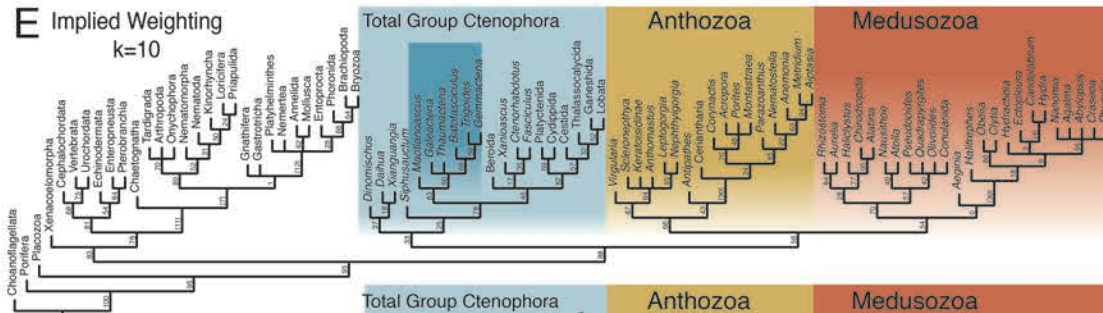


Figure S6. Comparison of cushion ring structures in extant and fossil ctenophores. Related to Figure 5. (A) Living ctenophore, *Beroe ovata* (juvenile) stained with phalloidin (actin filaments) highlighting the basal cushion plate structures of each ctene. (B) Close-up of specimen in (A) showing cushion ring. (C) Cushion plate structures in *Siphusauctum gregarium* (ROM 61419). (D) Close-up of specimen shown in (C). (E) *Galeactena hemispherica*, YKLP 13810, from Chengjiang. (F) Close-up of specimen in (E). (G) *Fasciculus vesanus* USNM 20215, Burgess Shale. (A,B) courtesy of Mark Q. Martindale and David Kainoa Simmons, Whitney Marine Labs, Florida. (C,D) courtesy of Jean-Bernard Caron, Royal Ontario Museum.





 Scleroctenophora

Figure S7. Additional phylogenetic results. Related to Figure 6 and Figure 7. (A) All taxa, implied weighting ($k=10$), numbers at nodes are support values from symmetric resampling. (B) All taxa, implied weighting ($k=3$), numbers at nodes are support values from symmetric resampling. (C) All taxa, equal character weighting, numbers at nodes are support values from bootstrap/jackknife/Bremer. (D) All taxa, Bayesian inference using mkv + gamma model. Numbers at nodes are posterior probabilities and scale bar and branch lengths are in units of number of substitutions per site. (E) Reduced taxon sample, implied weighting ($k=10$), numbers at nodes are support values from symmetric resampling. (F) Reduced taxon sample, implied weighting ($k=3$), numbers at nodes are support values from symmetric resampling. (G) Reduced taxon sample, equal character weighting, numbers at nodes are support values from bootstrap/jackknife/Bremer. (H) Reduced taxon sample, Bayesian inference using mkv + gamma model. Numbers at nodes are posterior probabilities and scale bar and branch lengths are in units of number of substitutions per site. The reduced taxon sample excludes *Eolympia*, *Sphenothallus* and *Namacalathus*.

Taxon	Specimen	Orientation			Stalk	Calyx	Mesentery	Gut tract & Oral cone	Tentacles	Cushion plate & Pinnules	Bracts
		Or	La	Ob							
<i>Daihua sanqiong</i> gen. et sp. nov	YKLP 13401	√			-	+	-	-	Sc&FI	Cu&Pi	+
	YKLP 13402			√	-	+	-	-	Sc	-	-
	YKLP 13404	√			-	+	-	-	Sc	-	-
	YKLP 13426		√		-	+	-	-	Sc	Pin	+
	YKLP 13428		√		-	+	-	-	Sc	-	+
<i>Dinomischus venustus</i>	YKLP 13405	√			-	+	-	-	Sc	-	-
	RCCBYU 10216	√			-	+	-	-	Sc&FI	-	-
	YKLP 13430		√		+	+	+	Gu	Sc	-	-
	YKLP 13431		√		+	+	+	-	Sc	-	-
	YKLP 13412		√		+	+	+	-	Sc	-	-
	YKLP 13406		√		+	+	+	Gu&Oc	Sc	-	-
	YKLP 13407		√		+	+	-	Oc	Sc	-	-
	YKLP 13408		√		+	+	+	Oc	Sc	-	-
	YKLP 13410		√		+	+	+	-	Sc	-	-
	YKLP 13411		√		+	+	+	Gu&Oc	Sc	-	-
	YKLP 13413		√		+	+	-	Gu	Sc	-	-
	YKLP 13432		√		-	+	-	Gu	Sc	-	-
	YKLP 13433		√		+	+	-	-	Sc	-	-
	YKLP 13434		√		-	+	-	Oc	Sc	-	-
	YKLP 13435		√		+	+	+	Gu	Sc	-	-
	YKLP 13436		√		+	+	+	Gu&Oc	Sc	-	-
	YKLP 13437		√		-	+	-	Gu&Oc	Sc	-	-
	YKLP 13438		√		-	+	-	Gu&Oc	Sc	-	-
	YKLP 13439		√		-	+	+	Gu	Sc	-	-
	YKLP 13440		√		+	+	-	Oc	Sc	-	-
	YKLP 13441		√		+	+	-	-	Sc	-	-
	YKLP 13414		√		+	+	-	-	Sc	Pin	-
	YKLP 13893		√		+	+	+	-	Sc	-	-
	CJHMD 00051		√		-	+	-	-	Sc	Cu	+
	YKLP 13442		√		+	+	-	-	Sc	-	-
	YKLP 13443		√		+	+	+	-	Sc	-	-
	YKLP 13444		√		+	+	-	-	Sc	-	-
<i>Xianguangia sinica</i>	YKLP 13415			√	-	+	+	-	Sc	-	-
	YKLP13421		√		-	+	+	Gu	Sc	-	-
	YKLP 13418		√		-	+	-	-	Sc&FI	-	-
	YKLP 13422		√		-	+	+	-	Sc	-	-
	YKLP 13416		√		-	+	+	-	Sc	-	-
	YKLP 13445		√		-	+	-	Gu	Sc	-	-
	YKLP 13446		√		-	+	+	-	Sc	-	-
	YKLP 13447		√		-	+	+	-	Sc	-	-
	YKLP 13448		√		-	+	-	-	Sc&FI	-	-

	YKLP 13449		√		-	+	-	-	Sc&FI	-	-
	YKLP 13450		√		-	+	+	-	Sc	-	-
	YKLP 13466		√		-	+	+	-	Sc	-	-
	YKLP 13467		√		-	+	-	-	Sc	-	-
	YKLP 13468		√		-	+	+	-	Sc	-	-
	YKLP 13469		√		-	+	-	-	Sc	-	-
	YKLP 13470		√		-	+	-	Gu	Sc	-	-
	YKLP 13471		√		-	+	-	-	Sc&FI	-	-
	YKLP 13472			√	-	+	-	-	Sc	-	-
	YKLP 13830		√		-	+	-	-	Sc&FI	Pin	-
	YKLP 13429		√		-	+	-	-	Sc&FI	Pin	-
	YKLP 13473		√		-	+	-	-	Sc&FI	Pin	-
	YKLP 13474			√	-	+	-	-	Sc	-	-
	YKLP 13475		√		-	+	-	-	Sc&FI	Pin	-
	YKLP 13476		√		-	+	-	-	Sc&FI	Pin	-
	YKLP 13477	√			-	+	-	-	Sc&FI	-	-
	YKLP 13478		√		-	+	-	-	Sc&FI	Pin	-
	YKLP 13479		√		-	+	-	-	Sc&FI	Pin	-
	YKLP 13480			√	-	+	-	-	Sc	-	-
	YKLP 13481		√		-	+	-	-	Sc	-	-
Sum	61	5	51	5	19	51	21	Gu 8 Oc 4 Gu&Oc 5	Sc 47 Sc&FI 14	Cu 1 Pin 9 Cu&Pin 1	4

Table S1 Specimens of 'dinomischids' from the Chengjiang biota available for this study. Related to Figures 1-5. Orientation of specimen: Or, Oral view; La, Lateral view; Ob, Oblique view. Characters state: "+", Structure can be observed; "-" Structure not be observed or not preserved; Gu, Gut tract preserved; Oc, Oral cone preserved; Gu&Oc, Both gut tract and oral cone preserved; Sc, Sclerotized tentacle preserved; Sc&Fi, Both sclerotized and flexible tentacles preserved; Cu, Cushion plate preserved; Pin, Pinnules preserved; Cu&Pin, Both cushion plate and pinnules preserved.